UNCLASSIFIED

SECURITY CLASSIFICATION OF THIS PAGE

REPORT DOCUMENTATION PAGE

1a. REPORT SECURITY CLASSIFICATION UNCLASSIFIED	1b. RESTRICTIVE MARKINGS
2a. SECURITY CLASSIFICATION AUTHORITY	3. DISTRIBUTION/AVAILABILITY OF REPORT Approved for public release; distribution unlimited.
2b. DECLASSIFICATION/DOWNGRADING SCHEDULE	
4. PERFORMING ORGANIZATION REPORT NUMBER(S) TR 7633	5. MONITORING ORGANIZATION REPORT NUMBER(S)
6a. NAME OF PERFORMING ORGANIZATION Naval Underwater Systems Center 6b. OFFICE SYMBOL (If applicable)	7a. NAME OF MONITORING ORGANIZATION
6c. ADDRESS (City, State, and ZIP Code) New London Laboratory New London, CT 06320	7b. ADDRESS (City, State, and ZIP Code)
8a. NAME OF FUNDING/SPONSORING ORGANIZATION 8b. OFFICE SYMBOL (If applicable)	9. PROCUREMENT INSTRUMENT IDENTIFICATION NUMBER
8c. ADDRESS (City, State, and ZIP Code)	10. SOURCE OF FUNDING NUMBERS PROGRAM ELEMENT NO. / PROJECT NO. / TASK NO. / WORK UNIT ACCESSION NO.

11. TITLE (Include Security Classification)
SIGNAL-TO-NOISE RATIO REQUIREMENTS FOR HALF-WAVE AND FULL-WAVE NONLINEAR DETECTORS WITH ARBITRARY POWER LAWS, SAMPLING RATES, INPUT SPECTRA, AND FILTER CHARACTERISTICS

12. PERSONAL AUTHOR(S)
Albert H. Nuttall

13a. TYPE OF REPORT	13b. TIME COVERED	14. DATE OF REPORT (Year, Month, Day)	15. PAGE COUNT
	FROM ____ TO ____	1986, June 10	

16. SUPPLEMENTARY NOTATION

17. COSATI CODES			18. SUBJECT TERMS (Continue on reverse if necessary and identify by block number)
FIELD	GROUP	SUB-GROUP	Signal-to-Noise Ratio; ν-th Law Detector; Broadband Spectra; Half-Wave Rectifier; Full-Wave Rectifier; Undersampling

19. ABSTRACT (Continue on reverse if necessary and identify by block number)

The output signal-to-noise ratio of a signal detection system consisting of a sampler, a nonlinear rectifier, and a low-pass filter is evaluated generally, for arbitrary half-wave or full-wave ν-th law rectifiers, sampling rates, input spectra, input signal-to-noise ratio, and filter characteristics. The usual assumption of a long averaging time, relative to the inverse bandwidth of the input spectrum, is not made, thereby affording an explanation of the anamalous behavior of a half-wave rectifier for low-Q input spectra. A pitfall of employing the long averaging time assumption is illustrated via numerical example.

A simple recurrence for the half-wave and full-wave ν-th law rectifier coefficients allows for a very fast and efficient high-order series evaluation of the output signal-to-noise ratio for any value of ν. For moderate-or-large-Q

20. DISTRIBUTION/AVAILABILITY OF ABSTRACT ☐ UNCLASSIFIED/UNLIMITED ☐ SAME AS RPT. ☐ DTIC USERS	21. ABSTRACT SECURITY CLASSIFICATION UNCLASSIFIED
22a. NAME OF RESPONSIBLE INDIVIDUAL Albert H. Nuttall	22b. TELEPHONE (Include Area Code) (203) 440-4618 — 22c. OFFICE SYMBOL Code 33

DD FORM 1473, 84 MAR — 83 APR edition may be used until exhausted. All other editions are obsolete.

SECURITY CLASSIFICATION OF THIS PAGE

UNCLASSIFIED

18. Subject Terms (Cont'd.)

Aliasing
Hypothesis Testing
Deflection Criterion
Impulsive Filters
Long Averaging Time Assumption

19. Abstract (Cont'd.)

input spectra, the possibility of using deliberate undersampling with no loss of performance is illustrated. The use of a half-wave rectifier generally requires a higher sampling rate than does a symmetric full-wave rectifier; also, the performance is somewhat poorer for the half-wave rectifier, and in some cases, significantly so.

Programs for all procedures employed are presented so that investigation of additional cases or combinations of filters and input spectra can be conducted. These results are a significant extension of the work of Faran and Hills; comparisons with their results are noted.

NUSC Technical Report 7633
10 June 1986

Signal-to-Noise Ratio Requirements for Half-Wave and Full-Wave Nonlinear Detectors with Arbitrary Power Laws, Sampling Rates, Input Spectra, and Filter Characteristics

Albert H. Nuttall
Surface Ship Sonar Department

Naval Underwater Systems Center
Newport, Rhode Island / New London, Connecticut

Preface

This research was conducted under NUSC Project No. A99622, "Threat Sonar Assessment and Performance Predictions," Principal Investigator Joseph Dlubac (Code 60), Sponsor M. Vlattas (Code 23), Naval Intelligence Support Center. Also this research was conducted under NUSC Project No.A75205, Subproject No. ZR0000101, "Applications of Statistical Commnication Theory to Acoustic Signal Processing," Principal Investigator Dr. Albert H. Nuttall (Code 33), sponsored by the NUSC In-House Independent Research Program, Mr. W. R. Hunt, Program Manager, Director of Navy Laboratories (SPAWAR 05).

The author would like to acknowledge several useful discussions with the Technical Reviewer of this report, Joseph J. Dlubac (Code 60).

Reviewed and Approved: 10 June 1986

W. A. Von Winkle
Associate Technical Director
for Technology

TABLE OF CONTENTS

TABLE OF CONTENTS (Cont'd)

LIST OF ILLUSTRATIONS

LIST OF ILLUSTRATIONS (Cont'd)

LIST OF TABLES

LIST OF SYMBOLS

ν	power law of rectifier, x^{ν}
t	time
$x(t)$	stationary input process
σ^2	variance of input $x(t)$
$\rho(\tau)$	normalized correlation of input $x(t)$
H_1, H_0	hypotheses 1 and 0
$g\{x\}$	nonlinearity characteristic
$y(t)$	nonlinearity output
$h(\tau)$	filter impulse response
f	frequency
$H(f)$	filter transfer function, (5), (113)
$w(n)$	impulsive filter weights, (8)
Δ	sampling time increment
$z(t)$	filter output
W	bandwidth of input spectrum
f_c	center frequency of input spectrum
Q	quality factor of input spectrum, (11)
f_h	highest frequency of input spectrum, (12), (115)
$\mathrm{sinc}(x)$	auxiliary function, (14)
m_z	mean of filter output $z(t)$
σ_z^2	variance of filter output $z(t)$
γ	filter output signal-to-noise ratio, (16)
overbar	ensemble average
$p^{(1)}(x)$	input first-order probability density function

LIST OF SYMBOLS (Cont'd)

$\phi(w)$	normalized Gaussian function, (21)
$\tilde{z}(t)$	ac (zero-mean) component of z(t)
$a(\tau)$	autocorrelation of $h(\tau)$, (26)
$R_y(\tau)$	correlation of process y(t), (29)
$P_y(f)$	power density spectrum of process y(t)
$p^{(2)}$	input second-order probability density function, (30)
$He_k(x)$	Hermite polynomial
$G(k)$	nonlinearity coefficient, (32)
$A(k)$	filter and spectrum coefficient, (38)
$P^{(k)}(f)$	spectrum of $\rho^k(\tau)$, (47)
γ_s	standard system output signal-to-noise ratio, (50)
γ_a	approximate output signal-to-noise ratio, (51), (55)
T	effective duration of filter, (52)
σ_1^2, σ_0^2	variances under hypotheses 1, 0, (56), (131)
N	input noise power, (56), (131)
S	input signal power, (56), (131)
γ_b	basis output signal-to-noise ratio, (57), (133)
$(S/N)_s$	standard system input signal-to-noise ratio, (59), (134)
dB	decibel difference, (60)
$b(n)$	autocorrelation of filter weights, (62)
M	effective number of filter samples, (67)
$\beta(n)$	normalized autocorrelation of weights, (68)
RC	time constant of RC filter, (70)

LIST OF SYMBOLS (Cont'd)

$\alpha(\tau)$	normalized autocorrelation of filter, (73)
r, ϕ	envelope, phase of narrowband correlation, (78)
L(k)	auxiliary function, (85)
$\Gamma(x)$	gamma function
U(k)	auxiliary sequence, (92)
f_ℓ	lowest frequency of input spectrum, (111)
$\tilde{P}(f)$	aliased version of P(f), (114)
f_s	sampling frequency = $1/\Delta$
$D(\nu)$	ratio of gamma functions, (126)
$F_F(\nu)$	full-wave rectifier factor, (137)
$F_H(\nu)$	half-wave rectifier factor, (145)
$\sum$	sum in (159)
$\tilde{S}(k)$	approximation to S(k), (166)
FWR	full-wave rectifier
SNR	signal-to-noise ratio

subscripts:

F	full-wave rectifier
H	half-wave rectifier
N	nonimpulsive
I	impulsive
NB	narrowband
IF	impulsive, full-wave rectifier
NF	nonimpulsive, full-wave rectifier
IH	impulsive, half-wave rectifier
NH	nonimpulsive, half-wave rectifier

SIGNAL-TO-NOISE RATIO REQUIREMENTS FOR HALF-WAVE AND FULL-WAVE NONLINEAR DETECTORS WITH ARBITRARY POWER LAWS, SAMPLING RATES, INPUT SPECTRA, AND FILTER CHARACTERISTICS

INTRODUCTION

The purpose of this report is to determine the signal-to-noise ratio requirements for various half-wave and full-wave rectifiers, arbitrary input spectra, and post-detector filter characteristics. Both continuous and sampled systems are considered, as well as broadband and narrowband spectra.

The system of interest is indicated in figure 1. The input x(t) is a real stationary zero-mean Gaussian process with variance σ^2 and normalized correlation $\rho(\tau)$. The following analysis will utilize these general parameters where possible; however, since the system of figure 1 is to be used for detection or a decision between two hypotheses, we will later specialize to the cases

$$\sigma^2 = \begin{Bmatrix} \sigma_1^2 \text{ under } H_1 \\ \sigma_0^2 \text{ under } H_0 \end{Bmatrix},$$

$$\rho(\tau) = \begin{Bmatrix} \rho_1(\tau) \text{ under } H_1 \\ \rho_0(\tau) \text{ under } H_0 \end{Bmatrix}, \tag{1}$$

where the subscript denotes the hypothesis number, 1 or 0. That is, H_1 denotes the signal plus noise hypothesis, while H_0 denotes the noise-only hypothesis.

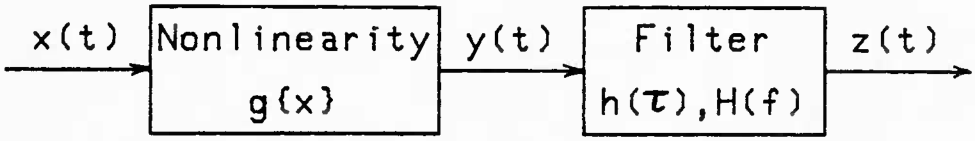

Figure 1. Detection System

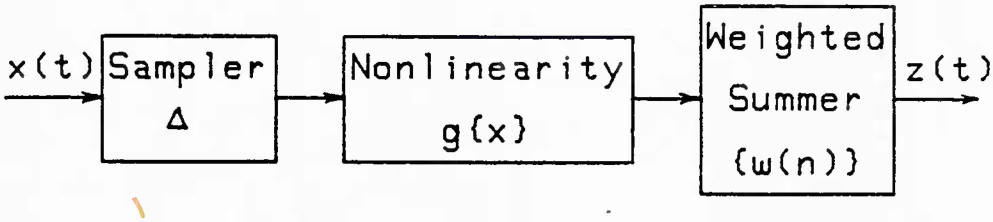

Figure 2. Discrete Detection System

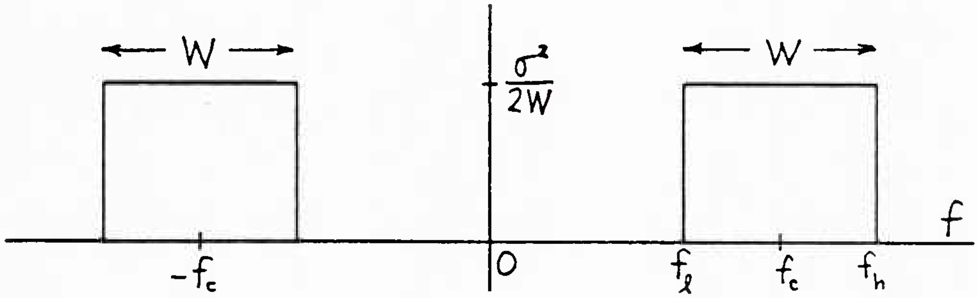

Figure 3. Flat Bandpass Input Spectrum

The nonlinearity $g\{x\}$ is characterized by output

$$y(t) = g\{x(t)\} \ ; \tag{2}$$

this is a memoryless transformation of the input at the same time instant. We shall be particularly interested in the class of half-wave rectifiers

$$g\{x\} = \begin{Bmatrix} x^{\upsilon} & \text{for } x > 0 \\ 0 & \text{for } x < 0 \end{Bmatrix} \tag{3}$$

and the class of symmetric full-wave rectifiers

$$g\{x\} = |x|^{\upsilon} \quad \text{for all } x \ . \tag{4}$$

The particular rectifier with $\upsilon = 0$ is not useful for detection purposes here, in either the full-wave or half-wave case. For the full-wave rectifier, $\upsilon = 0$ corresponds to a constant output, $y(t) = 1$, regardless of what the input $x(t)$ is. For the half-wave rectifier, $\upsilon = 0$ corresponds to $y(t) = 1$ whenever $x(t) > 0$; but if we are trying to decide between two zero-mean processes of different levels, this information is lost at the half-wave rectifier output. Hence, we assume $\upsilon > 0$ from this point on, when we deal with υ-th law rectifiers.

The low-pass filter is characterized either by its impulse response $h(\tau)$ or by its voltage transfer function*

---

*Integrals and sums without limits are over the entire range $(-\infty, +\infty)$ of nonzero integrands and summands, respectively.

$$H(f) = \int d\tau \exp(-i2\pi f\tau)\ h(\tau) . \tag{5}$$

Particular examples are the nonimpulsive filters,

$$h(\tau) = \left\{ \begin{matrix} \frac{1}{T} \text{ for } 0 < \tau < T \\ 0 \text{ otherwise} \end{matrix} \right\}, \text{ box car filter,} \tag{6}$$

and

$$h(\tau) = \left\{ \begin{matrix} \frac{1}{RC} \exp\left(-\frac{\tau}{RC}\right) & \text{for } \tau > 0 \\ 0 & \text{for } \tau < 0 \end{matrix} \right\}, \quad \text{RC filter .} \tag{7}$$

Another class of great interest is the impulsive filters with a response composed of a number of equispaced impulses:

$$h(\tau) = \sum_n w(n)\ \delta(\tau - n\Delta) . \tag{8}$$

Sample increment Δ is arbitrary; the sum is over all nonzero weights $\{w(n)\}$. Since the filter output in figure 1 in steady state is given, in this latter case, by

$$z(t) = \int d\tau\ h(\tau)\ y(t-\tau) = \int d\tau \sum_n w(n)\ \delta(\tau - n\Delta)\ g\{x(t-\tau)\} =$$

$$= \sum_n w(n)\ g\{x(t-n\Delta)\} , \tag{9}$$

an equivalent alternative form is that given in figure 2. Namely, the input $x(t)$ is sampled at increments Δ apart in time and subjected to nonlinearity $g\{x\}$. These quantities are then weighted and accumulated, to give output $z(t)$ at a time t equal to a multiple of Δ. As a special case, if

$$w(n) = \begin{Bmatrix} 1 \text{ for } 1 \leq n \leq M \\ 0 \text{ otherwise} \end{Bmatrix}, \quad \text{box car filter,} \tag{10}$$

then all M samples of the input are equiweighted.

The input spectrum that will be most closely considered is taken to be flat in a band W about center frequency $\pm f_c$; see figure 3. The Q of this spectrum is

$$Q = f_c/W \geq \frac{1}{2} , \tag{11}$$

and the highest frequency contained is

$$f_h = f_c + \frac{W}{2} = W\left(Q + \frac{1}{2}\right) . \tag{12}$$

The constraint on Q in (11) guarantees that W is always the bandwidth of the <u>positive</u> frequency components of the input spectrum.

The normalized correlation corresponding to figure 3 is

$$\rho(\tau) = \cos(2\pi f_c \tau) \ \mathrm{sinc}(W\tau) , \tag{13}$$

where we define

$$\mathrm{sinc}(x) = \frac{\sin(\pi x)}{\pi x} . \tag{14}$$

For the special case of a low-pass spectrum, $f_c = W/2$, (13) reduces to

$$\rho(\tau) = \mathrm{sinc}(2W\tau) \quad \text{for } Q = \frac{1}{2} ; \tag{15}$$

the input spectrum is flat over (-W,W) in this particular case.

Let m_z and σ_z^2 denote the mean and variance, respectively, of the output of the detection systems in figures 1 and 2. Our main interest here is in the evaluation of the output signal-to-noise ratio γ defined in accordance with the power deflection criterion:

$$\gamma = \frac{\left(m_{z1} - m_{z0}\right)^2}{\sigma_{z0}^2} . \tag{16}$$

The subscripts 1 and 0 denote the corresponding hypotheses, as already introduced in (1). We will determine the dependence of γ on all the parameters encountered above, such as σ_1, σ_0, $\rho_0(\tau)$, υ, T, Δ, M, W, Q, and compare the performance of different nonlinear systems for various sampling rates and spectra. These results will greatly extend those given in [1], for example, and will be much more accurate, since we will use 1000 terms in our series expansions, instead of the 3 or 4 terms used there. Observe that the absolute levels (gains) of the nonlinearity and filter cancel out in quantity γ; thus, we can assume any convenient level for them, as done in (3), (4), (6), (10), for example. Limitations of the output deflection criterion (16) will be discussed later.

DERIVATION OF OUTPUT MOMENTS

Output Mean

In order to determine the detection system output signal-to-noise ratio defined in (16), we need m_z and σ_z. For any filter $h(\tau)$, whether impulsive or not, since the output in steady state is

$$z(t) = \int d\tau \; h(\tau) \; y(t-\tau) \; , \tag{17}$$

then the mean of the output is

$$m_z = \overline{z(t)} = \int d\tau \; h(\tau) \; \overline{y(t-\tau)} = m_y \int d\tau \; h(\tau) \; , \tag{18}$$

in terms of the mean of nonlinearity output y(t). (An overbar denotes an ensemble average.) However, this latter quantity is given by

$$m_y = \overline{y(t)} = \overline{g\{x(t)\}} = \int dx \; g\{x\} \; p^{(1)}(x) \; , \tag{19}$$

in terms of the first-order probability density function $p^{(1)}$ of input x(t). Since the input is zero mean Gaussian, with variance σ^2, then

$$p^{(1)}(x) = \frac{1}{\sigma} \, \phi\left(\frac{x}{\sigma}\right) \; , \tag{20}$$

where we define

$$\phi(w) = (2\pi)^{-1/2} \exp(-w^2/2) \; . \tag{21}$$

Substitution of (20) in (19) yields for the mean of y(t),

$$m_y = \int dx\, g\{x\}\, \frac{1}{\sigma}\, \phi\!\left(\frac{x}{\sigma}\right) = \int dw\, g\{\sigma w\}\, \phi(w) \;. \tag{22}$$

Coupled with (18), system output mean m_z is now available as

$$m_z = \int dw\, g\{\sigma w\}\, \phi(w) \quad \int d\tau\, h(\tau) \;.$$

Output Variance

The ac (zero-mean) output of the detection system is

$$\tilde{z}(t) = z(t) - \overline{z(t)} = \int d\tau\, h(\tau)\, \tilde{y}(t-\tau) \;, \tag{23}$$

where the ac filter input is

$$\tilde{y}(t) = y(t) - \overline{y(t)} = y(t) - m_y \;. \tag{24}$$

Then the variance of the detection system output is

$$\sigma_z^2 = \overline{\tilde{z}^2(t)} = \iint du\, dv\, h(u)\, h(v)\, \overline{\tilde{y}(t-u)\, \tilde{y}(t-v)} =$$
$$= \iint du\, dv\, h(u)\, h(v)\, R_{\tilde{y}}(u-v) = \int d\tau\, a(\tau)\, R_{\tilde{y}}(\tau) \;, \tag{25}$$

where

$$R_{\tilde{y}}(\tau) = \overline{\tilde{y}(t)\, \tilde{y}(t-\tau)}$$

is the (auto) correlation of random process $\tilde{y}(t)$, and

$$a(\tau) = \int du\, h(u)\, h(u-\tau) \tag{26}$$

is the autocorrelation of the deterministic filter impulse response.

An alternative form to (25) is available via the frequency domain expression

$$\sigma_z^2 = \int df \; |H(f)|^2 \; P_{\tilde{y}}(f) \; , \tag{27}$$

where $|H(f)|^2$ is the filter power transfer function, and $P_{\tilde{y}}(f)$ is the power density spectrum of $\tilde{y}(t)$.

Now from (24), we see that correlation

$$R_{\tilde{y}}(\tau) = R_y(\tau) - m_y^2 \; . \tag{28}$$

Also, from (2), we have correlation

$$\begin{aligned} R_y(\tau) &= \overline{y(t)\; y(t-\tau)} = \overline{g\{x(t)\}\; g\{x(t-\tau)\}} = \\ &= \iint dx_a \, dx_b \; g\{x_a\} \; g\{x_b\} \; p^{(2)}(x_a, x_b, \tau) \; , \end{aligned} \tag{29}$$

in terms of the second-order probability density function of input process $x(t)$.

At this point, we use Mehler's expansion for a Gaussian process [2, (67)]:

$$p^{(2)}(x_a, x_b, \tau) = p^{(1)}(x_a)\; p^{(1)}(x_b) \sum_{k=0}^{\infty} \frac{1}{k!} \; \rho^k(\tau) \; He_k\!\left(\frac{x_a}{\sigma}\right) \; He_k\!\left(\frac{x_b}{\sigma}\right) , \tag{30}$$

where $p^{(1)}$ has already been encountered in (20)-(21), and $He_k(x)$ is the Hermite polynomial [3, (22.2.15)]. Substitution of (30) in (29) yields

$$R_y(\tau) = \sum_{k=0}^{\infty} \frac{1}{k!} \rho^k(\tau) \; G^2(k) \; , \tag{31}$$

where nonlinearity coefficients are defined as

$$G(k) = \int dx \; g\{x\} \; p^{(1)}(x) \; He_k(x/\sigma) =$$

$$= \int dw \; g\{\sigma w\} \; \phi(w) \; He_k(w) \quad \text{for } k \geq 0 \; . \tag{32}$$

Here we used (20) and (21).

In particular, we have from (32) and (19), the zero-th order coefficient

$$G(0) = \int dx \; g\{x\} \; p^{(1)}(x) = m_y \; . \tag{33}$$

Thus the $k = 0$ term in sum (31) is simply m_y^2. Combining this information with (28) and (31), we obtain correlation

$$R_{\tilde{y}}(\tau) = \sum_{k=1}^{\infty} \frac{1}{k!} \rho^k(\tau) \; G^2(k) \; . \tag{34}$$

It is worthwhile observing that coefficients $\{G(k)\}$ in (32) depend solely on the input standard deviation σ and the nonlinearity $g\{x\}$; they are independent of the input spectral shape or the filter characteristics. Of course, from (1), since

$$\sigma = \begin{Bmatrix} \sigma_1 \text{ under hypothesis } H_1 \\ \sigma_0 \text{ under hypothesis } H_0 \end{Bmatrix} , \tag{35}$$

then

$$G(k) = \begin{Bmatrix} G_1(k) \text{ under } H_1 \\ G_0(k) \text{ under } H_0 \end{Bmatrix} . \tag{36}$$

However, we will keep σ general for now, at least until we have to specialize to H_1 versus H_0, or to evaluate output signal-to-noise ratio γ in (16). A similar procedure has been adopted with respect to general $\rho(\tau)$ in (30), (31), and (34), above.

We now utilize (34) in (25) to obtain the detection system output variance

$$\sigma_z^2 = \int d\tau\, a(\tau) \sum_{k=1}^{\infty} \frac{1}{k!} \rho^k(\tau)\, G^2(k) =$$

$$= \sum_{k=1}^{\infty} \frac{1}{k!} G^2(k)\, A(k) , \tag{37}$$

where we define coefficient

$$A(k) = \int d\tau\, a(\tau)\, \rho^k(\tau) \quad \text{for } k \geq 1 . \tag{38}$$

This sequence $\{A(k)\}$ depends solely on filter $h(\tau)$ and input normalized correlation $\rho(\tau)$; it is independent of σ and $g\{x\}$. Thus sequences $\{G(k)\}$ and $\{A(k)\}$ in (32) and (38), respectively, completely separate the dependence of the system output variance on the relevant parameters of the problem. However, just as in (1) and (36), since

$$\rho(\tau) = \begin{Bmatrix} \rho_1(\tau) \text{ under } H_1 \\ \rho_0(\tau) \text{ under } H_0 \end{Bmatrix}, \tag{39}$$

then

$$A(k) = \begin{Bmatrix} A_1(k) \text{ under } H_1 \\ A_0(k) \text{ under } H_0 \end{Bmatrix}. \tag{40}$$

The results above for output mean m_z in (18) and output variance σ_z^2 in (37) are exact. There are no assumptions regarding small input signal-to-noise ratio, large averaging time, or large time-bandwidth product. They hold for arbitrary input strength σ, input normalized correlation $\rho(\tau)$, filter impulse response $h(\tau)$, and nonlinearity $g\{x\}$. Also σ and $\rho(\tau)$ can vary with the hypothesis, as in (1). The input spectrum can be low-pass, broadband, or narrowband. The filter can be impulsive as in (8), or otherwise as in (6) and (7); the sampling interval Δ and weights $\{w(n)\}$ in (8), and the duration T or time constant RC in (6) or (7), are arbitrary. The nonlinearity $g\{x\}$ can be a ν-th law power device as described in (3) or (4), but need not be; also, ν is not limited to being an integer. The effects of deliberately undersampling the input process in figure 2 can be investigated by choosing sampling increment Δ larger than the inverse of twice the highest frequency, (12), in figure 3; conversely, the effects of a continuous filter impulse response can be deduced by choosing Δ very small. All of these effects will be investigated here.

The major assumption utilized is that the input signal and noise must be Gaussian; this precludes the presence of pure tones in the input signal.

Output Signal-to-Noise Ratio

The system output signal-to-noise ratio was defined in (16). We now employ (18), (33), and (37) to obtain it in the form

$$\gamma = \left[\int d\tau \; h(\tau)\right]^2 \frac{\left[G_1(0) - G_0(0)\right]^2}{\sum_{k=1}^{\infty} \frac{1}{k!} \, G_0^2(k) \; A_0(k)} \, . \tag{41}$$

The utility of this result depends on the ability to accurately and efficiently evaluate the single integrals for G(k) and A(k) in (32) and (38), respectively, for high-order k.

A note of caution is worthwhile here: since output signal-to-noise ratio, γ, in (16) and (41) only uses second-order moment information, it will have limited capability insofar as determining the system operating characteristics, that is, detection probability versus false alarm probability, unless output z(t) is fairly well approximated by a Gaussian random variable. This latter situation will obtain when the product of averaging time and input bandwidth is large relative to 1; furthermore, that means that low input signal-to-noise ratios can be tolerated and yet decent performance predictions can be realized. Hence, although we concentrate here on the statistic γ, we are aware of its limitations as a performance measure. To accurately determine the exact operating characteristics, the techniques of [4] could be advantageously employed.

BASIS OF COMPARISON

In order to compare the various nonlinear systems subject to different input spectra and averaging filters, a standard performance level for output signal-to-noise ratio γ will be adopted. All comparisons will then be made with this standard, which will now be derived.

The standard system of interest is depicted in figure 4; it is a special case of figure 1 with $g\{x\} = x^2$ for all x, that is, the full-wave square-law rectifier. Since the output for figure 4 is

$$z(t) = \int d\tau \; h(\tau) \; x^2(t-\tau) \; , \tag{42}$$

then mean

$$m_z = \overline{z(t)} = H(0) \; \sigma^2 \; , \tag{43}$$

where we utilized (5). The total output power (ac and dc) is

$$\overline{z^2(t)} = \int df \; |H(f)|^2 \; P_{x^2}(f) \; , \tag{44}$$

in terms of the spectrum of process $x^2(t)$. But since the correlation of $x^2(t)$ is, for Gaussian process $x(t)$,

$$R_{x^2}(\tau) = \overline{x^2(t) \; x^2(t-\tau)} = \sigma^4 + 2\sigma^4 \; \rho^2(\tau) \; , \tag{45}$$

then the spectrum of $x^2(t)$ is

$$P_{x^2}(f) = \sigma^4 \; \delta(f) + 2\sigma^4 \; P^{(2)}(f) \; . \tag{46}$$

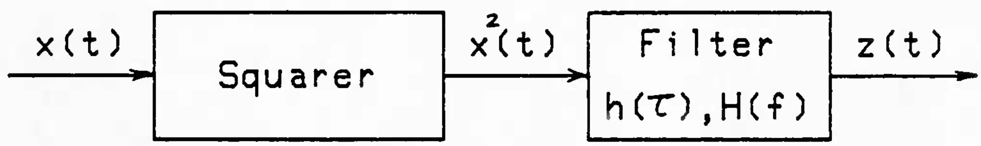

Figure 4. Full-Wave Square-Law Detection System

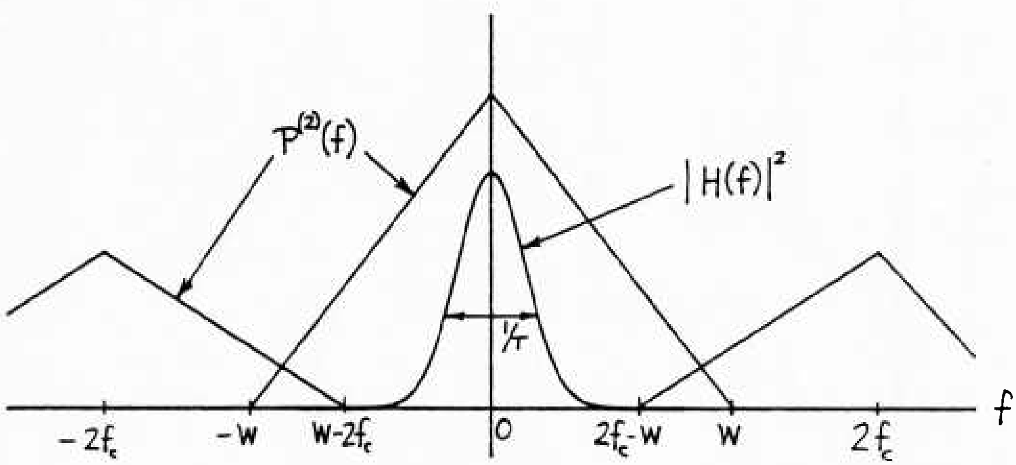

Figure 5. Spectral Quantities for Variance σ_z^2, (49)

Here, and in the following, we will use the notation

$$P^{(k)}(f) = \int d\tau \exp(-i2\pi f\tau)\ \rho^k(\tau) \ . \tag{47}$$

Thus, $P^{(k)}(f)$ is the k-fold convolution of

$$P^{(1)}(f) = \int d\tau \exp(-i2\pi f\tau)\ \rho(\tau) \ . \tag{48}$$

For the flat bandpass spectrum of major interest, $P^{(1)}(f)$ is just the spectrum of figure 3, without the factor σ^2. More generally, $P^{(1)}(f)$ is the spectrum of input x(t), normalized to unit area. $P^{(2)}(f)$ is depicted in figure 5. Combining (43), (44), and (46), we find output variance

$$\sigma_z^2 = 2\sigma^4 \int df\ |H(f)|^2\ P^{(2)}(f) \ . \tag{49}$$

The output signal-to-noise ratio of our <u>standard</u> system follows upon using (43) and (49) in (16):

$$\gamma_s = \frac{H^2(0)\left(\sigma_1^2 - \sigma_0^2\right)^2}{2\sigma_0^4 \int df\ |H(f)|^2\ P_0^{(2)}(f)} \ , \tag{50}$$

where we have added subscripts to differentiate hypotheses H_1 and H_0. If we wanted to maximize γ_s by choice of the filter, (50) indicates that the relative power transfer function $|H(f)/H(0)|^2$ of the low-pass filter should be made as sharp (narrow) as possible about f = 0, where the power ratio must necessarily be 1. But since, in practice, the effective duration T of filter impulse response $h(\tau)$ is limited, there is an upper limit to γ_s.

Rather than attempt to derive this absolute optimum value of γ_s, we develop an approximation to γ_s in the case where the filter width, 1/T, is much narrower than the input spectral width, W; that is, TW >> 1, which corresponds to a long averaging time assumption. In this case, (50) yields the approximation

$$\gamma_s \cong \frac{H^2(0)\left(\sigma_1^2/\sigma_0^2 - 1\right)^2}{2P_0^{(2)}(0) \int df \, |H(f)|^2} =$$

$$= \frac{\left[\int d\tau \, h(\tau)\right]^2 \left(\sigma_1^2/\sigma_0^2 - 1\right)^2}{2 \int df \, P_0^{(1)^2}(f) \int d\tau \, h^2(\tau)} =$$

$$= \frac{T\left(\sigma_1^2/\sigma_0^2 - 1\right)^2}{2 \int df \, P_0^{(1)^2}(f)} \equiv \gamma_a \, , \tag{51}$$

where

$$T = \frac{\left[\int d\tau \, h(\tau)\right]^2}{\int d\tau \, h^2(\tau)} \tag{52}$$

is defined as the effective duration of filter impulse response $h(\tau)$. The last quantity in (51) is the desired <u>approximation</u>, γ_a, to be utilized as a basis of comparison. In deriving this result, we have utilized (47) in the form

$$P_0^{(2)}(0) = \int d\tau \, \rho_0^2(\tau) = \int df \, P_0^{(1)^2}(f) \, , \tag{53}$$

and Parseval's theorem for the Fourier transform pair in (48).

For the flat bandpass spectrum of figure 3, where W measures the width of the positive frequency components of the input spectrum, that is,

$$P_0^{(1)}(f) = \frac{1}{2W} \quad \text{for } |f \pm f_c| < \frac{W}{2} , \qquad \left(f_c > \frac{W}{2} , \; Q > \frac{1}{2}\right) , \tag{54}$$

the approximation in (51) becomes

$$\gamma_a = TW\left(\frac{\sigma_1^2}{\sigma_0^2} - 1\right)^2 \quad \text{for flat bandpass spectrum with } Q \geq \frac{1}{2} . \tag{55}$$

If the input spectrum is modified from figure 3, this result must be re-evaluated from (51). In fact, the interpretation of bandwidth W must be done carefully and with precision.

In the further special case where hypothesis H_0 corresponds to noise only, and H_1 to signal plus noise, then

$$\sigma^2 = \left\{\begin{array}{lll} \sigma_1^2 = S + N & \text{under } H_1 \\ \sigma_0^2 = \quad\;\; N & \text{under } H_0 \end{array}\right\} , \tag{56}$$

where N and S are the input noise and signal powers, respectively, and (55) reduces to

$$\gamma_b = TW\left(\frac{S}{N}\right)^2 \quad \text{for flat bandpass spectrum} . \tag{57}$$

This, finally, is the basis of comparison, for the standard system signal-to-noise ratio, to be used for all the quantitative results for the flat bandpass spectrum, and for the two hypotheses described in (56). There is a certain amount of arbitrariness in adopting (57) as a basis; however, if two systems are both compared with (57), then the difference of those two relative signal-to-noise ratios is exact, regardless of the basis.

It is very important to observe that the approximation for the standard system output signal-to-noise ratio γ_a in (51) is not the optimum or maximum value of the more general result γ_s in (50) for the square-law system depicted in figure 4. Rather, γ_s will be greater than γ_a in some cases. To see this, the terms in the system output variance (denominator of (50)), are illustrated in figure 5. It is obvious, since everything is nonnegative, that

$$\int df\ |H(f)|^2\ P_0^{(2)}(f) \leq\ P_0^{(2)}(0)\ \int df\ |H(f)|^2\ . \tag{58}$$

Since this right-hand side is just the quantity in the denominator of the top line of approximation (51), this means that $\gamma_s \geq \gamma_a$.

More generally, this means that we have to expect the possibility that the general system output signal-to-noise ratio in (16) will have $\gamma > \gamma_b$ in some cases. Nevertheless, because of its simplicity, γ_b in (57) will be kept as our basis of comparison for the various systems. However, the interpretation of T and W must be carefully noted for each case.

The exact way in which we use the basis γ_b in (57) is as follows: for the general nonlinear system in figure 1, we set its <u>output</u> signal-to-noise ratio γ equal to the basis, that is, set

$$\gamma = \gamma\left(\frac{S}{N}\right) = TW\left(\frac{S}{N}\right)_s^2 , \tag{59}$$

where S/N is the actual input signal-to-noise ratio to the general nonlinear system, and $(S/N)_s$ is the input signal-to-noise ratio to the standard system. Then we solve (59) for the required <u>input</u> signal-to-noise ratio S/N to achieve this level of performance, and compute the decibel difference at the input,

$$dB = 10 \log\left[\frac{S/N}{(S/N)_s}\right], \tag{60}$$

relative to the standard system input signal-to-noise ratio.

In general, this quantity will be a function of the standard system input signal-to-noise ratio $(S/N)_s$; however, for low input signal-to-noise ratio, it is independent of $(S/N)_s$. It affords a measure of how much more input signal-to-noise ratio is required for the general nonlinear system of interest, relative to the square-law standard of figure 4. In keeping with the discussion above, we can expect that the quantity, dB, in (60) will become negative in some cases; this simply means that the performance of that particular nonlinear system is somewhat better than the arbitrary basis γ_b adopted in (57).

OUTPUT SIGNAL-TO-NOISE RATIO FOR TWO FILTER CLASSES

The system output signal-to-noise ratio γ was derived in (41) in terms of the general filter impulse response $h(\tau)$. In this section, we shall develop γ in more detail for impulsive filters, as in (8), and nonimpulsive filters, as in (6) and (7). The latter case correponds to an analog filtering procedure.

Impulsive Filters

The impulse response $h(\tau)$ takes the form (8) in this case, and the corresponding system block diagram is given in figure 2. We substitute (8) in (26) to obtain the autocorrelation of $h(\tau)$ as

$$a(\tau) = \sum_n b(n)\ \delta(\tau - n\Delta) \ , \tag{61}$$

where sequence $\{b(n)\}$ is the autocorrelation of the filter weights:

$$b(n) = \sum_m w(m)\ w(m-n) \quad \text{for all } n \ . \tag{62}$$

The evaluation of $A(k)$ in (38) is immediate in this case, yielding

$$A(k) = \sum_n b(n)\ \rho^k(n\Delta) \quad \text{for } k \geq 1 \ . \tag{63}$$

There follows from (18), (33), and (8), the system output mean in the form

$$m_z = G(0) \sum_n w(n) \ , \tag{64}$$

while from (37) and (63), the variance is given by

$$\sigma_z^2 = \sum_{k=1}^{\infty} \frac{1}{k!} G^2(k) \sum_n b(n)\, \rho^k(n\Delta) \; . \tag{65}$$

Combining these last two expressions in (16), the output signal-to-noise ratio for the impulsive class of filters can be expressed as

$$\gamma_I = \frac{M \left[G_1(0) - G_0(0)\right]^2}{\sum_{k=1}^{\infty} \frac{1}{k!} G_0^2(k) \sum_n \beta(n)\, \rho_0^k(n\Delta)} \; , \tag{66}$$

where

$$M = \frac{\left[\sum_n w(n)\right]^2}{\sum_n w^2(n)} \tag{67}$$

is the effective number of samples in impulsive filter response $h(\tau)$ in (8), and

$$\beta(n) = \frac{b(n)}{b(0)} = \frac{\sum_m w(m)\, w(m-n)}{\sum_m w^2(m)} \tag{68}$$

is the normalized autocorrelation of the filter sampling weights $\{w(n)\}$. The result (66) holds for any impulsive filter with any weight sequence $\{w(n)\}$, sampling increment Δ, input levels σ_1, σ_0, input correlation $\rho_0(\tau)$, and nonlinearity $g\{x\}$.

Nonimpulsive Filters

Examples of filter impulse responses in this class were presented in (6) and (7). In the former case, the autocorrelation (26) is

$$a(\tau) = \left\{ \begin{array}{ll} \frac{1}{T}\left(1 - \frac{|\tau|}{T}\right) & \text{for} \quad |\tau| < T \\ 0 \text{ otherwise} & \end{array} \right\}, \quad \text{box car filter,} \tag{69}$$

while in the latter case,

$$a(\tau) = \frac{1}{2\,RC} \exp\left(-\frac{|\tau|}{RC}\right) \quad \text{for all } \tau\,, \quad \text{RC filter .} \tag{70}$$

If we substitute (38) in (41), the output signal-to-noise ratio for the nonimpulsive class of filters can be expressed as

$$\gamma_N = \frac{T\left[G_1(0) - G_0(0)\right]^2}{\sum_{k=1}^{\infty} \frac{1}{k!}\, G_0^2(k) \int d\tau\, \alpha(\tau)\, \rho_0^k(\tau)}\,, \tag{71}$$

where

$$T = \frac{\left[\int d\tau\, h(\tau)\right]^2}{\int d\tau\, h^2(\tau)} \tag{72}$$

is the effective duration of filter impulse response $h(\tau)$, and

$$\alpha(\tau) = \frac{a(\tau)}{a(0)} = \frac{\int du\, h(u)\, h(u-\tau)}{\int du\, h^2(u)} \tag{73}$$

is the normalized autocorrelation of the filter response. The result (71) holds for any input levels σ_1, σ_0, input correlation $\rho_0(\tau)$, and nonlinearity $g\{x\}$. However, it does not cover a filter containing any impulses, since the denominator integral in (72) and (73) is infinite then. Nevertheless, the corresponding result in (66) for the impulsive filters can be derived as a limit of a set of progressively narrower pulses at multiples of increment Δ. Thus, (71) does have the capability of covering the most general filter structure, if manipulated properly.

Long Averaging Time Assumption

The results in (66) and (71) for the output signal-to-noise ratio simplify somewhat when the averaging time of the filter ($M\Delta$ or T) is much larger than the correlation time ($1/W$) of the input process $x(t)$ under hypothesis H_0. In the impulsive filter case, this means that the sum on n in the denominator of (66) can be approximated according to

$$\sum_n \beta(n)\, \rho_0^k(n\Delta) \cong \beta(0) \sum_n \rho_0^k(n\Delta) = \sum_n \rho_0^k(n\Delta) \quad \text{for } k \geq 1 , \tag{74}$$

leading to approximation

$$\gamma_I \cong \frac{M\left[G_1(0) - G_0(0)\right]^2}{\sum_{k=1}^{\infty} \frac{1}{k!}\, G_0^2(k) \sum_n \rho_0^k(n\Delta)} . \tag{75}$$

It is interesting to observe that the exact detailed values of the weights $\{w(n)\}$ in impulsive filter response (8) are immaterial to the value of (75), except insofar as they affect effective number M via (67). This simplification is not possible for the general averaging time result in (66), which depends on the weights through their normalized autocorrelation sequence $\{\beta(n)\}$ in (68).

On the other hand, for nonimpulsive filters, the long averaging time assumption means that the integral on τ in the denominator of (71) can be approximated according to

$$\int d\tau \; \alpha(\tau) \; \rho_0^k(\tau) \cong \alpha(0) \int d\tau \; \rho_0^k(\tau) = \int d\tau \; \rho_0^k(\tau) \quad \text{for } k \geq 1 \; , \tag{76}$$

leading to approximation

$$\gamma_N \cong \frac{T\left[G_1(0) - G_0(0)\right]^2}{\sum_{k=1}^{\infty} \frac{1}{k!} \, G_0^2(k) \int d\tau \; \rho_0^k(\tau)} \; . \tag{77}$$

Analogous to the observation above, the shape of the detailed impulse response $h(\tau)$ is immaterial to the value of (77), except as it affects the effective duration T via (72).

The approximations in (75) and (77) for the long averaging time assumption are not used in the numerical results that follow later. Rather, the exact result (66) for impulsive filters, and (71) for nonimpulsive filters, are extensively utilized. Also the danger of using the long averaging time assumption when inappropriate is illustrated by a numerical example in a later section.

Narrowband Input Spectrum

We now return to general output signal-to-noise ratio γ_N for arbitrary averaging time in (71) and consider, for the moment, the case of a very narrowband input spectrum under H_0. That is, let normalized correlation

$$\rho_0(\tau) = r(\tau)\cos(2\pi f_c \tau + \phi(\tau)) , \tag{78}$$

where center frequency f_c is much larger than the highest frequency contents of envelope $r(\tau)$ and phase $\phi(\tau)$; this is called a high-Q input spectrum. Then the integral in the denominator of (71) becomes

$$\int d\tau\, \alpha(\tau)\, \rho_0^k(\tau) = \int d\tau\, \alpha(\tau)\, r^k(\tau)\cos^k(2\pi f_c \tau + \phi(\tau)) =$$

$$\cong \overline{\cos^k \theta} \int d\tau\, \alpha(\tau)\, r^k(\tau) = \begin{Bmatrix} 0 & \text{for } k \text{ odd} \\ \frac{1}{2^k}\binom{k}{k/2} \int d\tau\, \alpha(\tau)\, r^k(\tau) & \text{for } k \text{ even} \end{Bmatrix} . \tag{79}$$

Here, the k-th power of the cosine varies so quickly with τ that we replaced it by its average value and removed it from under the integral on τ. Substitution of (79) in (71) yields the system output signal-to-noise ratio

$$\gamma_{NB} = \frac{T\left[G_1(0) - G_0(0)\right]^2}{\sum\limits_{\substack{k=2 \\ \text{even}}}^{\infty} \frac{1}{k!} G_0^2(k) \frac{1}{2^k}\binom{k}{k/2} \int d\tau\, \alpha(\tau)\, r^k(\tau)} \tag{80}$$

for a narrowband input spectrum.

This form for γ_{NB} leads to an interesting conclusion regarding symmetric full-wave rectifiers versus half-wave rectifiers. Namely, reference to the defining relation (32) for nonlinearity coefficient $G(k)$ reveals that, for k even, a symmetric full-wave rectifier has a value of $G(k)$ exactly double that for the corresponding half-wave rectifier. However, since (80) only involves the even k values, whether a full-wave rectifier or half-wave rectifier, this factor of 2 cancels, and output signal-to-noise ratio γ_{NB} in (80) is exactly the <u>same</u> for a symmetric full-wave rectifier as for a half-wave rectifier. This conclusion holds for any rectifier $g\{x\}$, not just the ν-th law rectifiers in (3) and (4). It also holds for any filter $h(\tau)$ and normalized correlation envelope and phase $r(\tau)$ and $\phi(\tau)$ in (78), and is not limited to large averaging times or small input signal-to-noise ratio. The only restriction is the required high Q of the input spectrum.

This conclusion regarding identical γ_{NB} values for symmetric full-wave rectifiers and half-wave rectifiers is also physically reasonable for a high-Q input, in that no significantly different information is contained by the negative lobes of the waveform x(t) when its envelope and phase are slowly varying relative to the center frequency.

ν-TH LAW RECTIFIERS

Up to this point, all the relations involving nonlinearity coefficient G(k), defined in (32), have been general. We now specialize to the symmetric full-wave and half-wave ν-th law rectifiers mentioned in (3) and (4).

Full-Wave Rectifiers

The nonlinearity of interest here is

$$g\{x\} = |x|^{\nu} \quad \text{for all } x \qquad (\nu > 0) , \tag{81}$$

which is a symmetric full-wave rectifier. Substitution of (81) in (32) yields

$$G(k) = \sigma^{\nu} \int dw \; |w|^{\nu} \, \phi(w) \, He_k(w) \quad \text{for } k \geq 0 , \tag{82}$$

where $\phi(w)$ is defined in (21), and $He_k(w)$ is a Hermite polynomial [3, (22.2.15)]. Since $He_k(w)$ is odd in w for k odd, it immediately follows that

$$G(k) = 0 \quad \text{for } k \text{ odd} . \tag{83}$$

On the other hand,

$$G(k) = 2\sigma^{\nu} \int_0^{\infty} dw \; w^{\nu} \, \phi(w) \, He_k(w) \quad \text{for } k \text{ even } (0, 2, 4, \ldots) . \tag{84}$$

In order to evaluate this integral, we first define the quantity

$$L(k) = \int_0^\infty dw\ w^\upsilon\ \phi(w)\ He_k(w) \quad \text{for all } k \geq 0 \ . \tag{85}$$

It should be noted that L(k) is a function of υ, in addition to the explicitly indicated dependence on k; however, it is independent of σ. A recurrence for L(k) is derived in appendix A:

$$L(k) = (\upsilon+2-k)\ L(k-2) \quad \text{for all } k \geq 2 \ , \tag{86}$$

with starting values

$$L(0) = 2^{\frac{\upsilon}{2}-1}\ \pi^{-\frac{1}{2}}\ \Gamma\left(\frac{\upsilon+1}{2}\right) \ , \quad L(1) = 2^{\frac{\upsilon-1}{2}}\ \pi^{-\frac{1}{2}}\ \Gamma\left(\frac{\upsilon}{2}+1\right) \ . \tag{87}$$

Thus very high order values of L(k) can be quickly evaluated with the aid of just two gamma function computations.

The nonlinearity coefficient in (84) is therefore expressible as

$$G(k) = 2\sigma^\upsilon\ L(k) \quad \text{for } k = 0, 2, 4, \ldots \ , \tag{88}$$

or

$$G(k) = (\upsilon+2-k)\ G(k-2) \quad \text{for } k = 2, 4, 6, \ldots \ , \tag{89}$$

with starting value

$$G(0) = \sigma^\upsilon\ 2^{\frac{\upsilon}{2}}\ \pi^{-\frac{1}{2}}\ \Gamma\left(\frac{\upsilon+1}{2}\right) \ . \tag{90}$$

We now utilize the results in (88) and (83) to express the impulsive filter system output signal-to-noise ratio in (66) as

$$\gamma_{IF} = \frac{M\left(\sigma_1^{\nu}/\sigma_0^{\nu} - 1\right)^2}{\sum\limits_{\substack{k=2\\ \text{even}}}^{\infty} U(k) \sum\limits_{n} \beta(n)\, \rho_0^k(n\Delta)} , \tag{91}$$

where subscripts IF denote the impulsive filter full-wave rectifier case and where we have also defined sequence

$$U(k) = \frac{1}{k!} \frac{L^2(k)}{L^2(0)} \quad \text{for all } k \geq 0 . \tag{92}$$

This latter sequence has a simple recurrence, as seen by reference to (86), namely

$$U(k) = U(k-2) \frac{(\nu+2-k)^2}{k(k-1)} \quad \text{for all } k \geq 2 , \tag{93}$$

with starting values, from (87),

$$U(0) = 1 , \quad U(1) = 2 \frac{\Gamma^2\left(\frac{\nu}{2} + 1\right)}{\Gamma^2\left(\frac{\nu+1}{2}\right)} . \tag{94}$$

In fact, since (91) only involves even k, γ_{IF} can actually be evaluated without the aid of any gamma functions.

An exactly analogous procedure applied to nonimpulsive result (71) leads to output signal-to-noise ratio

$$\gamma_{NF} = \frac{T\left(\sigma_1^{\upsilon}/\sigma_0^{\upsilon} - 1\right)^2}{\sum\limits_{\substack{k=2\\ \text{even}}}^{\infty} U(k) \int d\tau\, \alpha(\tau)\, \rho_0^k(\tau)}\,, \tag{95}$$

where subscripts NF denote a nonimpulsive filter and a symmetric full-wave rectifier.

Full-Wave Square-Law Rectifier

Here we specialize the above results to the case of $\upsilon = 2$, that is, $g\{x\} = x^2$ for all x. There follows, upon use of (93) and (94), the significantly simpler results

$$\gamma_{IF}(\upsilon = 2) = \frac{M\left(\sigma_1^2/\sigma_0^2 - 1\right)^2}{2 \sum\limits_{n} \beta(n)\, \rho_0^2(n\Delta)} \tag{96}$$

from (91), and

$$\gamma_{NF}(\upsilon = 2) = \frac{T\left(\sigma_1^2/\sigma_0^2 - 1\right)^2}{2 \int d\tau\, \alpha(\tau)\, \rho_0^2(\tau)} \tag{97}$$

from (95). This fortuitous situation occurs because the recurrence (93) generates zero coefficients for $k \geq 4$, when $\upsilon = 2$. More generally, υ even would also terminate the recurrence at $k = \upsilon + 2$.

Full-Wave Linear Rectifier

This special case corresponds to $\nu = 1$, that is, $g\{x\} = |x|$ for all x.

Then

$$\gamma_{IF}(\nu = 1) = \frac{M\left(\sigma_1/\sigma_0 - 1\right)^2}{\sum\limits_{\substack{k=2\\ \text{even}}}^{\infty} U(k) \sum\limits_{n} \beta(n)\ \rho_0^k(n\Delta)} \tag{98}$$

from (91), where $\{U(k)\}$ is given by (93) with $\nu = 1$. Also, from (95),

$$\gamma_{NF}(\nu = 1) = \frac{T\left(\sigma_1/\sigma_0 - 1\right)^2}{\sum\limits_{\substack{k=2\\ \text{even}}}^{\infty} U(k) \int d\tau\ \alpha(\tau)\ \rho_0^k(\tau)} . \tag{99}$$

Half-Wave Rectifiers

We now return to general values of power law ν, but to half-wave rectifiers characterized by

$$g\{x\} = \begin{Bmatrix} x^\nu & \text{for } x > 0 \\ 0 & \text{for } x < 0 \end{Bmatrix} . \tag{100}$$

Substitution of (100) in (32) yields nonlinearity coefficient

$$G(k) = \sigma^\nu\ L(k) \quad \text{for all } k \geq 0 , \tag{101}$$

where L(k) was defined in (85). When (101) is utilized in (66), the result for the output signal-to-noise ratio is

$$\gamma_{IH} = \frac{M\left(\sigma_1^{\upsilon}/\sigma_0^{\upsilon} - 1\right)^2}{\sum\limits_{k=1}^{\infty} U(k) \sum\limits_{n} \beta(n)\ \rho_0^k(n\Delta)}\ , \tag{102}$$

where IH denotes impulsive filters and half-wave rectifiers. This result is identical to γ_{IF} in (91), except for the inclusion of all the odd k values here. Similarly, (71) leads to

$$\gamma_{NH} = \frac{T\left(\sigma_1^{\upsilon}/\sigma_0^{\upsilon} - 1\right)^2}{\sum\limits_{k=1}^{\infty} U(k) \int d\tau\ \alpha(\tau)\ \rho_0^k(\tau)} \tag{103}$$

for nonimpulsive filters and half-wave rectifiers, NH. This is identical to γ_{NF} in (95) except for the inclusion of all the odd k values here, in the case of half-wave rectification.

Half-Wave Square-Law Rectifier

When we set $\upsilon = 2$ in the results above, and refer to (93), we find that

$$\gamma_{IH}(\upsilon = 2) = \frac{M\left(\sigma_1^2/\sigma_0^2 - 1\right)^2}{2\sum\limits_{n} \beta(n)\ \rho_0^2(n\Delta) + \sum\limits_{\substack{k=1\\ \text{odd}}}^{\infty} U(k) \sum\limits_{n} \beta(n)\ \rho_0^k(n\Delta)}\ , \tag{104}$$

while

$$\gamma_{NH}(\upsilon = 2) = \frac{T\left(\sigma_1^2/\sigma_0^2 - 1\right)^2}{2\int d\tau\ \alpha(\tau)\ \rho_0^2(\tau) + \sum\limits_{\substack{k=1\\ \text{odd}}}^{\infty} U(k) \int d\tau\ \alpha(\tau)\ \rho_0^k(\tau)} . \tag{105}$$

Neither of the series in odd k terminate, since the numerator in recurrence (93) is $(4-k)^2$, which is always nonzero for k odd.

Half-Wave Linear Rectifier

Upon setting $\upsilon = 1$ in (93) and (94), we obtain

$$U(0) = 1\ ,\ U(1) = \frac{\pi}{2}\ ,\ U(k) = U(k-2)\ \frac{(3-k)^2}{k(k-1)} \quad \text{for } k = 2, 4, 6, \ldots , \tag{106}$$

with all other U(k) zero. Then (102) and (103) yield

$$\gamma_{IH}(\upsilon = 1) = \frac{M\left(\sigma_1/\sigma_0 - 1\right)^2}{\frac{\pi}{2} \sum\limits_{n} \beta(n)\ \rho_0(n\Delta) + \sum\limits_{\substack{k=2\\ \text{even}}}^{\infty} U(k) \sum\limits_{n} \beta(n)\ \rho_0^k(n\Delta)} \tag{107}$$

and

$$\gamma_{NH}(\upsilon = 1) = \frac{T\left(\sigma_1/\sigma_0 - 1\right)^2}{\frac{\pi}{2}\int d\tau\ \alpha(\tau)\ \rho_0(\tau) + \sum\limits_{\substack{k=2\\ \text{even}}}^{\infty} U(k) \int d\tau\ \alpha(\tau)\ \rho_0^k(\tau)} , \tag{108}$$

respectively.

The programs to be furnished later are not limited to the special cases in (96)-(99) and (104)-(108), but, in fact, cover arbitrary values of υ.

Equality of Performance for $\upsilon = 1$

It is interesting to observe that these last two results for the linear half-wave rectifier are identical to the corresponding earlier results for the symmetric linear full-wave rectifier in (98) and (99), except for the additional term for k = 1 here. Thus, for nonimpulsive filters,

$$\text{if} \quad \int d\tau \, \alpha(\tau) \, \rho_0(\tau) = 0 \tag{109}$$

in (108), then the output signal-to-noise ratios of the linear symmetric full-wave rectifier and linear half-wave rectifier are the same. But since, from appendix B,

$$\int d\tau \, \alpha(\tau) \, \rho_0(\tau) = \frac{\int df \, |H(f)|^2 \, P_0^{(1)}(f)}{\int df \, |H(f)|^2} , \tag{110}$$

the only way (109) can be true is if the filter power transfer function $|H(f)|^2$ and the input spectrum under H_0, namely $P_0^{(1)}(f)$, do not overlap; see figure 6 for the flat bandpass input spectrum example. Then approximately, if

$$\frac{4}{T} < f_\ell = f_c - \frac{W}{2} , \quad \text{i.e.,} \; Q - \frac{1}{2} > \frac{4}{TW} , \tag{111}$$

then (109) is substantially satisfied and the linear half-wave rectifier and the symmetric linear full-wave rectifier have similar output signal-to-noise

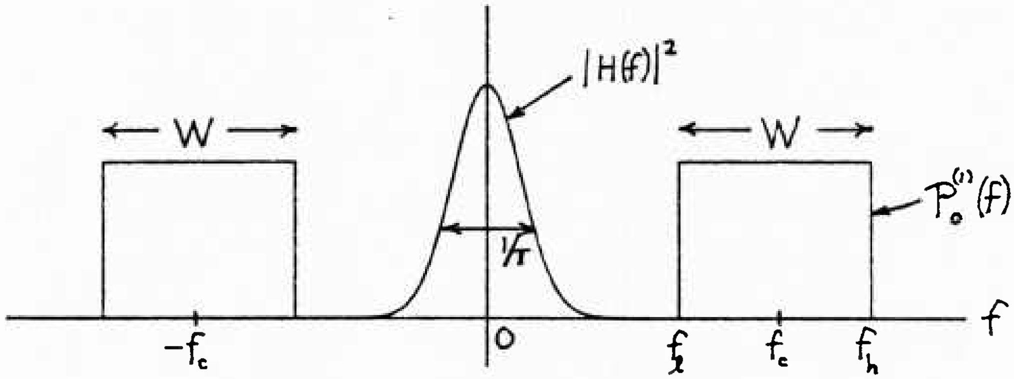

Figure 6. Spectral Quantities for (110) and (112)

ratios. This lower bound on Q in (111), relative to the inverse time-bandwidth product, will be encountered again later, when we investigate general ν-th law rectifiers for general bandpass spectra, as delineating a distinct dichotomy in performance for half-wave rectifiers.

It will be recalled, in an earlier section dealing with narrowband input spectra, (78)-(80), that the output signal-to-noise ratios of a ν-th law half-wave rectifier and a symmetric full-wave rectifier were identical for all ν, if the Q of the input spectrum was very large. The result here, particularly (111), is a much milder requirement that achieves the same result, but only for the linear device, $\nu = 1$. The reason that a much more moderate requirement on Q will suffice for $\nu = 1$ is that all the odd terms for $k > 1$ are already absent from (107) and (108), whereas they were suppressed in

(79) only by the use of the very large Q assumption. So, for a linear rectifier, virtual equality of performance for a half-wave rectifier and a symmetric full-wave rectifier can be expected for a very moderate value of Q. Larger values of ν would require larger Q values for the same result to obtain. These observations will be borne out by numerical results to follow later.

For the impulsive filter result of (107), the analogous result to (110) is also derived in appendix B, giving

$$\Delta \sum_n \beta(n)\ \rho_0(n\Delta) = \frac{\int df\ |H(f)|^2\ P_0^{(1)}(f)}{\int_{1/\Delta} df\ |H(f)|^2}\ , \tag{112}$$

where the filter voltage transfer function is now

$$H(f) = \sum_n w(n)\ \exp(-i2\pi f\Delta n) \tag{113}$$

from (5) and (8). The integral in the denominator of (112) is over any frequency interval of length $1/\Delta$, which is the period in f of the filter voltage transfer function H(f). The numerator integral in (112) is over all f, but could be limited, if desired, to the fundamental frequency interval $(-1/2\Delta,\ 1/2\Delta)$ if normalized input spectrum $P_0^{(1)}(f)$ is replaced by its aliased version

$$\tilde{P}_0^{(1)}(f) = \sum_n P_0^{(1)}\left(f - \frac{n}{\Delta}\right) \quad \text{for all f}\ , \tag{114}$$

where the sum is over all n from $-\infty$ to $+\infty$.

In any event, (112) will be zero if the filter power transfer function $\left|H(f)\right|^2$ and input spectrum $P_0^{(1)}(f)$ do not overlap. Figure 6 is again applicable, but now with the addition of major lobes of $\left|H(f)\right|^2$ at $f = n/\Delta$ for all n. Not only must (111) be met in order to avoid overlap near f = 0, but the other major lobes of $\left|H(f)\right|^2$ must not overlap $P_0^{(1)}(f)$. This requirement can be met, for example, by keeping the lower skirt, of the lobe of $\left|H(f)\right|^2$ centered at $f = 1/\Delta$, above the highest frequency of the input spectrum:

$$\frac{1}{\Delta} - \frac{4}{T} > f_h = f_c + \frac{W}{2} = W\left(Q + \frac{1}{2}\right) ; \tag{115}$$

that is, sampling frequency $f_s = 1/\Delta$ must satisfy

$$\frac{f_s}{W} > \frac{4}{TW} + Q + \frac{1}{2} . \tag{116}$$

This requirement is in addition to that of (111).

Actually, (116) is a sufficient condition for non-overlap in figure 6, but is not always necessary. In particular, for larger Q, the possibility exists of deliberately undersampling (violating (115)) and yet achieving nonoverlap of the aliased spectral components of (114) with the filter lobe at f = 0. This will be demonstrated by example in the results section, not only for $\upsilon = 1$, but for other υ values as well. Here we have resorted to the equality

$$\int df \ \left|H(f)\right|^2 P_0^{(1)}(f) = \int_{1/\Delta} df \ \left|H(f)\right|^2 \tilde{P}_0^{(1)}(f) , \tag{117}$$

based upon the use of aliased spectrum (114) and the periodic character of filter H(f).

INDEPENDENT SAMPLES

This section will address the discrete detection system of figure 2, where sampling increment Δ in (8) is taken such that the samples of Gaussian process x(t) are statistically independent. This can be accomplished by taking Δ large, in general. However, at least in the special case of a flat low-pass spectrum under H_0, as in figure 3 with

$$f_c = \frac{W}{2}\ ,\ Q = \frac{1}{2}\ ,\ P_0^{(1)}(f) = \frac{1}{2W} \quad \text{for } |f| < W\ , \tag{118}$$

then the choice $\Delta = (2W)^{-1}$ in corresponding normalized correlation (15) gives

$$\rho_0(n\Delta) = \mathrm{sinc}(n) = \begin{Bmatrix} 1 & \text{for } n = 0 \\ 0 & \text{otherwise} \end{Bmatrix}, \tag{119}$$

which also means independent samples. (Another special case is afforded in the flat bandpass spectrum case, by choosing $\Delta = W^{-1}$, irrespective of center frequency f_c; see (13) and refer to (119).)

For this section only, dealing exclusively with independent samples, we will not yet specialize to the case of ν-th law rectifiers, but temporarily allow general nonlinearities. Then general result (66) for the system output signal-to-noise ratio reduces to

$$\gamma_I = \frac{M\left[G_1(0) - G_0(0)\right]^2}{\sum_{k=1}^{\infty} \frac{1}{k!}\, G_0^2(k)} \quad \text{for independent samples,} \tag{120}$$

by use of (119). We observe immediately that the only way the filter weights $\{w(n)\}$ enter this result is via effective number M defined in (67), whether large or small; normalized autocorrelation sequence $\{\beta(n)\}$ in (68) is not relevant in this special case.

Numerical evaluation of the particular infinite series in the denominator of (120) can be circumvented, as follows; from (34) and (28),

$$R_{\tilde{y}}(0) = \sum_{k=1}^{\infty} \frac{1}{k!} G^2(k) = \sigma_y^2 . \tag{121}$$

Then, also using (33), (120) becomes

$$\gamma_I = \frac{M\left(m_{y1} - m_{y0}\right)^2}{\sigma_{y0}^2} \quad \text{for independent samples} . \tag{122}$$

But these latter quantities can be obtained directly from the moments of the nonlinearity output,

$$\begin{aligned} m_y &= \overline{y(t)} = \overline{g\{x(t)\}} = \int dx\; g\{x\}\; p^{(1)}(x) , \\ \overline{y^2(t)} &= \overline{g^2\{x(t)\}} = \int dx\; g^2\{x\}\; p^{(1)}(x) , \end{aligned} \tag{123}$$

by numerical integration if necessary, once the nonlinearity $g\{x\}$ and first-order input probability density function $p^{(1)}(x)$ are specified.

Symmetric Full-Wave Rectifier

We now specialize to symmetric υ-th law full-wave rectifiers as in (4) and a Gaussian input as in (20). (123) immediately yields moments

$$m_y = \sigma^{\upsilon}\, 2^{\upsilon/2}\, \pi^{-1/2}\, \Gamma\left(\frac{\upsilon+1}{2}\right) ,$$

$$\overline{y^2(t)} = \sigma^{2\upsilon}\, 2^{\upsilon}\, \pi^{-1/2}\, \Gamma\left(\upsilon + \frac{1}{2}\right) . \qquad (124)$$

Appropriate substitution into (122) gives output signal-to-noise ratio

$$\gamma_{IF} = \frac{M\left(\sigma_1^{\upsilon}/\sigma_0^{\upsilon} - 1\right)^2}{D(\upsilon) - 1} \quad \text{for independent samples ,} \qquad (125)$$

where we define quantity

$$D(\upsilon) = \frac{\pi^{1/2}\, \Gamma\left(\upsilon + \frac{1}{2}\right)}{\Gamma^2\left(\frac{\upsilon+1}{2}\right)} . \qquad (126)$$

Equation (125) is a compact expression for the system output signal-to-noise ratio for any $\upsilon > 0$, requiring no summations.

Special cases of (126) are

$$D(1) = \frac{\pi}{2} \;,\; D(2) = 3 \;,\; D(3) = \frac{15\pi}{8} \;,\; D(4) = \frac{35}{3} . \qquad (127)$$

Thus, for example, (125) yields

$$\gamma_{IF}(\upsilon = 2) = \frac{M}{2}\left(\frac{\sigma_1^2}{\sigma_0^2} - 1\right)^2 , \qquad (128)$$

in agreement with (96) in this case of independent samples.

More generally, since from (91) and (119), we have output signal-to-noise ratio

$$\gamma_{IF} = \frac{M\left(\sigma_1^\upsilon/\sigma_0^\upsilon - 1\right)^2}{\sum\limits_{\substack{k=2\\ \text{even}}}^{\infty} U(k)} \quad \text{for independent samples}\ , \tag{129}$$

then comparison with (125) yields the following identity on the $\{U(k)\}$ sequence in (92)-(94):

$$\sum_{\substack{k=0\\ \text{even}}}^{\infty} U(k) = D(\upsilon) = \frac{\pi^{1/2}\,\Gamma\left(\upsilon + \frac{1}{2}\right)}{\Gamma^2\left(\frac{\upsilon+1}{2}\right)} . \tag{130}$$

This result has been confirmed directly, by letting $m = k/2$, converting the recursion on $\{U(k)\}$ to one on $\{U(2m)\}$, recognizing it as a hypergeometric function, and using [3, (15.1.20)]. This identity will prove to be very useful in the accurate numerical evaluation of general result (91) for symmetric full-wave rectifiers with statistically dependent samples.

We now consider the case where hypothesis H_0 corresponds to noise-only and H_1 to signal plus noise, that is,

$$\sigma^2 = \begin{Bmatrix} \sigma_1^2 = S + N \text{ under } H_1 \\ \sigma_0^2 = \quad\; N \text{ under } H_0 \end{Bmatrix} , \tag{131}$$

where N and S are the independent input noise and signal powers, respectively. When utilized in (125), we have output signal-to-noise ratio

$$\gamma_{IF} = \frac{M}{D(\upsilon) - 1} \left[\left(1 + \frac{S}{N}\right)^{\upsilon/2} - 1\right]^2 , \tag{132}$$

which is valid for independent samples and all values of M, υ, and S/N.

The basis of comparison (in this section alone, for independent samples) will be the full-wave square-law detector, which simply corresponds to taking $\upsilon = 2$ in (132):

$$\gamma_b = \frac{M}{2} \left(\frac{S}{N}\right)^2 . \tag{133}$$

In keeping with the discussion surrounding (59), we now equate these last two expressions above:

$$\frac{M}{D(\upsilon) - 1} \left[\left(1 + \frac{S}{N}\right)^{\upsilon/2} - 1\right]^2 = \frac{M}{2} \left(\frac{S}{N}\right)_s^2 , \tag{134}$$

where $(S/N)_s$ is the input signal-to-noise ratio to the square-law system, and S/N is that for the general υ-th law symmetric full-wave rectifier. The solution of (134) is

$$\frac{S}{N} = \left[\left(\frac{D(\upsilon) - 1}{2}\right)^{1/2} \left(\frac{S}{N}\right)_s + 1\right]^{2/\upsilon} - 1 \quad \text{for all } \upsilon, \left(\frac{S}{N}\right)_s . \tag{135}$$

This is the input signal-to-noise ratio required for the ν-th law system to achieve the same output signal-to-noise ratio as for the full-wave square-law system, for the independent samples case. It is independent of M, the effective number of samples.

Although generally a function of the actual square-law input signal-to-noise ratio $(S/N)_s$, in the case of low input signal-to-noise ratio, (135) becomes approximately

$$\frac{S}{N} \cong \frac{1}{\nu}\left(2D(\nu) - 2\right)^{1/2}\left(\frac{S}{N}\right)_s \quad \text{for} \left(\frac{S}{N}\right)_s \ll 1 . \tag{136}$$

This leads to the factor

$$F_F(\nu) = \frac{1}{\nu}\left(2D(\nu) - 2\right)^{1/2} \tag{137}$$

by which the input signal-to-noise ratio must be increased for the ν-th law device relative to the full-wave square-law system, and which is independent of the actual input signal-to-noise ratio $(S/N)_s$. Subscript F denotes symmetric full-wave rectifiers.

The factor $F_F(\nu)$ is tabulated in decibels in table 1 and plotted versus ν in figure 7. They both reveal that, for low input signal-to-noise ratio,

ν	.5	1	1.5	2	2.5	3	3.5	4
$10 \log F_F(\nu)$	.796	.288	.062	0	.049	.181	.376	.625

Table 1. Additional Input Signal-to-Noise Ratio Relative to Full-Wave Square-Law System; Low Input Signal-to-Noise Ratio, Symmetric Full-Wave Rectifiers, Selected ν, Independent Samples

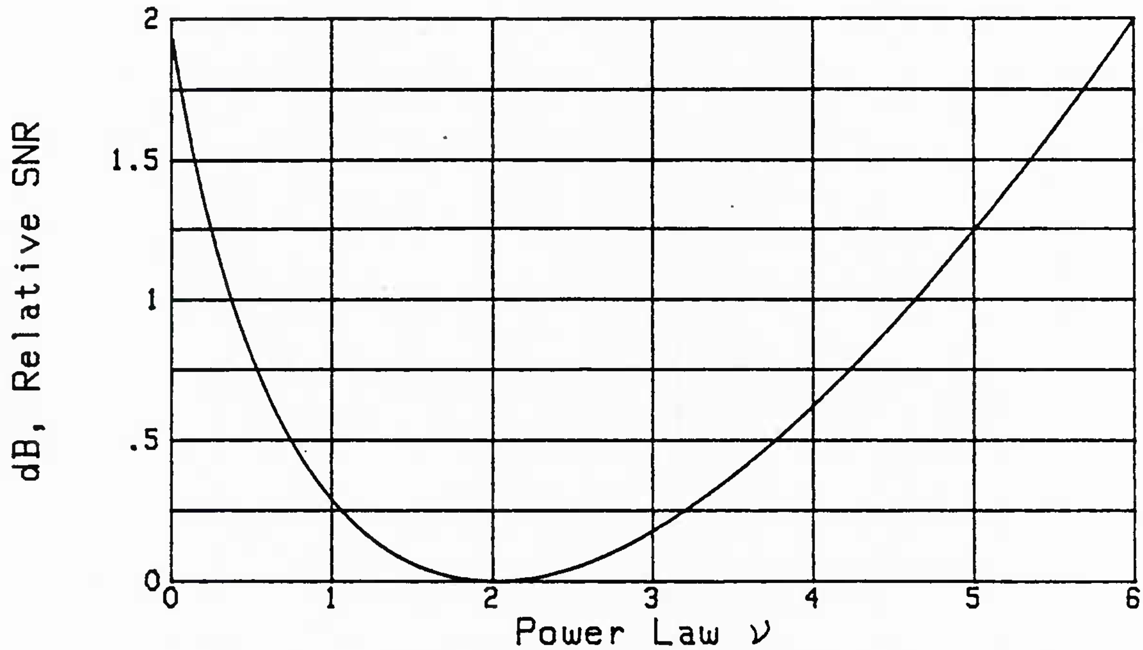

Figure 7. Additional Input Signal-to-Noise Ratio Relative to Square-Law System; Symmetric FWRs, Low Input Signal-to-Noise Ratio

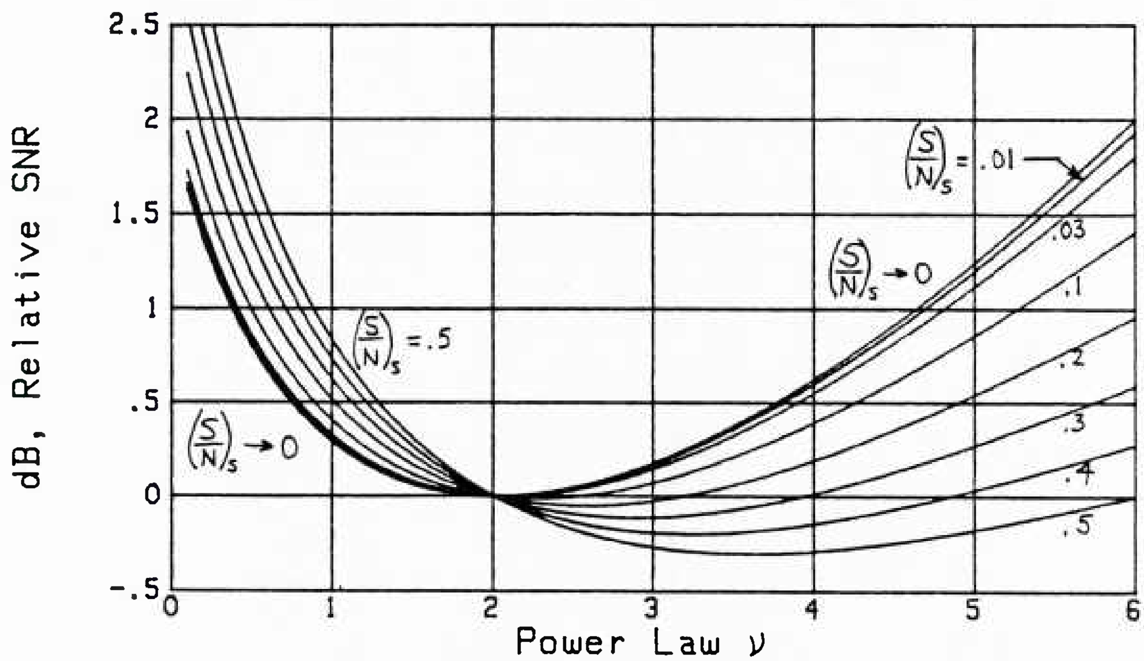

Figure 8. Additional Input Signal-to-Noise Ratio Relative to Square-Law System; Symmetric Full-Wave Rectifiers

the full-wave square-law detector is best. The linear full-wave rectifier (FWR), for example, requires .29 dB more input signal-to-noise ratio than the square-law full-wave rectifier, in order to achieve the same output signal-to-noise ratio (SNR).

More generally, exact result (135) is plotted in figure 8, for various values of the full-wave square-law input signal-to-noise ratio $(S/N)_s$. The curve labelled $(S/N)_s \to 0$ is exactly that already plotted in figure 7. The other results for larger $(S/N)_s$ seem to indicate that better performance can be achieved by choosing υ larger than 2, for example, $\upsilon = 3.5$ for $(S/N)_s = 0.5$. However, this conclusion is completely spurious, because the square-law detector is, in fact, the <u>optimum</u> device to use in this particular case of independent samples of the input; furthermore, the input samples should all be equi-weighted. These conclusions are based on the likelihood ratio derivation in appendix C. This situation serves to accentuate the earlier caution that the output signal-to-noise ratio of a system with nonlinearities is not a complete descriptor of performance, and care must be exercised in the use and interpretation of the system output signal-to-noise ratio; see (41) et seq. The results in figure 8 for the higher signal-to-noise ratios cannot be used.

Half-Wave Rectifier

We now return to general results (122) and (123), and consider half-wave rectifiers as described in (3) and a Gaussian input as in (20). Substitution in (123) yields moments which are half of the values listed in (124). When employed in (122), there follows for the output signal-to-noise ratio,

$$\gamma_{IH} = \frac{M\left(\sigma_1^{\nu}/\sigma_0^{\nu} - 1\right)^2}{2D(\nu) - 1} \quad \text{for independent samples} , \tag{138}$$

where $D(\nu)$ was defined in (126). For example,

$$\gamma_{IH}(\nu = 2) = \frac{M}{5}\left(\frac{\sigma_1^2}{\sigma_0^2} - 1\right)^2 \tag{139}$$

for the square-law half-wave rectifier; compare this result with (128) for the full-wave rectifier.

Generally, from (102) and (119), we have

$$\gamma_{IH} = \frac{M\left(\sigma_1^{\nu}/\sigma_0^{\nu} - 1\right)^2}{\sum_{k=1}^{\infty} U(k)} \quad \text{for independent samples} . \tag{140}$$

Comparison with (138) yields the identity

$$\sum_{k=0}^{\infty} U(k) = 2D(\nu) . \tag{141}$$

Coupled with (130), this yields

$$\sum_{\substack{k=1 \\ \text{odd}}}^{\infty} U(k) = D(\nu) = \frac{\pi^{1/2}\,\Gamma\left(\nu + \frac{1}{2}\right)}{\Gamma^2\left(\frac{\nu+1}{2}\right)} . \tag{142}$$

Thus, both the even and odd sums on U_k give exactly the same value, $D(\nu)$. The result in (142) has been confirmed directly by letting $m = (k-1)/2$, converting the recursion on $\{U(k)\}$ to one on $\{U(2m+1)\}$, recognizing it as a hypergeometric function, and using [3, (15.1.20)]. This identity will prove to be very useful in the accurate numerical evaluation of general result (102) for half-wave rectifiers with statistically dependent samples.

We now again consider the case where hypothesis H_0 corresponds to noise-only and H_1 to signal plus noise; see (131). Then (138) for the output signal-to-noise ratio becomes

$$\gamma_{IH} = \frac{M}{2D(\nu) - 1} \left[\left(1 + \frac{S}{N}\right)^{\nu/2} - 1\right]^2 , \tag{143}$$

which is valid for independent samples and all values of M, ν, and S/N.

For small input signal-to-noise ratio, this is approximately

$$\gamma_{IH} \cong \frac{M}{2D(\nu) - 1} \; \frac{\nu^2}{4} \left(\frac{S}{N}\right)^2 . \tag{144}$$

When this is compared with the basis in (133) for the full-wave square-law detector, we see that the input signal-to-noise ratio for the ν-th law half-wave detector must be increased by the factor

$$F_H(\nu) = \frac{1}{\nu} \left(4D(\nu) - 2\right)^{1/2} , \tag{145}$$

in order to maintain the same output signal-to-noise ratio. This factor is tabulated in table 2 and plotted in figure 9. The most striking feature of

ν	.5	1	1.5	2	2.5	2.633	3	3.5	4
$10 \log F_H(\nu)$	5.18	3.16	2.35	1.99	1.87	1.865	1.90	2.03	2.23

Table 2. Additional Input Signal-to-Noise Ratio Relative to Full-Wave Square-Law System; Low Input Signal-to-Noise Ratio, Half-Wave Rectifiers, Selected ν, Independent Samples

these results is the large degradation, relative to the full-wave square-law system, suffered by employing a half-wave rectifier for independent samples. For example, a linear half-wave rectifier requires an additional 3.16 dB input signal-to- noise ratio in order to realize the same output signal-to-noise ratio as a full-wave square-law detector, while the square-law half-wave rectifier requires 1.99 dB additional input signal-to-noise ratio. Amelioration of this degradation in the case of statistically dependent samples will be demonstrated later for bandpass spectra with various values of Q.

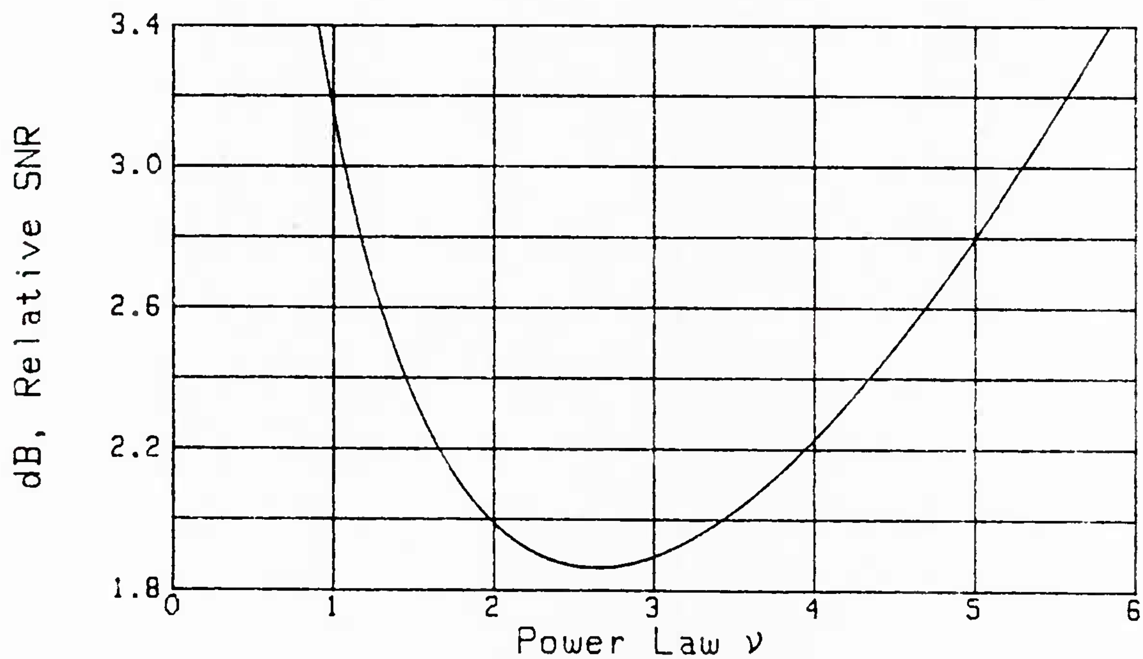

Figure 9. Additional Input Signal-to-Noise Ratio Relative to Square-Law System; Half-Wave Rectifiers, Low Input Signal-to-Noise Ratio

FLAT BANDPASS SPECTRUM AND BOX CAR FILTER

In this section, the input spectrum is taken to be flat in a bandwidth W about center frequency $\pm f_c$; see figure 3. The Q of the spectrum will be varied from its minimum of 1/2 to values large enough that the limiting performance achieved by a narrowband spectrum is virtually achieved.

The sampled version of the detection system, depicted in figure 2, will be considered, with the weights $\{w(n)\}$ in the accumulator set equal to the same value; this is the box car filter of (10). Sampling increment Δ is arbitrary, as is the power law ν of the half-wave and full-wave rectifiers to be considered. When Δ is taken very small, the system performance will approach that for a nonimpulsive filter; thus, there is no need to additionally evaluate the nonimpulsive results of (95) and (103). On the other hand, when Δ is taken large, the effects of undersampling will become apparent.

The basis of comparison for the ν-th law rectifiers considered here has been delineated in an earlier section, in particular, in the discussion surrounding (59) and (60). We confine the numerical results for the decibel difference in (60) to low input signal-to-noise ratio, and specialize the general results in (91) and (102) for symmetric full-wave and half-wave rectifiers, accordingly. The detailed computational procedure is presented in appendix D, for both the symmetric full-wave rectifier and the half-wave rectifier. Sampling increment Δ is related to integration time or observation time T according to

$$T = M\Delta \, , \tag{146}$$

where M is the number of samples employed in box car filter (10).

Full-Wave Rectifier; Variable Sampling Increment

In this subsection, the nonlinear detector is taken to be a ν-th law full-wave rectifier. The first result in figure 10 gives the additional signal-to-noise ratio in dB required by the full-wave rectifier relative to the standard of (57), for TW = 50, Q = 1/2, and M varied from 50 up to 500. Since Δ is given by (146) in terms of integration time T and number of samples M, there follows, for the sampling frequency $f_s = 1/\Delta$, the ratio

$$\frac{f_s}{W} = \frac{1}{W\Delta} = \frac{M}{TW} \, . \tag{147}$$

Thus, for example, M = 100 here corresponds to a ratio of sampling frequency f_s to bandwidth W of 100/50 = 2; since Q = 1/2, this value of M corresponds to sampling of an input process with a lowpass spectrum, at twice the highest frequency, meaning independent samples. These frequencies are indicated in the figure. The dB numbers entered at this value of M on figure 10 for $\nu = 1$, 2, 3, are in fact exactly those already listed earlier in table 1 for independent samples.

Increasing M to 200 leads to a sampling frequency 4 times $f_h (= W)$, and to dB values virtually equal to the saturation values entered at M = 500. Thus, it is possible to lower the required input signal-to-noise ratio by .133, .018, .077 dB for $\nu = 1$, 2, 3, respectively, by employing larger M values than lead to independent samples. The slightly negative dB values for

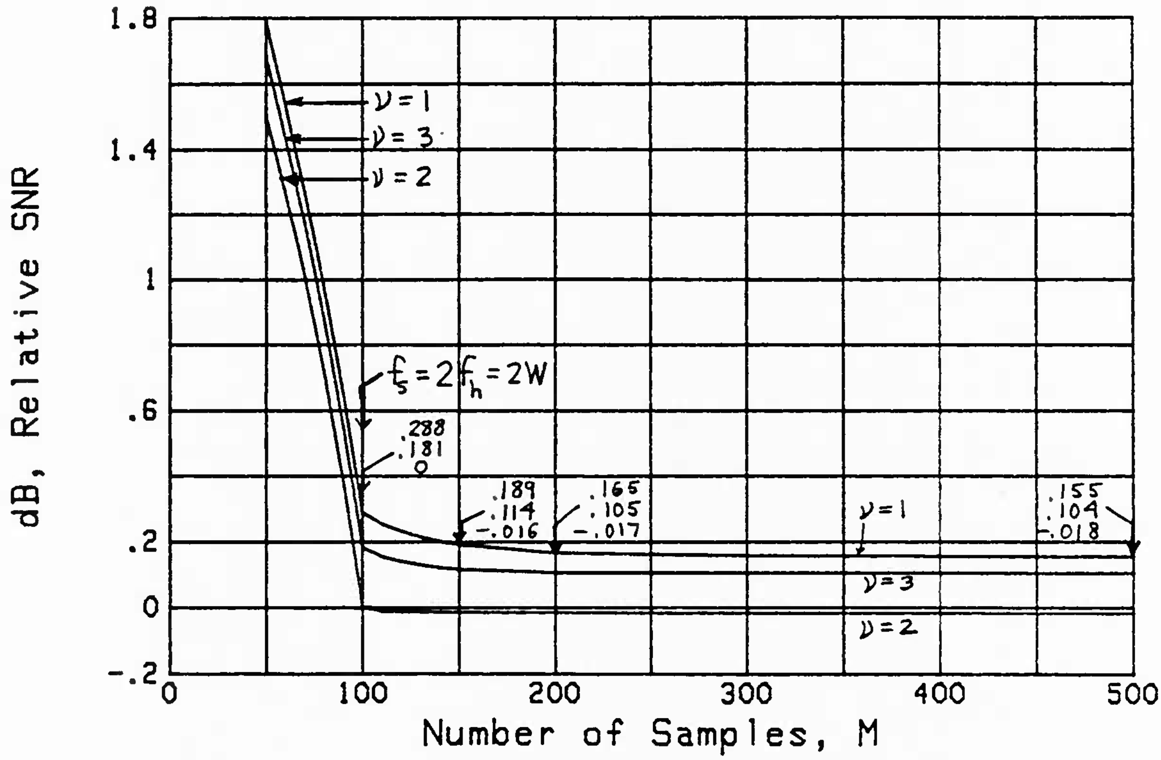

Figure 10. Flat Spectrum, Box Car Filter, Full-Wave Rectifier, TW = 50, Q = 1/2

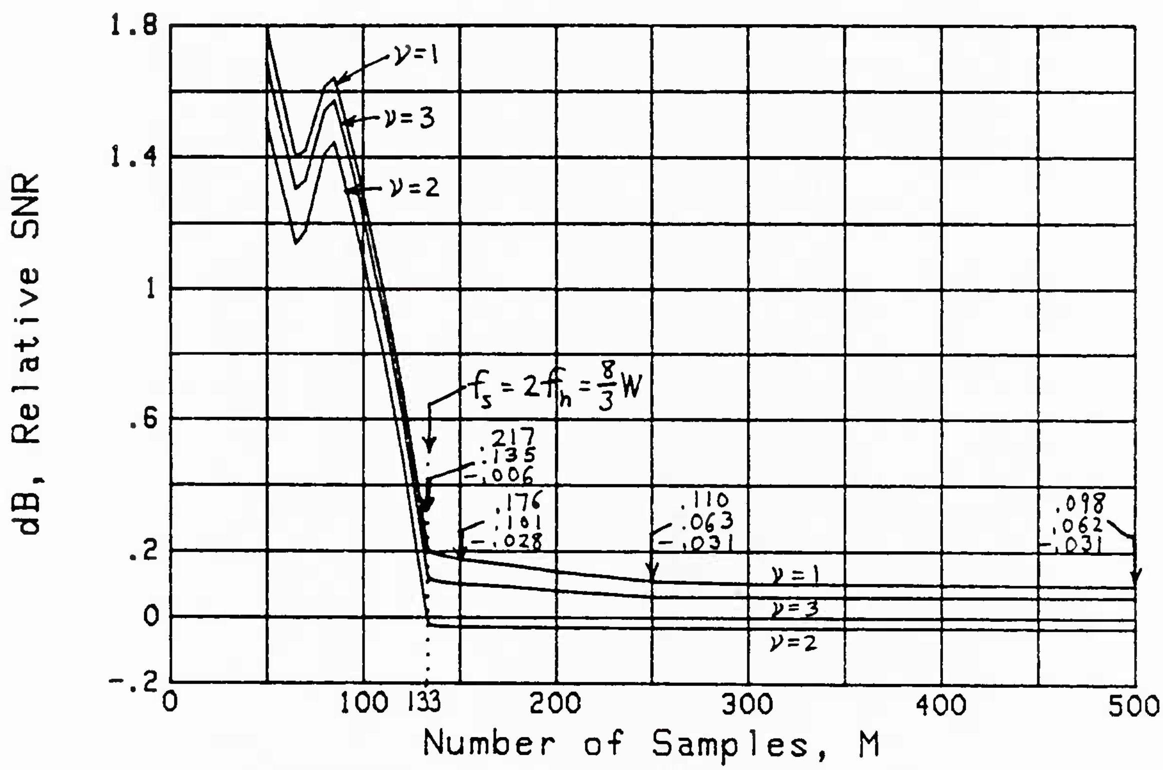

Figure 11. Flat Spectrum, Box Car Filter, Full-Wave Rectifier, TW = 50, Q = 5/6

large M, achieved by the full-wave rectifier with $\nu = 2$, are consistent with the discussion surrounding (58), and merely reflect the fact that the standard is not the absolute optimum output signal-to-noise ratio.

On the other hand, decreasing the sampling frequency below $2f_h$, that is, decreasing M below 100 for this example of TW = 50, leads to a significant degradation of performance, as witnessed by the rapid rise of the dB curves in figure 10, to the left of M = 100.

In figure 11, the only change is to increase Q to 5/6; this is a flat bandpass spectrum. Since, in general, using (12) and (146), the ratio

$$\frac{f_s}{f_h} = \frac{2}{\Delta W(1 + 2Q)} = \frac{M}{TW} \frac{1}{Q + \frac{1}{2}} , \tag{148}$$

then the value of M = 133 in figure 11 corresponds to $f_s = 2f_h = (8/3)W$. Again, this is seen to correspond to a prominent knee of the performance degradation curve. Increasing M to 250 realizes essentially the same input dB values as for M = 500; however, for $\nu = 2$, M need only be increased to 150 in order to essentially attain the large-M asymptote. It is worthwhile noting for future reference that the frequency ratios in (147) and (148) are directly proportional to M, the number of samples employed in the box car filter. The seemingly anomalous behavior of figure 11 near M = 75 is more pronounced in the next figure and will be explained there.

In figure 12, the only change is to increase Q to 2, while keeping TW = 50. Reference to (147) and (148) reveals that M = 250 now corresponds to

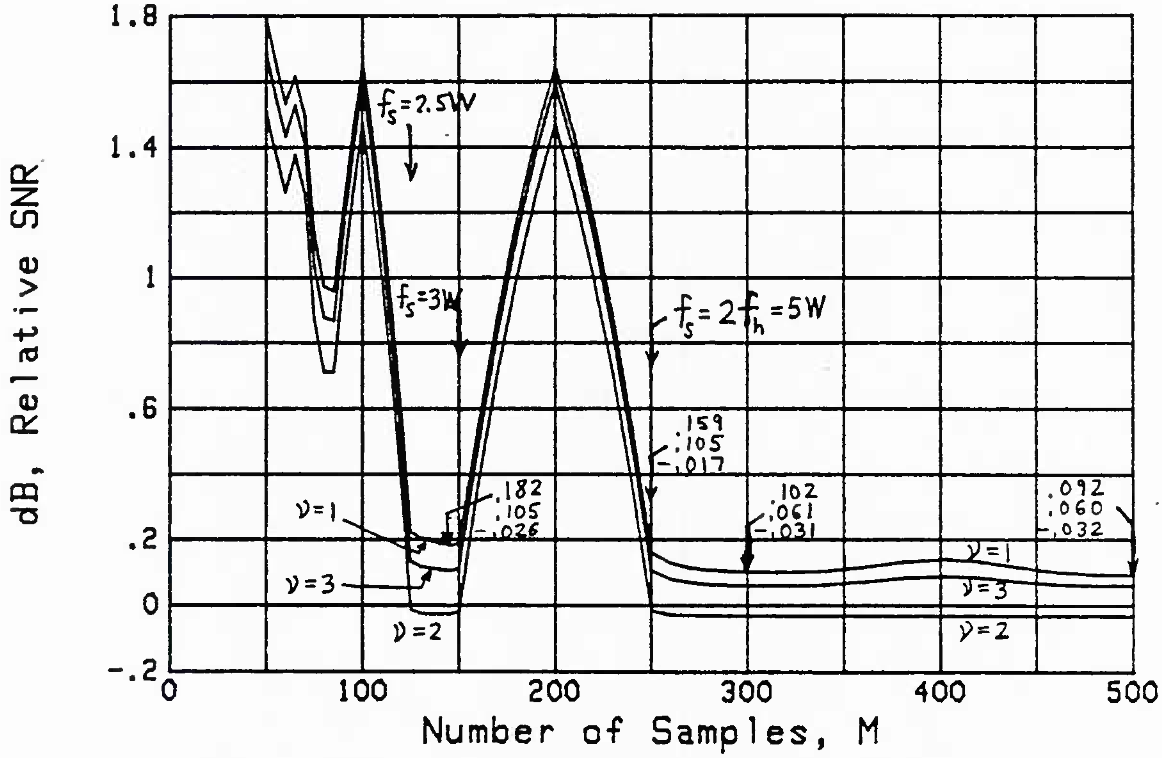

Figure 12. Flat Spectrum, Box Car Filter, Full-Wave Rectifier, TW = 50, Q = 2

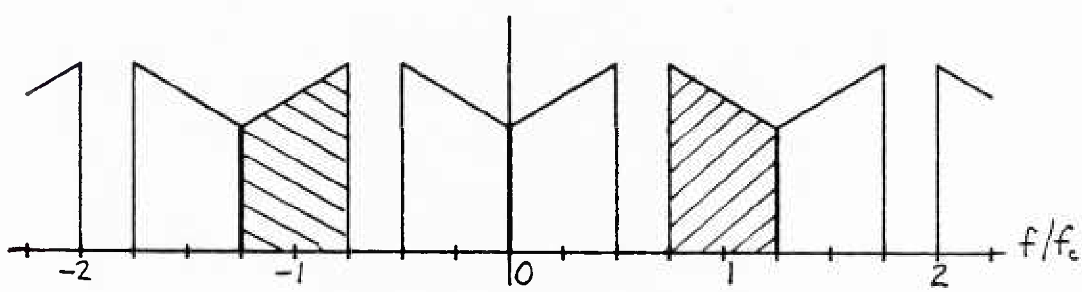

Figure 13. $\tilde{P}^{(1)}(f)$ for $f_s = f_h = 2.5W$; Q=2, M=125

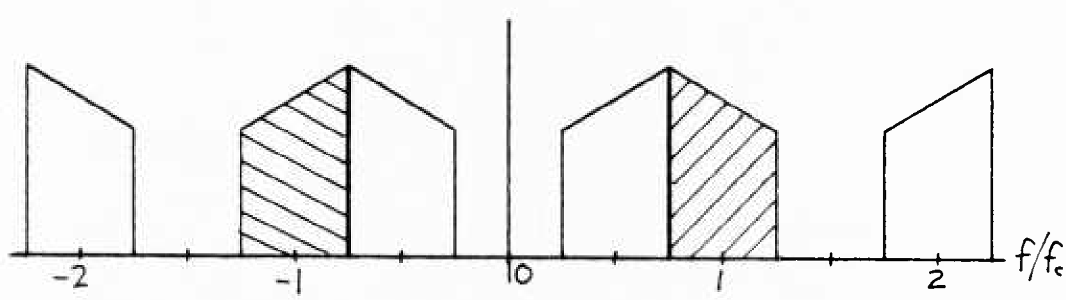

Figure 14. $\tilde{P}^{(1)}(f)$ for $f_s = 1.2f_h = 3W$; Q=2, M=150

$f_s = 2f_h = 5W$; there is a slight improvement by increasing M to 300. However, the most striking feature of this figure is the return of the required input signal-to-noise ratio dB values to very low levels for M in the range (125,150). To explain this behavior, we first note from (147) and (148) that $f_s = f_h = 2.5W$ at $M = 125$, while $f_s = 1.2f_h = 3W$ at $M = 150$; thus, the sampling rate is still larger than twice the bandwidth W of the input process (and remains so until M decreases to 100). However, since f_s is smaller than $2f_h$, we have an example of undersampling, without significant loss in performance.

The mathematical explanation of what is happening requires a close examination of the denominator of the system output signal-to-noise ratio, γ_{IF}, in (91). In appendix E, some useful frequency domain representations of the denominator of (91) are derived. In particular, a combination of (E-8) and (E-12) yields the approximate result

$$\sum_n \beta(n)\, \rho^2(n\Delta) \cong \frac{1}{\Delta} \int_{1/\Delta} df \left[\tilde{P}^{(1)}(f)\right]^2 , \tag{149}$$

where

$$\tilde{P}^{(k)}(f) \equiv \sum_n P^{(k)}\left(f - \frac{n}{\Delta}\right) \quad \text{for all } f \tag{150}$$

is the aliased (periodic) version of $P^{(k)}(f)$, which, in turn, is the Fourier transform of $\rho^k(\tau)$; see (47). The approximation (149) is valid when the TW product is large; see (E-8) for details.

The leading term in the denominator of signal-to-noise ratio γ_{IF} in (91) is equal to U(2) times the result (149). The latter quantity is the average value under the square of the aliased input spectrum. In order to realize large values of γ_{IF}, then (149) should be small. Plots* of $\tilde{P}^{(1)}(f)$ in figures 13 and 14 for Q = 2, with M = 125 and M = 150, respectively, reveal that none of the aliased lobes overlap, despite the undersampling; the cross-hatched lobes represent the input (unaliased) spectrum. Thus, the integral of (149) remains constant (and small) for M in the range (125,150).

However, if M is decreased below 125, the aliasing lobes in figure 13 bordering f = 0, for example, begin to overlap, thereby doubling the value of $\tilde{P}^{(1)}(f)$ in this region. Similarly, if M is increased above 150, the lobes in figure 14 bordering $f/f_c = \pm.75$ begin to overlap. In both these cases, the value of (149) would increase significantly, thereby decreasing the system output signal-to-noise ratio γ_{IF} in (91), or alternatively increasing the required input signal-to-noise ratio. In order to avoid this degradation, overlapped aliasing lobes must be avoided, either by looking for "clean" regions for high Q, as in figures 13 and 14, or by sampling at rates greater than twice the highest frequency of the input spectrum.

---

*A slight tilt has been added to the spectral shape in order to more easily identify which lobes result from positive and negative frequency components.

The results in figure 12, as well as all the other figures, have not been limited to considering just the k = 2 term in the denominator of the system output signal-to-noise ratio γ, nor have they utilized the approximations (149) or (E-8). Instead, they have been obtained by utilizing K = 1000 terms in the series, and by actually conducting the exact summations in the denominators of (91) and (102). The discussion above, relative to figures 13 and 14, was presented in order to give a simple physical explanation of what is happening, and thereby furnish guidance to further cases of interest.

In figure 15, Q is further increased to 3, again keeping TW at 50. Reference to (147) and (148) indicates that M = 350 corresponds to $f_s = 2f_h = 7W$; slightly improved performance can be achieved by increasing M to 400. Substantially the same performance level can be achieved, however, for M in the range (175,250), corresponding, respectively, to undersampling with f_s in the range 3.5W to 5W. Furthermore, there is an additional possibility for M in the range (117,125), with sampling frequencies in the range f_s = (2.34W, 2.5W); it may be verified by use of (147) and (148) that the aliasing lobes of $\widetilde{P}^{(1)}(f)$ do not overlap for this range of sampling frequencies (as shown in figures 13 and 14). However, only the $\upsilon = 2$ full-wave rectifier achieves the level attainable at large M, whereas the $\upsilon = 1$ and $\upsilon = 3$ rectifiers suffer additional degradation. This is due to the fact that the denominator series in (91) terminates for $\upsilon = 2$, but does not terminate for $\upsilon = 1$ or 3; thus, the higher-order terms in (91) cause additional unavoidable degradation through leakage of higher-order spectral terms, as indicated in appendix E.

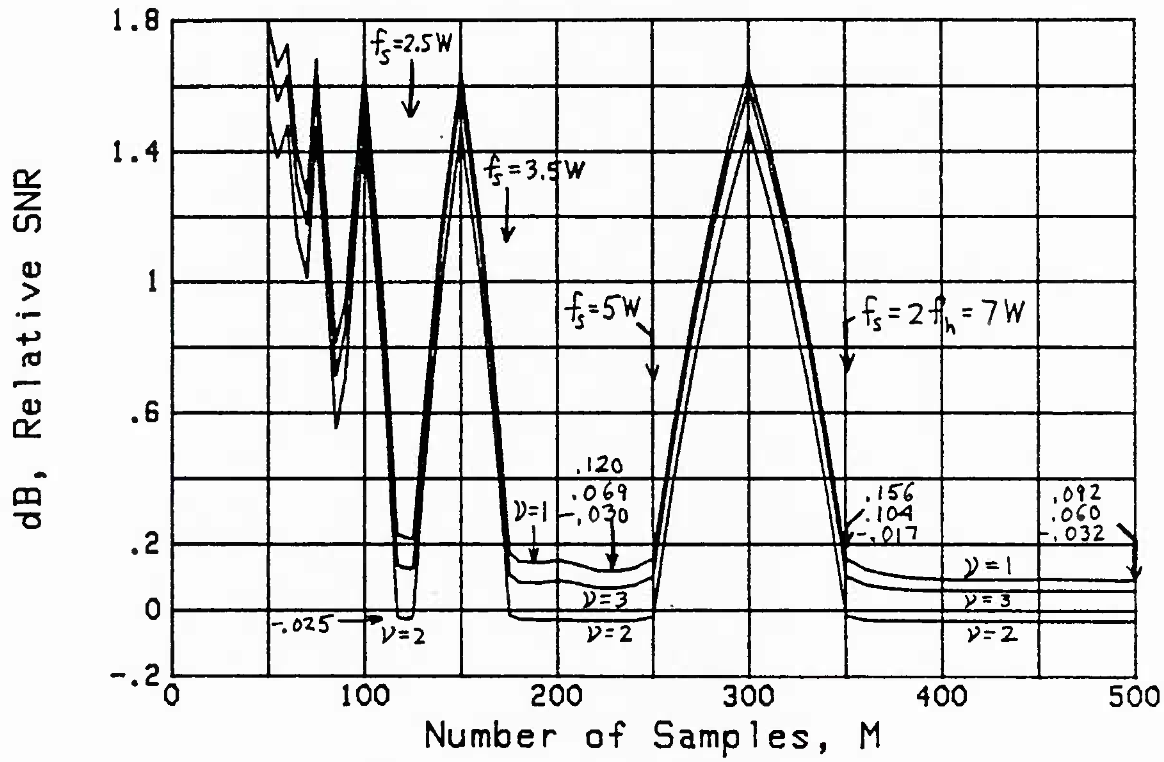

Figure 15. Flat Spectrum, Box Car Filter, Full-Wave Rectifier, TW = 50, Q = 3

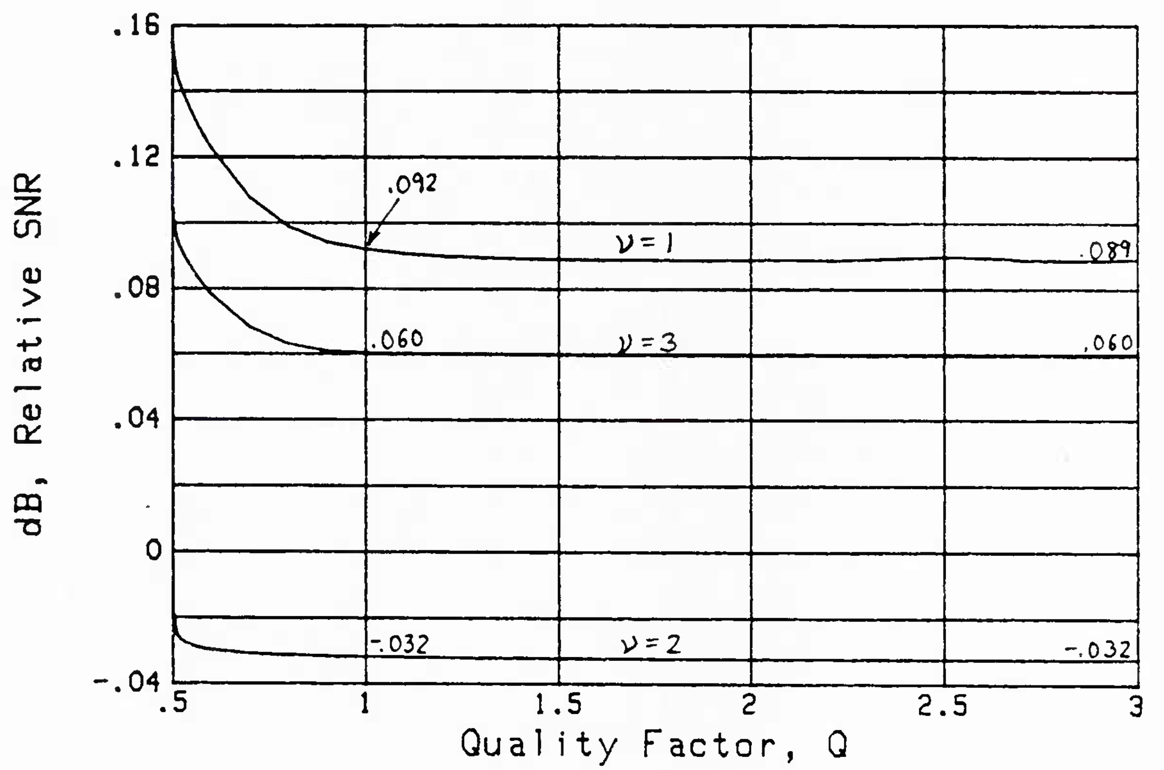

Figure 16. Variation with Q, Full-Wave Rectifier, TW = 50, M = 1000

Full-Wave Rectifier; Variable Q

The curves in the previous subsection all saturated for large numbers of samples, M; that is, the required input signal-to-noise ratio approached that for a continuous box car filter. Here, we will take M = 1000, meaning that we are effectively considering only the continuous box car filter, and look now at the required system input signal-to-noise ratio as a function of the Q of the spectrum, but not limited to the four discrete values of 1/2, 5/6, 2, and 3 earlier. The first result in figure 16 indicates a rapid drop in required input signal-to-noise ratio as Q increases above .5. The region (.5,.6) for Q is blown up in figure 17 to better illustrate the decay. The main conclusion from these two figures is that once Q-.5 is larger than approximately 1, the required input signal-to-noise ratio is essentially independent of Q.

To illustrate the relative independence of the results on the specific TW product (once it is large), figure 18 was computed and plotted for TW = 100; this result can be compared with figure 17 which utilized TW = 50.

Finally, in a similar comparison, figure 11 for TW = 50, Q = 5/6 was rerun for TW = 100, Q = 5/6 in figure 19. Except for the doubling of the abscissa values (M = 1000 vs 500 earlier), figures 19 and 11 are very similar. The fact that M must be doubled if TW is doubled is reasonable, whether that doubling comes about from increased T (more observation time) or increased W (higher bandwidth, meaning faster sampling).

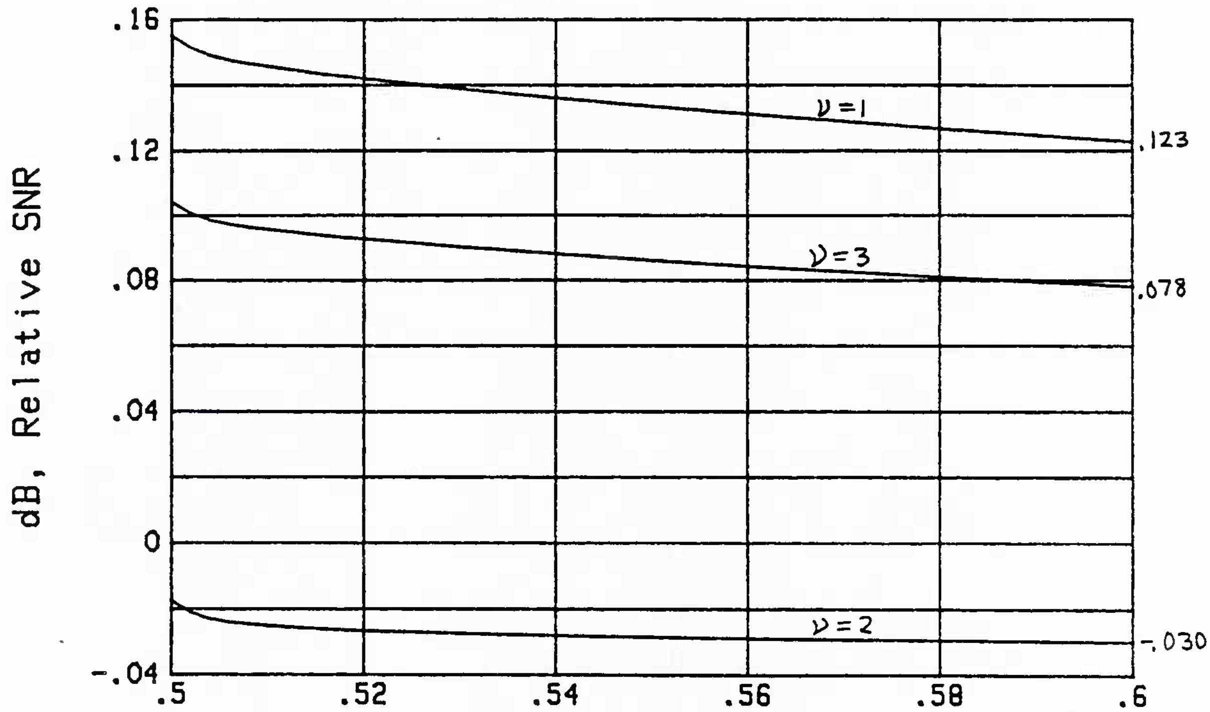

Figure 17. Small Q Variation, Full-Wave Rectifier, TW = 50, M = 1000

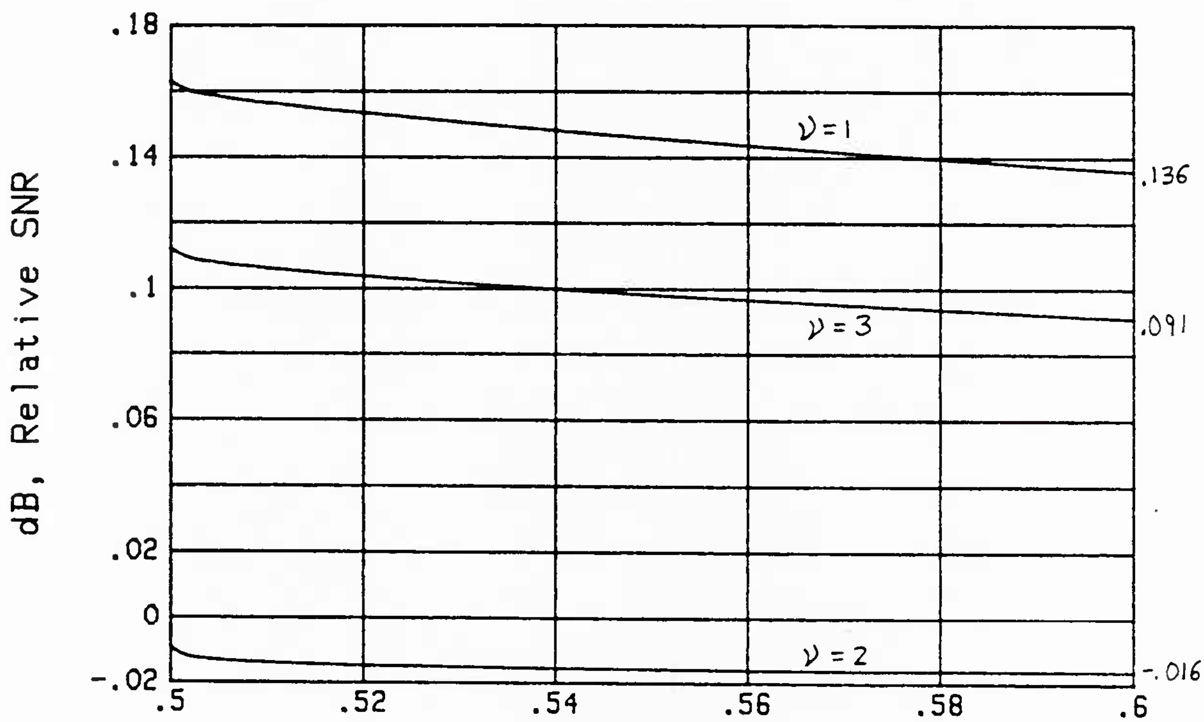

Figure 18. Small Q Variation, Full-Wave Rectifier, TW = 100, M = 1000

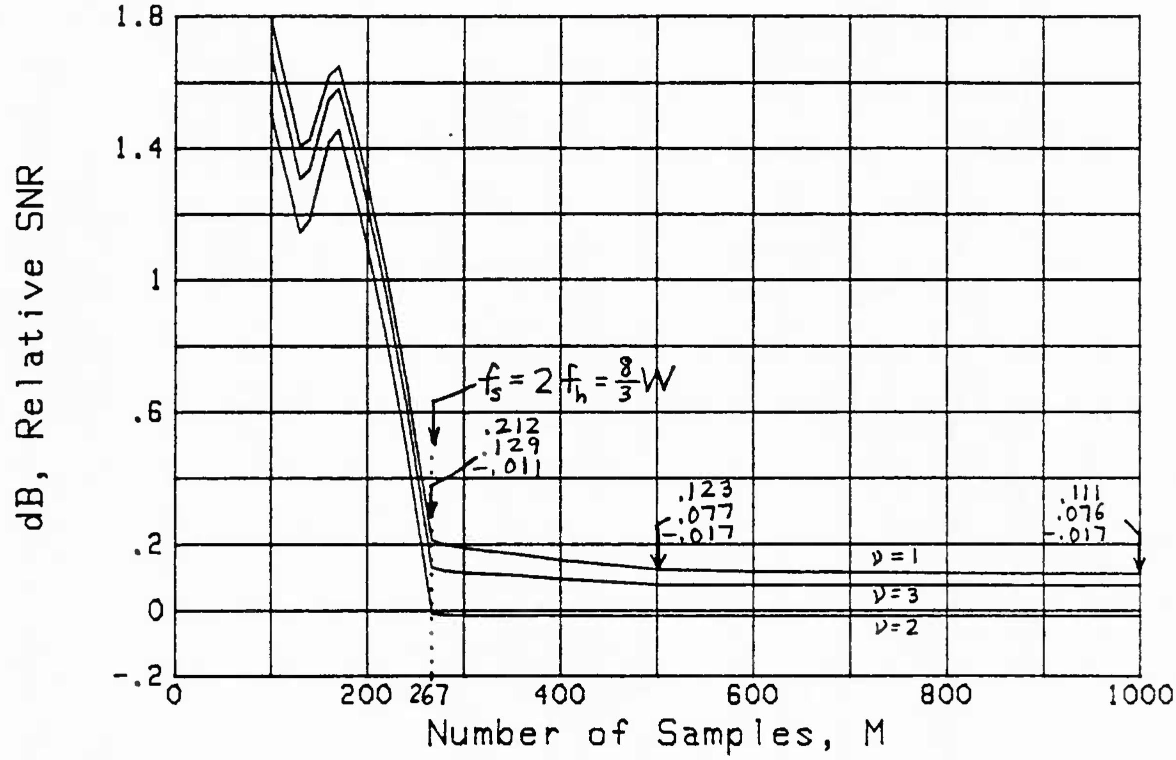

Figure 19. Flat Spectrum, Box Car Filter,
Full-Wave Rectifier, TW = 100, Q = 5/6

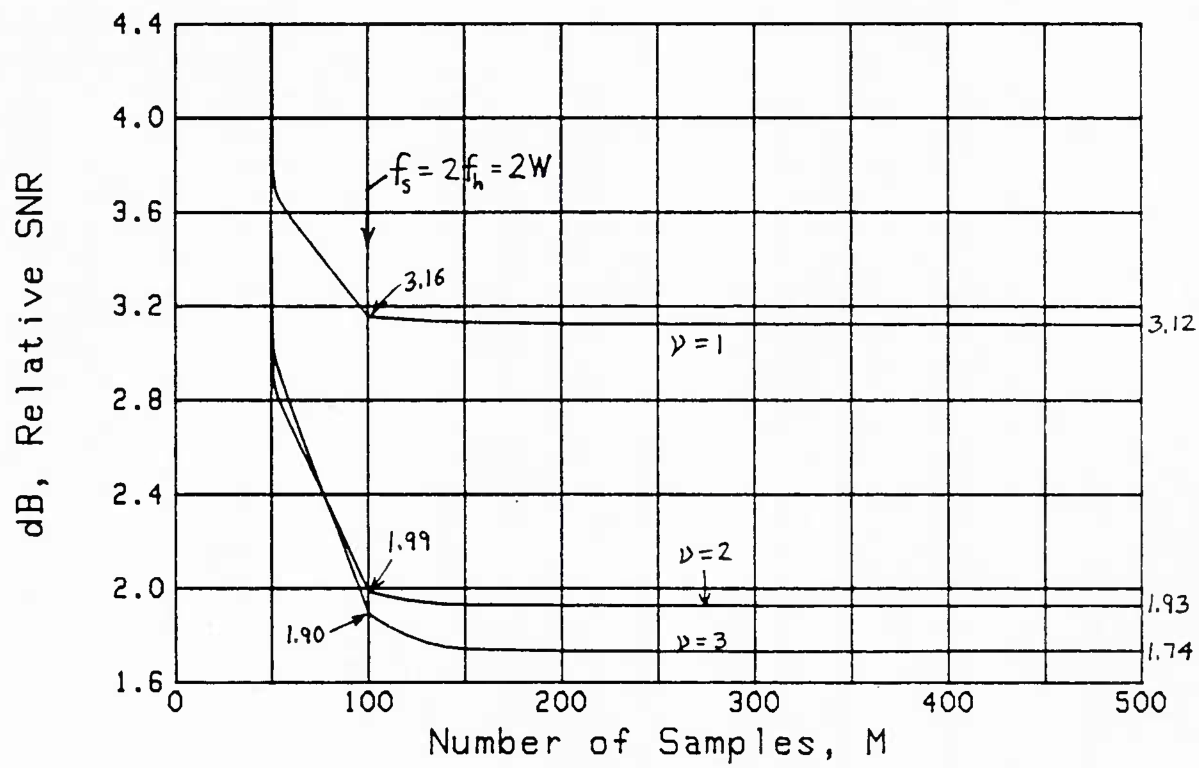

Figure 20. Flat Spectrum, Box Car Filter,
Half-Wave Rectifier, TW = 50, Q = 1/2

Half-Wave Rectifier; Variable Sampling Increment

We will repeat the series of plots given earlier in figures 10, 11, 12, 15, but now for ν-th law half-wave rectifiers. The first result in figure 20 gives the required input signal-to-noise ratio (relative to the standard) for Q = 1/2, a low-pass spectrum. The levels of required signal-to-noise ratios are much greater here for the half-wave rectifiers than for the corresponding full-wave rectifiers in figure 10. M = 100 corresponds to sampling frequency $f_s = 2f_h = 2W$; increasing M to 200 essentially reaches the saturation value attained for large M (continuous filtering). The dB numbers entered at M = 100 agree with those given earlier in table 1, since this corresponds to independent samples. (When TW is doubled to the value 100, virtually the same plot results when the abscissa scale, M, is also doubled.)

When Q is increased to 5/6 in figure 21, a marked improvement in performance occurs. The value M = 133 corresponds to $f_s = 2f_h = (8/3)W$; increasing M to 200 achieves saturation values, at which point $f_s = 3f_h = 4W$. However, the performance relative to the corresponding full-wave rectifier result in figure 11 is still poorer.

For Q = 2 in figure 22, although there is a marked dip in the required input signal-to-noise ratio for M in the range (130,150), the levels achieved are not as low as those possible for larger M. For example, an additional .24 dB is required at M = 150 for $\nu = 1$ than at M = 400 for $\nu = 2$. At M = 125, the dB values in figure 22 are very large; this is due to an aliased component, a la figures 13 and 14, abutting frequency f = 0. This result is

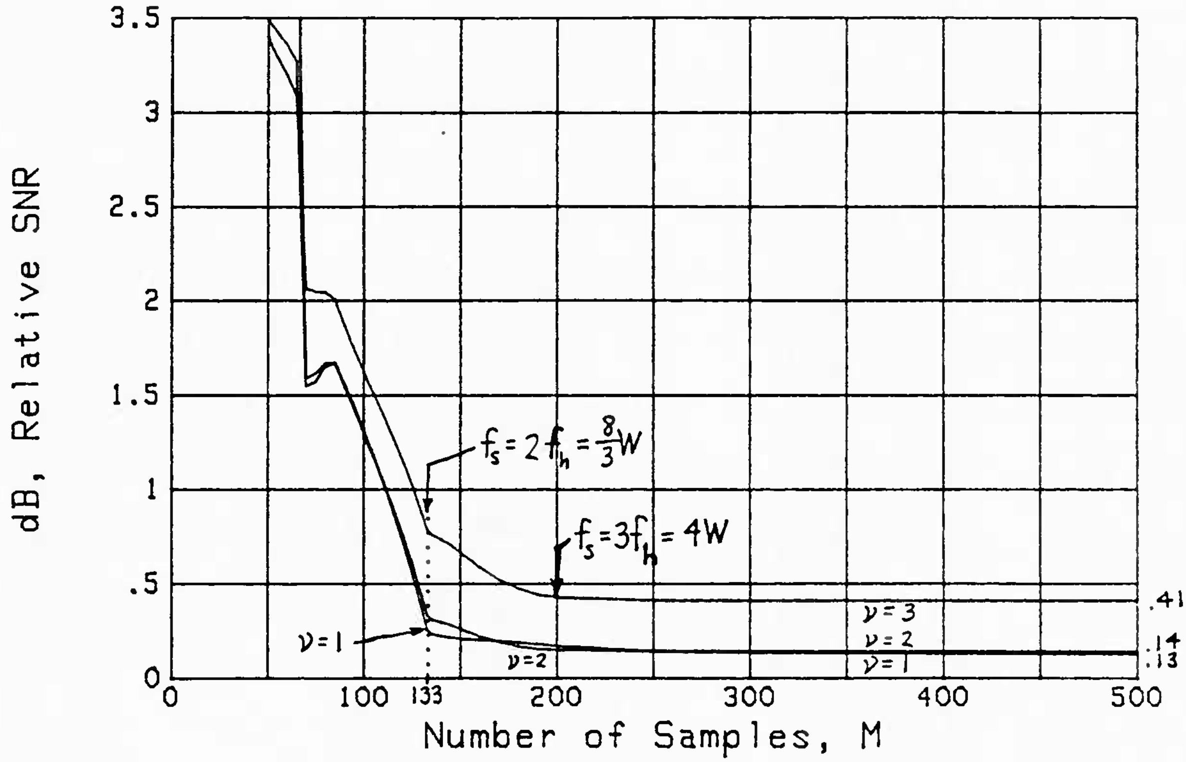

Figure 21. Flat Spectrum, Box Car Filter, Half-Wave Rectifier, TW = 50, Q = 5/6

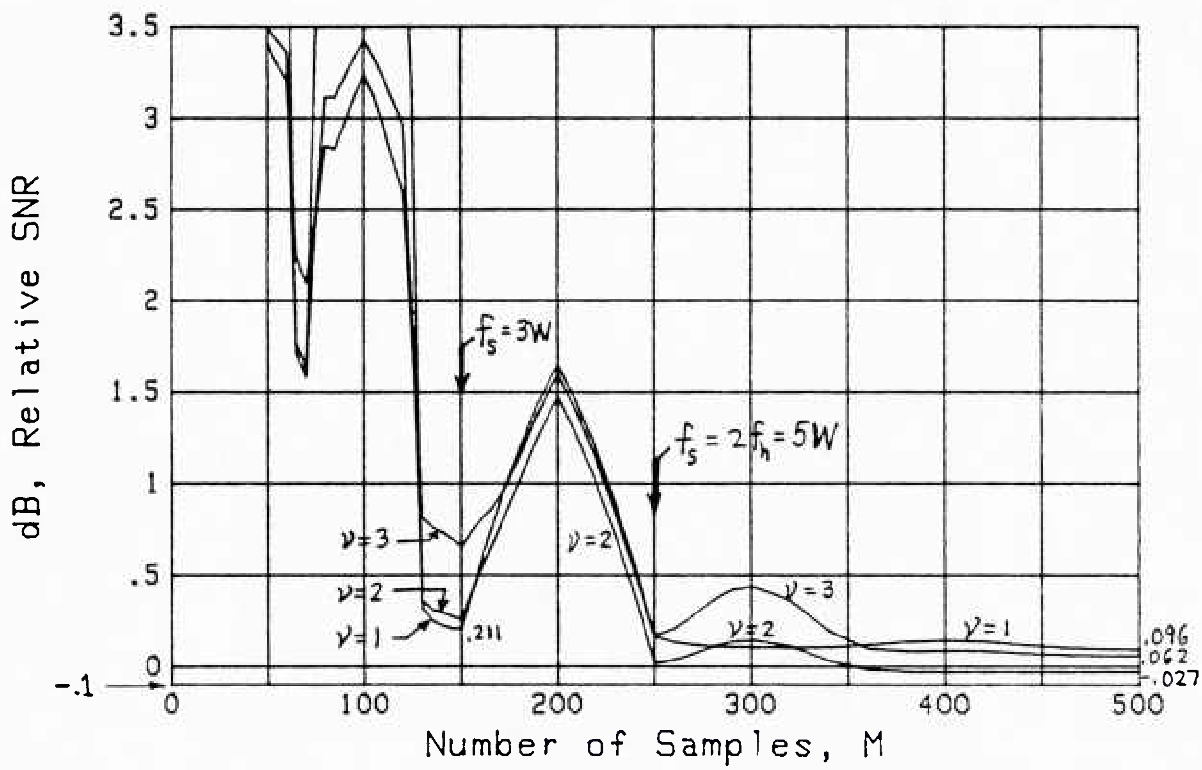

Figure 22. Flat Spectrum, Box Car Filter, Half-Wave Rectifier, TW = 50, Q = 2

distinctly different from the corresponding one for a full-wave rectifier in figure 12.

The half-wave rectifier result for Q = 3 in figure 23 is somewhat similar to the corresponding full-wave rectifier result in figure 15. However, there is much more degradation here for M near 120, and moderate degradation for M in the range (180,250). Essentially the same performance for $\nu = 2$ is achieved at M = 350, $f_s = 2f_h$ as at M = 500, $f_s = (20/7)f_h$, but losses are encountered for sampling rates between these values.

Half-Wave Rectifier; Variable Q

To determine the explicit dependence of performance on the Q of the input spectrum, we eliminate the dependence on M, by setting M equal to a large value, namely 1000, thereby essentially realizing a continuous box car filter. Then we vary Q over the range (.5,3) and plot the results for TW = 50 in figure 24. Saturation is achieved for Q > 1.5 at acceptably low values; however the performance degrades considerably for small Q.

Comparison of figure 24 with the corresponding result in figure 16 for a full-wave rectifier (both with TW = 50 and M = 1000) reveals that by the time Q reaches 1.5, the half-wave and full-wave rectifiers realize virtually the same performance level, regardless of the value of ν. For example, the dB numbers listed above Q = 3 are almost identical. This confirms the results anticipated in the analysis presented earlier in (78)-(80) et seq.

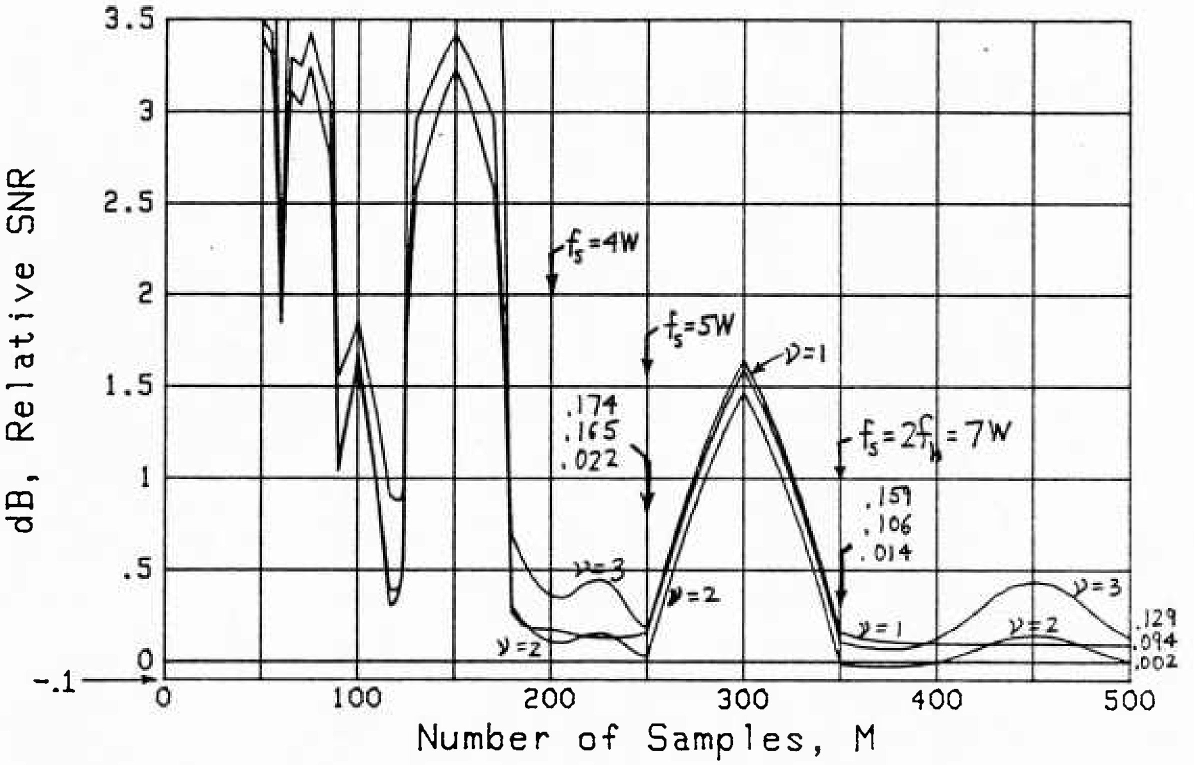

Figure 23. Flat Spectrum, Box Car Filter, Half-Wave Rectifier, TW = 50, Q = 3

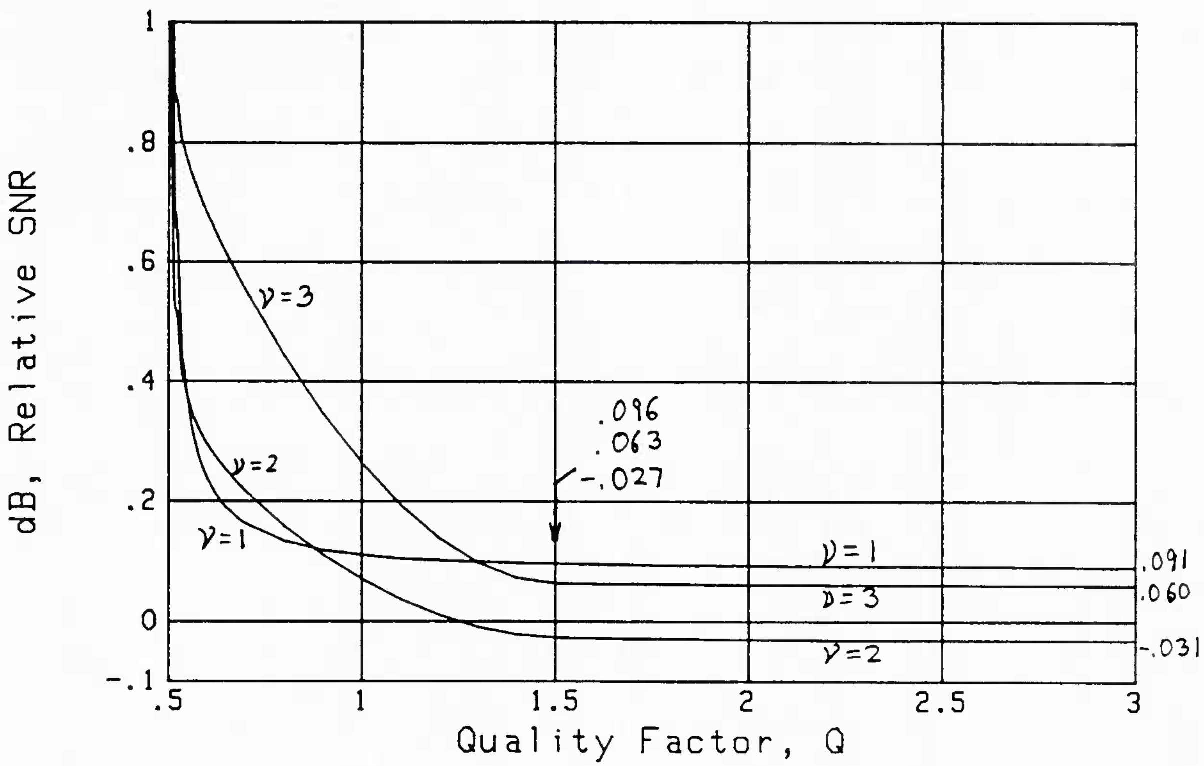

Figure 24. Variation with Q, Half-Wave Rectifier, TW = 50, M = 1000

The region (.5,.6) for Q is blown up in figure 25; it indicates approximately that if

$$Q - \frac{1}{2} > \frac{4}{TW} , \tag{151}$$

a plateau in performance is essentially realized, while a more gradual improvement takes place for larger Q. This same bound on Q was previously encountered in (111) when we discovered the condition under which the linear half-wave rectifier and the symmetric linear full-wave rectifier have similar performance. The analysis in (109)-(117) is again directly relevant here in regards to overlapping aliased spectral lobes.

If TW is increased to 100, figure 26 illustrates very similar behavior, except that the sharp transition region near Q = 1/2 is approximately half as wide; this is consistent with (151).

In a similar vein, for a fixed Q of 5/6, a comparison of results for TW = 100 in figure 27 can be made with the corresponding earlier result for TW = 50 in figure 21. Except for the doubling of the M scale in figure 27, the two sets of curves are virtually identical.

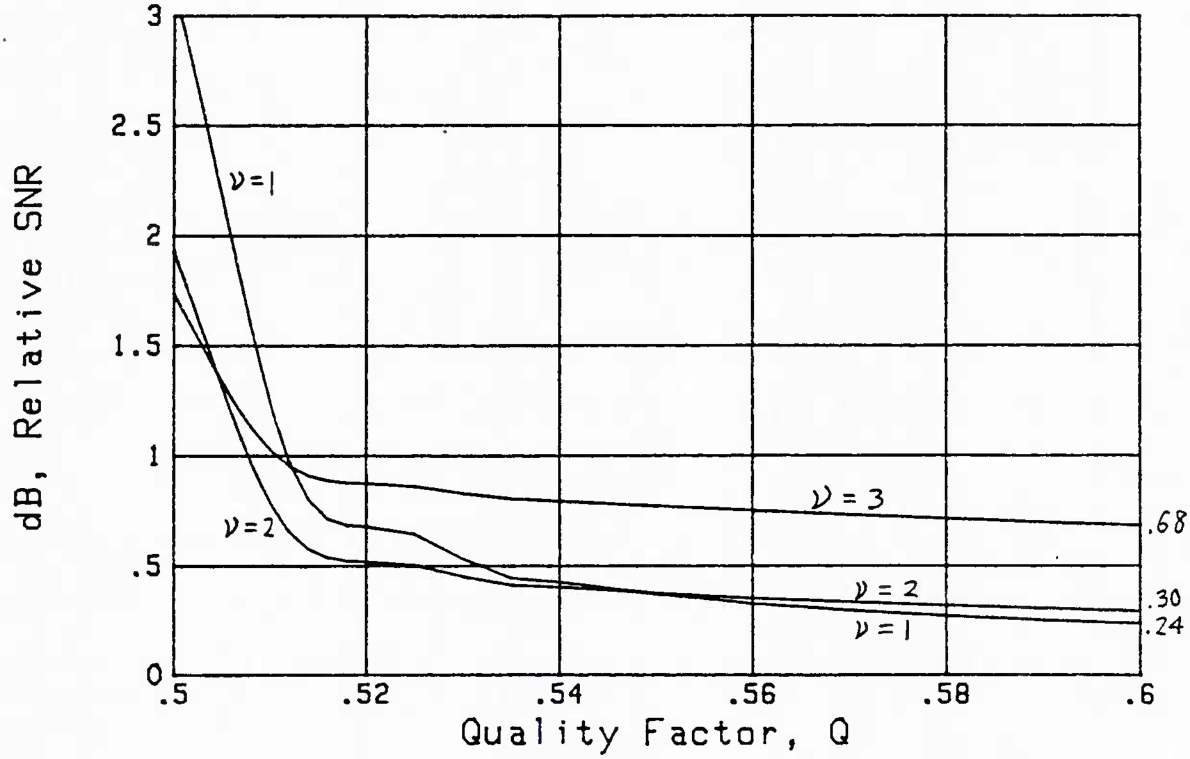

Figure 25. Small Q Variation, Half-Wave Rectifier, TW = 50, M = 1000

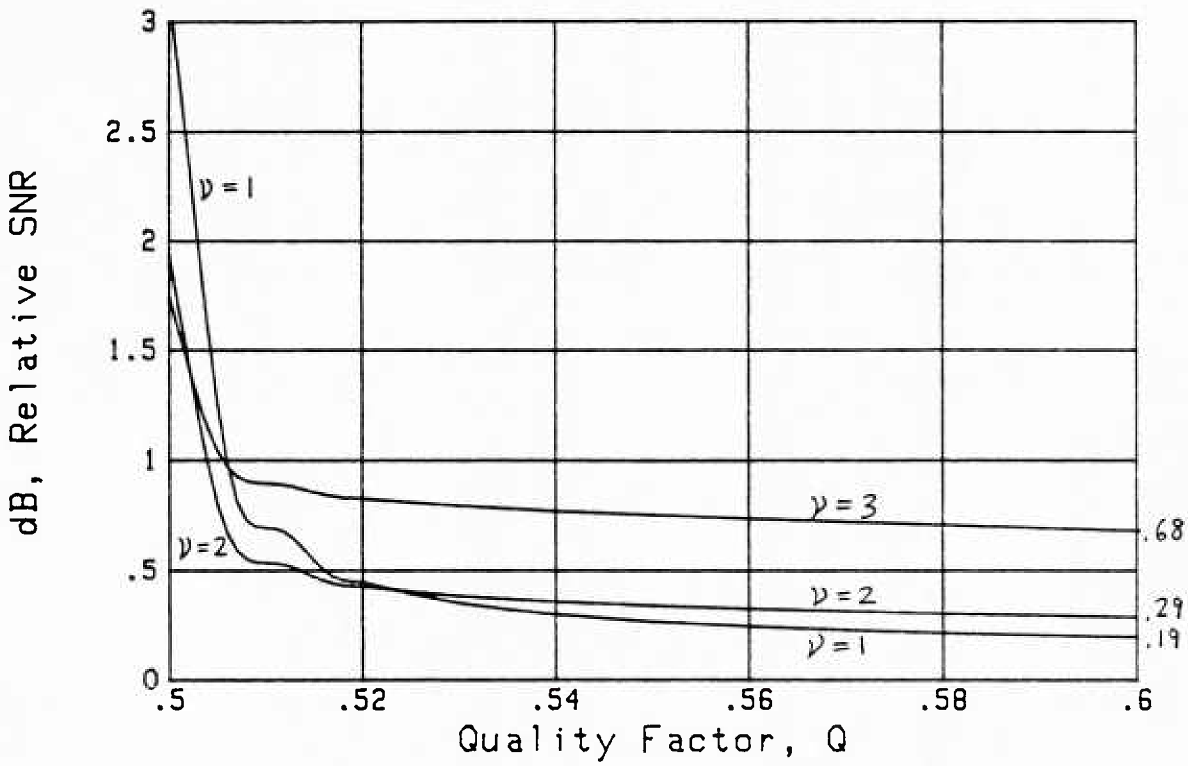

Figure 26. Small Q Variation, Half-Wave Rectifier, TW = 100, M = 1000

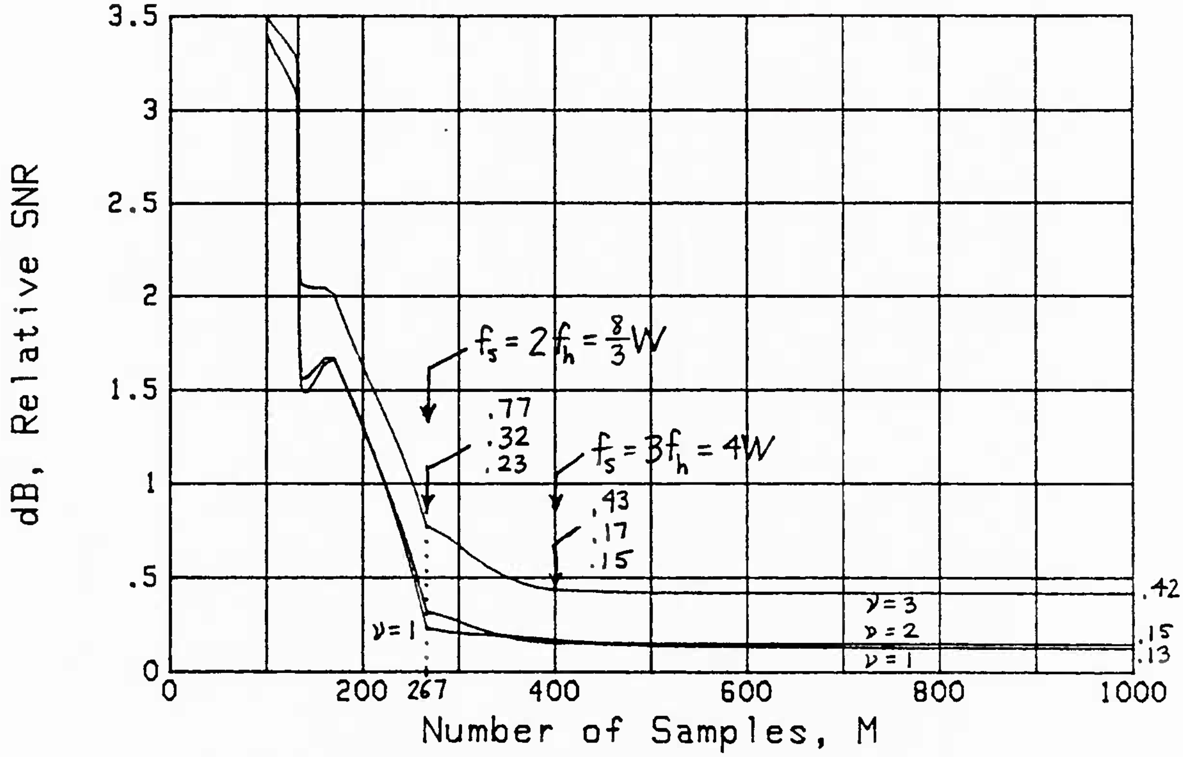

Figure 27. Flat Spectrum, Box Car Filter, Half-Wave Rectifier, TW = 100, Q = 5/6

OTHER SPECTRA AND FILTERS

Gaussian Spectrum

All the previous results pertained to the flat bandpass spectrum of figure 3. In order to ascertain how important the details of the input spectrum are, we consider in this subsection the input normalized correlation

$$\rho(\tau) = \cos(2\pi f_c \tau)\ \exp\left(-\frac{\pi}{2} W^2 \tau^2\right), \tag{152}$$

with corresponding spectrum given by (47) as

$$p^{(1)}(f) = \frac{1}{2^{1/2} W}\left\{\exp\left[-2\pi\left(\frac{f - f_c}{W}\right)^2\right] + \exp\left[-2\pi\left(\frac{f + f_c}{W}\right)^2\right]\right\}. \tag{153}$$

This is a pair of Gaussian lobes centered at $\pm f_c$.

It should be observed that

$$\frac{\left\{\int df\ \exp\left[-2\pi\left(\frac{f - f_c}{W}\right)^2\right]\right\}^2}{\int df\ \exp^2\left[-2\pi\left(\frac{f - f_c}{W}\right)^2\right]} = W\ , \tag{154}$$

independent of center frequency f_c. Thus W in (152) and (153) is the effective or statistical bandwidth of the <u>positive lobe</u> of input spectrum $p^{(1)}(f)$, as if the negative lobe were absent. Also, the relative value of the positive lobe at frequencies $f = f_c \pm W/2$ is $\exp(-\pi/2) = .208 = -6.82$ dB.

More generally, the effective bandwidth of the complete spectrum $p^{(1)}(f)$ is

$$\frac{\left[\int df\ p^{(1)}(f)\right]^2}{\int df\ p^{(1)^2}(f)} = \frac{1}{\int df\ p^{(1)^2}(f)} = \frac{2W}{1 + \exp(-4\pi Q^2)} \ . \tag{155}$$

Unfortunately, this depends on $Q = f_c/W$. If we were to use this latter result in standard output signal-to-noise ratio γ_a in (51), we would have

$$\gamma_a = TW \frac{\left(\sigma_1^2/\sigma_0^2 - 1\right)^2}{1 + \exp(-4\pi Q^2)} \tag{156}$$

and (56) would yield

$$\gamma_b = TW\left(\frac{S}{N}\right)^2 \frac{1}{1 + \exp(-4\pi Q^2)} \ . \tag{157}$$

The dependence on Q is undesirable, although it is a weak dependence; for example, for Q = 1/2, the exponential in (157) is .043. Hence we drop this dependence, and use the usual basis (57) again.

If we use (91) for γ_{IF}, or (102) for γ_{IH}, with the S+N versus N hypotheses of (56), and a small input signal-to-noise ratio, we have

$$\gamma_{I(F,H)} = \frac{M \frac{\upsilon^2}{4} \left(\frac{S}{N}\right)^2}{\sum} \ , \tag{158}$$

where

$$\sum \equiv \sum_k U(k) \sum_n \beta(n)\ \rho_0^k(n\Delta) \ , \tag{159}$$

the sum being over k = 2, 4, 6, ... for full-wave rectifiers, and over k = 1, 3, 5, ... for half-wave rectifiers. If we now equate the output signal-to-noise ratios, that is, set

$$\gamma_{I(F,H)} = \frac{M \frac{v^2}{4} \left(\frac{S}{N}\right)^2}{\sum} = TW\left(\frac{S}{N}\right)_s^2 , \tag{160}$$

then there follows factor

$$\frac{S/N}{(S/N)_s} = \frac{2}{v}\left(\frac{TW}{M} \sum\right)^{1/2} . \tag{161}$$

This is the input signal-to-noise ratio required, relative to basis (57). Recall that W is now the effective BW of the positive frequency lobe; see (154).

Plots of the relative increase in input signal-to-noise ratio, as given by (161) and (159), are presented in figures 28 and 29 for the full-wave and half-wave rectifiers, respectively, for TW = 50 and Q = 5/6. These should be compared with the corresponding flat bandpass spectrum results in figures 11 and 21, respectively. Except for a general smoothing in figures 28 and 29, due to the smoother Gaussian spectrum (153), the results are very similar. Saturation is essentially reached at M = 200, which corresponds to sampling frequency $f_s = 3f_h = 4W$.

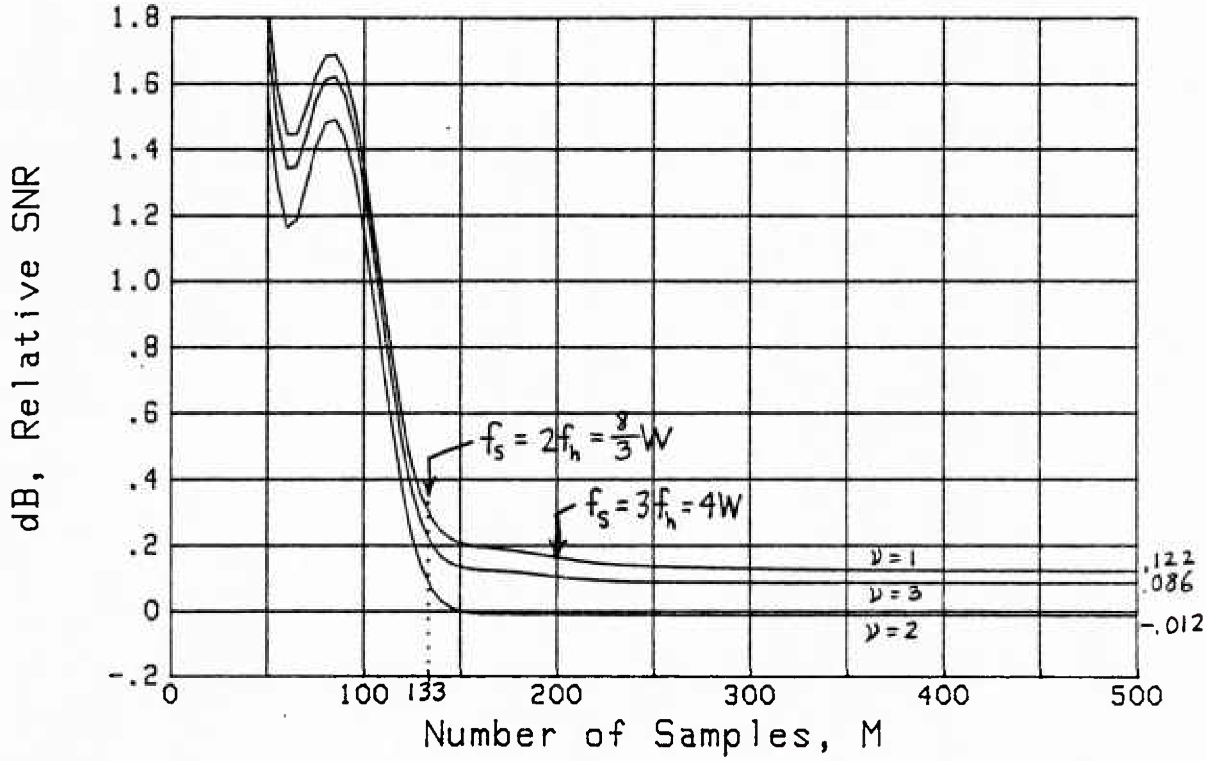

Figure 28. Gaussian Spectrum, Box Car Filter, Full-Wave Rectifier, TW = 50, Q = 5/6

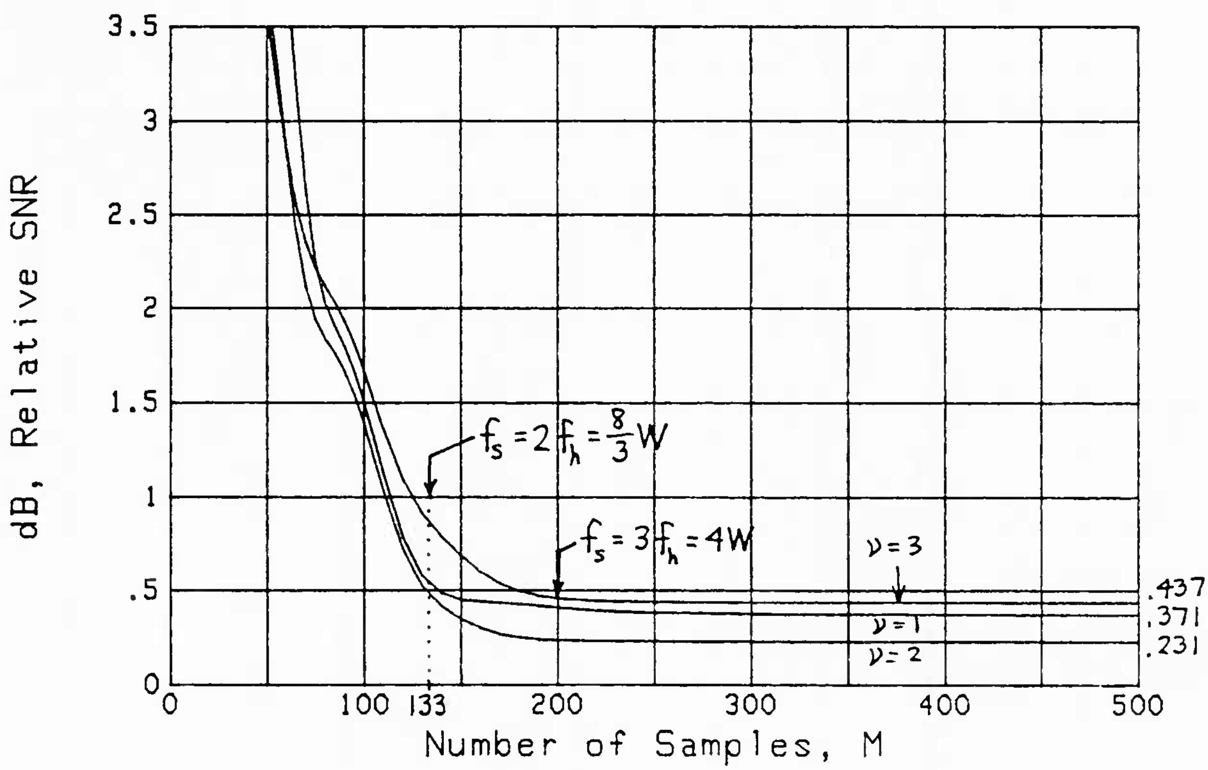

Figure 29. Gaussian Spectrum, Box Car Filter, Half-Wave Rectifier, TW = 50, Q = 5/6

-6 dB/Octave Spectrum

In this section, the input spectrum is taken to have a $1/f^2$ shape in the band (f_1,f_2). There is a difference in this example between the bandwidth $W = f_2 - f_1$ and the effective bandwidth, W_e, which is developed in appendix F. The pertinent equations for this case (as well as the spectral shapes f^n for $n = -2,-1,0,1,2$) are also presented in appendix F. The results for $TW = 50$ and $Q = 5/6$ are given in figures 30 and 31 for full-wave and half-wave rectifiers, respectively. They are very similar to the corresponding earlier results with the same parameter values.

RC Filter

All the previous examples have employed a box car impulse response, as given by (10). We now replace this assumption by one in which the impulsive filter weights are given by samples of an RC filter response, with effective duration T = 2 RC; see (52) or (72). That is,

$$w(n) = \frac{1}{RC} \exp\left(-\frac{n\Delta}{RC}\right) \quad \text{for } n \geq 0 . \tag{162}$$

The effective number of samples is, from (67),

$$M = \frac{\left[\sum\limits_n w(n)\right]^2}{\sum\limits_n w^2(n)} = \frac{1 + \exp\left(-\frac{\Delta}{RC}\right)}{1 - \exp\left(-\frac{\Delta}{RC}\right)} =$$

$$\cong \frac{2\ RC}{\Delta}\left(1 + \frac{\Delta^2}{12\ R^2C^2}\right) \quad \text{for} \quad \frac{RC}{\Delta} > 1 . \tag{163}$$

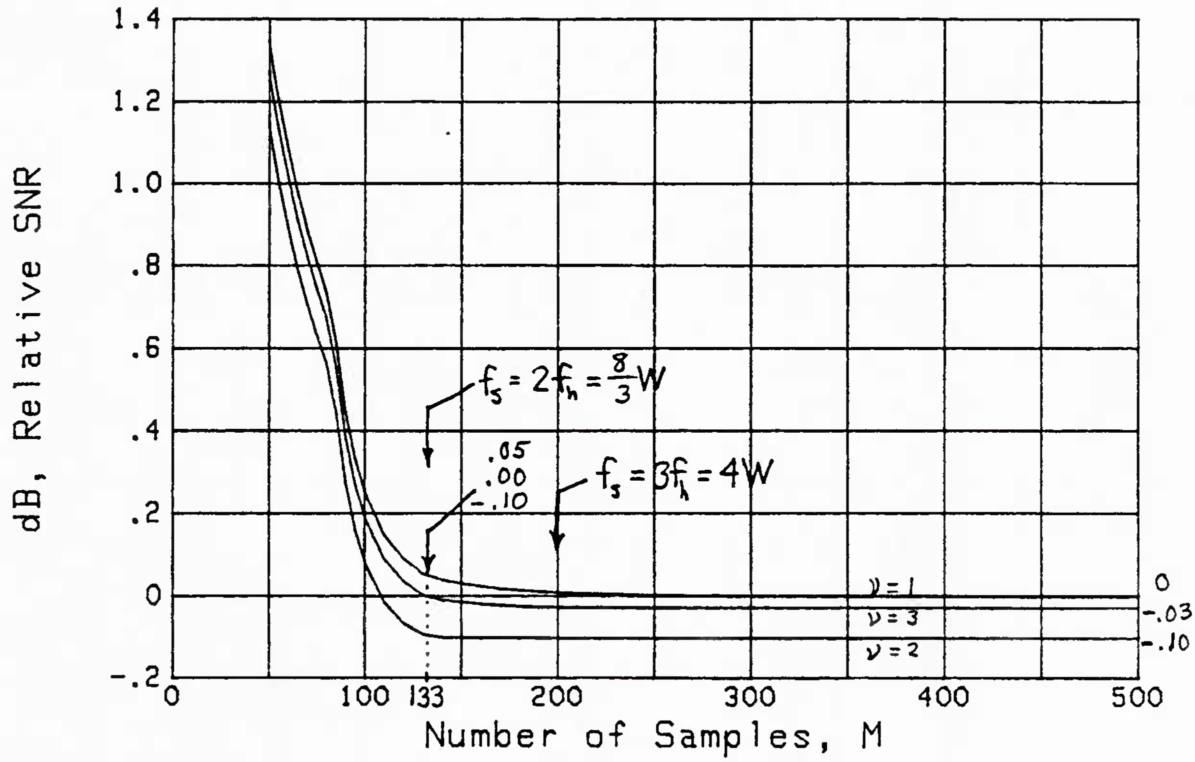

Figure 30. -6 dB/Octave Spectrum, Box Car Filter, Full-Wave Rectifier, TW = 50, Q = 5/6

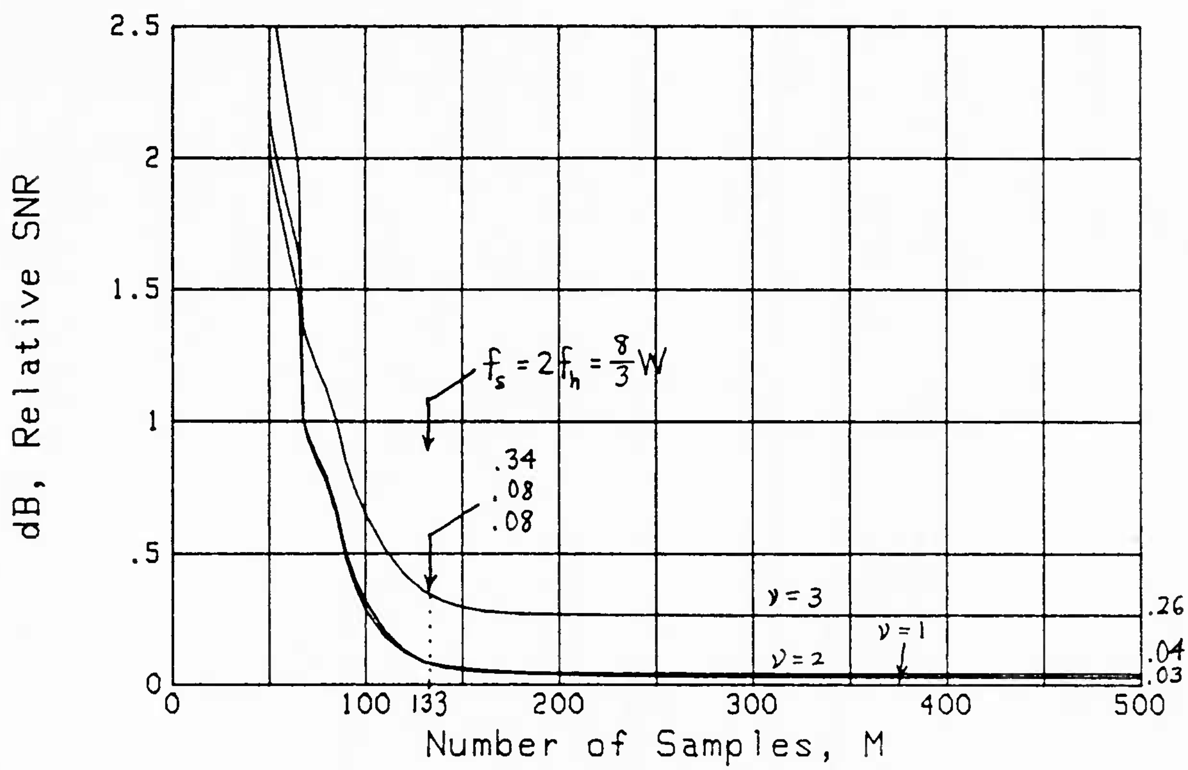

Figure 31. -6 dB/Octave Spectrum, Box Car Filter, Half-Wave Rectifier, TW = 50, Q = 5/6

For example, for $\frac{RC}{\Delta} = 10$, $M \cong 20\left(1 + \frac{1}{1200}\right)$. Accordingly we set

$$M = \frac{2\ RC}{\Delta} = \frac{T}{\Delta} \quad (\text{for } M >> 1)\ . \tag{164}$$

This is consistent with (146) employed for the box car filter. The normalized autocorrelation is, via (68),

$$\beta(n) = \exp\left(-\frac{\Delta}{RC}\ |n|\right) \cong \exp\left(-\frac{2}{M}\ |n|\right)\ . \tag{165}$$

A plot of the relative input signal-to-noise ratio is given in figure 32 for a half-wave rectifier with TW = 50, Q = 5/6, and a flat bandpass input spectrum. It indicates the same general behavior as corresponding earlier results for different input spectra and/or filters; the precise numerical values are a little different, and are a reflection of the particular filter employed here, namely (162).

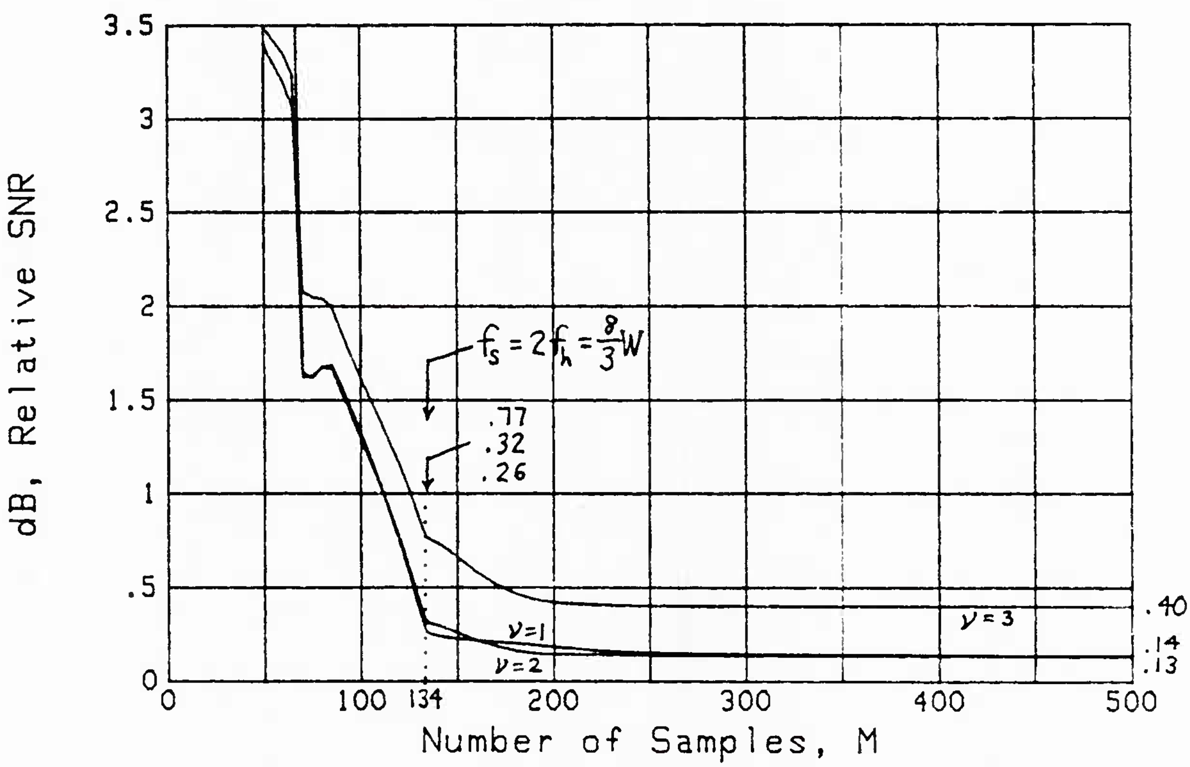

Figure 32. Flat Spectrum, RC Filter, Half-Wave Rectifier, TW = 50, Q = 5/6

A PITFALL OF THE LONG AVERAGING TIME ASSUMPTION

The general factor by which the input signal-to-noise ratio for a half-wave ν-th law rectifier must be increased, relative to the standard full-wave square-law rectifier, is given in (D-5). Here, Sum_H is given in (D-1), in terms of the normalized autocorrelation (68) of the filter weights. Under the long averaging time assumption, as discussed earlier with regard to (74) et seq., the quantity $\beta(n)$ is replaced by its origin value of 1 for all n. Then the quantity S(k) in (D-3) is replaced by

$$\tilde{S}(k) \equiv \sum_{n=1}^{\infty} \rho_0^k(n\Delta) \quad \text{for } k \geq 1 , \tag{166}$$

and factor (D-5) is replaced by

$$\tilde{F}_H = \frac{2}{\nu} \left(\frac{TW}{M} \tilde{S}_H \right)^{1/2} , \tag{167}$$

where

$$\tilde{S}_H = 2D(\nu) - 1 + 2 \sum_{k=1}^{\infty} U(k)\ \tilde{S}(k) \tag{168}$$

is an obvious modification of (D-2).

A similar approach for full-wave ν-th law rectifiers yields signal-to-noise ratio factor

$$\tilde{F}_F = \frac{2}{\nu} \left(\frac{TW}{M} \tilde{S}_F \right)^{1/2} , \tag{169}$$

where

$$\tilde{S}_F = D(\nu) - 1 + 2 \sum_{\substack{k=2 \\ \text{even}}}^{\infty} U(k)\ \tilde{S}(k) \ . \qquad (170)$$

It will be seen from (168) and (170) that a fundamental calculation required is that described in (166), whether utilizing the full-wave or the half-wave rectifier. In particular, for the flat bandpass input spectrum given by figure 3, with normalized correlation (13), the summation in (166) is very slowly convergent for low order k. This problem is treated in appendix G, through a judicious combination of Poisson's formula and numerical calculation.

Results for the long averaging time assumption are superposed as dotted lines in figures 33 and 34 over the earlier results from figures 24 and 25, respectively, for half-wave rectifiers, TW = 50, M = 1000. As Q approaches .5, there is a marked difference between the two results. For example, for $\nu = 2$, the approximation yields .34 dB whereas the exact results is 1.93 dB. And for $\nu = 1$, the comparison is .17 dB versus exact value 3.12 dB, almost a 3 dB discrepancy. This serves to point out the pitfall of employing the long averaging time assumption when inappropriate. Regardless of the size of the TW product, there will always be a narrow range near Q = 1/2 where the exact signal-to-noise ratio drops sharply from the values listed in tables 1 and 2 to their eventual asymptotic values for large Q. This transition is ignored by the long averaging time assumption and can be overly optimistic in its performance prediction.

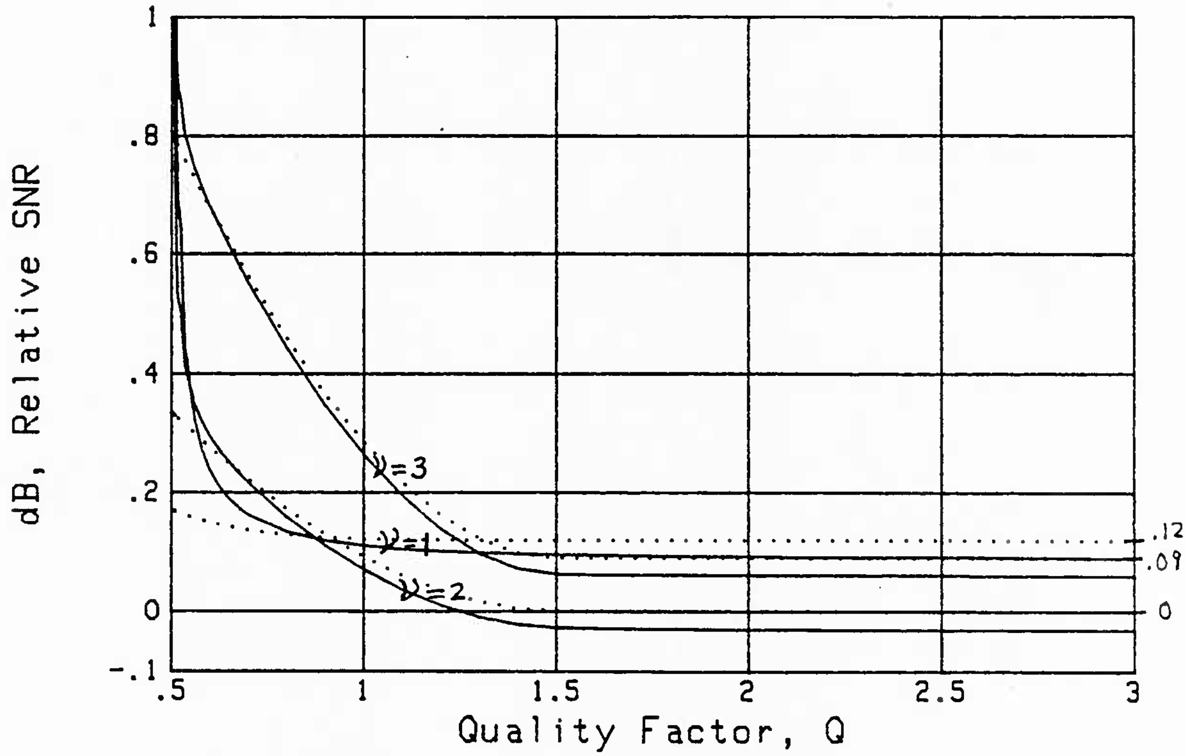

Figure 33. Long Averaging Time Assumption, Half-Wave Rectifier, TW = 50, M = 1000

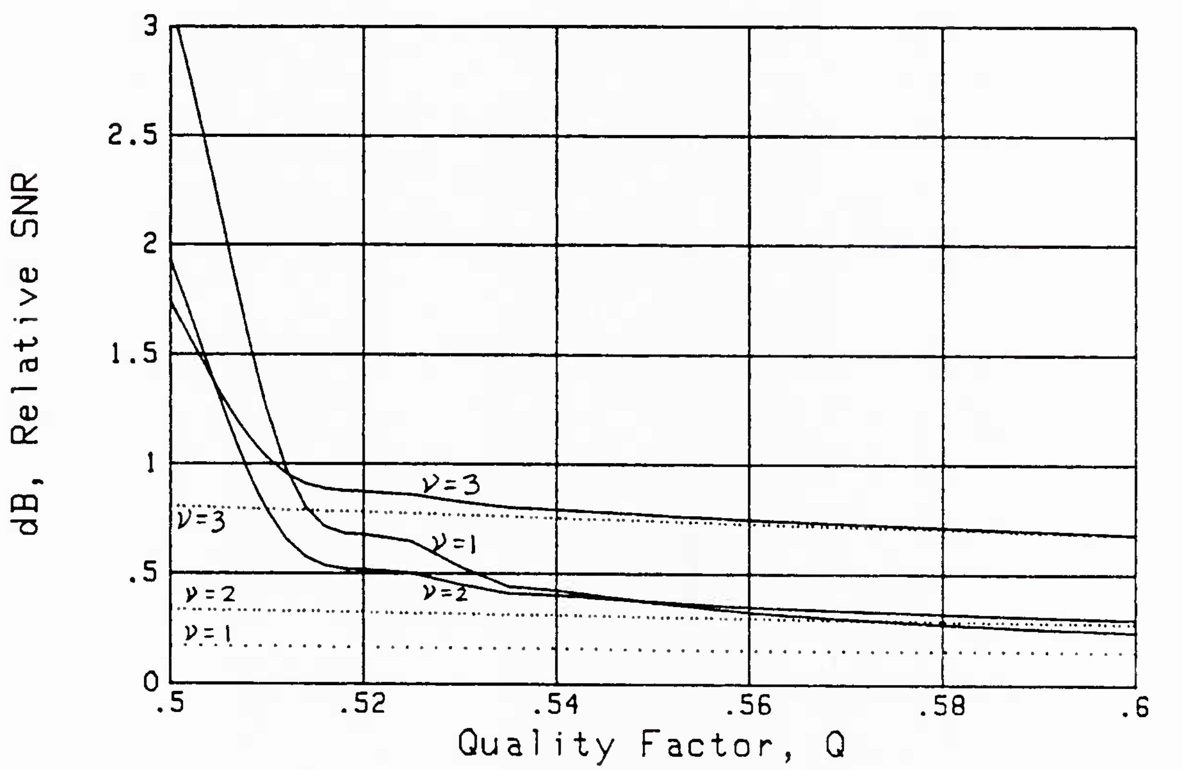

Figure 34. Long Averaging Time Assumption, Half-Wave Rectifier, TW = 50, M = 1000, Small Q

SUMMARY

The losses incurred by using various full-wave and half-wave ν-th law rectifiers with different filter characteristics, sampling rates, and input spectra have been evaluated and plotted for a number of cases. These results allow for a ready comparison of many alternative choices and give quantitative bases for a selection procedure.

The possibility of deliberately undersampling an input process with a high-Q spectrum, with insignificant loss of performance, has been analyzed and numerically investigated. The exact choice of sampling frequency is crucial, but can be easily calculated once the lower and upper frequencies of the band-limited input spectrum are specified. Even though the system nonlinearity $g\{x\}$ creates harmonics and intermodulation products, and the undersampling process creates aliased spectral replicas, it is still possible, through proper choice of the sampling rate, to control all these undesirable by-products and achieve a near-minimum input signal-to-noise ratio for specified output deflection.

The danger of using the long averaging time assumption when inappropriate has been demonstrated via numerical example. All the results presented in this report have not employed this assumption, but have utilized the precise filter characteristics and finite time extent. Programs for these evaluations are presented in tables H-1 through H-4 in appendix H. Changes required to handle the Gaussian spectrum or the RC filter, instead of the flat bandpass spectrum or box car filter, respectively, are also presented there.

The losses incurred by a half-wave rectifier for low-Q inputs are very significant and should be avoided, either by utilizing a full-wave rectifier or by filtering out the low frequency components of the input, prior to sampling and nonlinear distortion. Generally speaking, the square-law detector, $\nu = 2$, offers the best performance.

Direct comparisons of these results with those in [1] are not possible, because there are no common examples. Also, most of the results in [1] are for very narrowband spectra and employ a long averaging time assumption, in addition to using very few terms in the series expansion for the output variance.

APPENDIX A. DERIVATION OF RECURRENCE

The quantity of interest is given by (85):

$$L(k) = \int_0^\infty dw\, w^{\upsilon}\, \phi(w)\, He_k(w) \quad \text{for all } k \geq 0 . \tag{A-1}$$

First of all, using (21),

$$L(0) = \int_0^\infty dw\, w^{\upsilon}\, \phi(w) = (2\pi)^{-1/2} \int_0^\infty dw\, w^{\upsilon} \exp(-w^2/2) =$$

$$= (2\pi)^{-1/2} \int_0^\infty dx\, (2x)^{\frac{\upsilon-1}{2}} \exp(-x) = 2^{\frac{\upsilon}{2}-1}\, \pi^{-\frac{1}{2}}\, \Gamma\!\left(\frac{\upsilon+1}{2}\right). \tag{A-2}$$

In a similar fashion, there follows

$$L(1) = \int_0^\infty dw\, w^{\upsilon+1}\, \phi(w) = 2^{\frac{\upsilon-1}{2}}\, \pi^{-\frac{1}{2}}\, \Gamma\!\left(\frac{\upsilon}{2}+1\right) . \tag{A-3}$$

We now employ the recurrence [3, (22.7.14)]

$$He_k(w) = w\, He_{k-1}(w) - (k-1)\, He_{k-2}(w) \quad \text{for } k \geq 2 . \tag{A-4}$$

Substitution in (A-1) yields

$$L(k) = \int_0^\infty dw\, w^{\upsilon+1}\, \phi(w)\, He_{k-1}(w) - (k-1)\, L(k-2) \quad \text{for } k \geq 2 . \tag{A-5}$$

We now integrate by parts, using

$$u = w^{\upsilon+1} , \quad dv = dw\, \phi(w)\, He_{k-1}(w) ,$$

$$du = dw\, (\upsilon+1)\, w^{\upsilon} , \quad v = -\phi(w)\, He_{k-2}(w) , \tag{A-6}$$

the last relation from [3, (22.11.8)]. The integral in (A-5) then becomes, since $v > 0$,

$$\left[-w^{v+1}\ \phi(w)\ He_{k-2}(w)\right]_0^\infty + (v+1) \int_0^\infty dw\ w^v\ \phi(w)\ He_{k-2}(w) =$$

$$= (v+1)\ L(k-2)\ . \tag{A-7}$$

Use of this result in (A-5) immediately yields

$$L(k) = (v+2-k)\ L(k-2) \quad \text{for all } k \geq 2\ . \tag{A-8}$$

The starting values for this recurrence have already been furnished in (A-2) and (A-3).

APPENDIX B. DERIVATIONS OF (110) AND (112)

We employ (73) and (48) to develop the left-hand side of (110) according to

$$\int d\tau\, \alpha(\tau)\, \rho(\tau) = \int d\tau \frac{\int du\, h(u)\, h(u-\tau)}{\int du\, h^2(u)} \int df\, \exp(i2\pi f\tau)\, P^{(1)}(f) =$$

$$= \left[\int du\, h^2(u)\right]^{-1} \int df\, P^{(1)}(f) \int du\, h(u) \int d\tau\, h(u-\tau)\, \exp(i2\pi f\tau) =$$

$$= \frac{\int df\, P^{(1)}(f)\, |H(f)|^2}{\int df\, |H(f)|^2}\,, \tag{B-1}$$

where we let x = u-τ in the innermost τ integral in the second line, and used Parseval's theorem for the denominator term.

For the impulsive filter case, we utilize (68) and (48) to express the left-hand side of (112) as

$$\sum_n \beta(n)\, \rho(n\Delta) = \sum_n \frac{\sum_m w(m)\, w(m-n)}{\sum_m w^2(m)} \int df\, \exp(i2\pi f\Delta n)\, P^{(1)}(f) =$$

$$= \left[\sum_m w^2(m)\right]^{-1} \int df\, P^{(1)}(f) \sum_m w(m) \sum_n w(m-n)\, \exp(i2\pi f\Delta n) =$$

$$= \frac{\int df\, P^{(1)}(f)\, |H(f)|^2}{\sum_m w^2(m)}\,, \tag{B-2}$$

where we let k = m-n in the innermost sum on n in the second line, and used

$$H(f) = \sum_n w(n) \exp(-i2\pi f\Delta n) \; , \tag{B-3}$$

which follows from (5) and (8). Since H(f) obviously has period $1/\Delta$ in f, an integral over any period of the power transfer function becomes

$$\int_{1/\Delta} df \; |H(f)|^2 = \int_{1/\Delta} df \sum_{mn} w(m)\; w(n) \exp(i2\pi f\Delta(m-n)) =$$

$$= \frac{1}{\Delta} \sum_m w^2(m) = \frac{1}{\Delta}\, b(0) \; , \tag{B-4}$$

using orthogonality of the exponentials for $m \neq n$. Thus (B-2) translates into

$$\sum_n \beta(n)\; \rho(n\Delta) = \frac{\int df \; P^{(1)}(f) \; |H(f)|^2}{\Delta \int_{1/\Delta} df \; |H(f)|^2} \; . \tag{B-5}$$

Equation (B-4) is a special case of the useful result that

$$\int_{1/\Delta} df \; |H(f)|^2 \exp(i2\pi f\Delta n) = \frac{1}{\Delta} \sum_m w(m)\; w(m-n) = \frac{1}{\Delta}\, b(n) \; . \tag{B-6}$$

The method of derivation is similar to (B-4), and (62) has been employed for the final identification.

APPENDIX C. LIKELIHOOD RATIO PROCESSOR FOR INDEPENDENT SAMPLES

For a zero mean Gaussian input process with variance σ^2, the joint probability density function of M independent samples $x_1, \ldots, x_M$ is

$$p(x_1, \ldots, x_M) = \prod_{m=1}^{M} \left\{ \frac{1}{\sqrt{2\pi}\,\sigma} \exp\left(-\frac{x_m^2}{2\sigma^2}\right) \right\} . \qquad \text{(C-1)}$$

The likelihood ratio for hypothesis H_1 versus H_0 is

$$\frac{p_1(x_1, \ldots, x_M)}{p_0(x_1, \ldots, x_M)} = \left(\frac{\sigma_0}{\sigma_1}\right)^M \exp\left[\frac{1}{2}\left(\frac{1}{\sigma_0^2} - \frac{1}{\sigma_1^2}\right) \sum_{m=1}^{M} x_m^2\right] . \qquad \text{(C-2)}$$

The sufficient statistic of the samples is obviously

$$\sum_{m=1}^{M} x_m^2 , \qquad \text{(C-3)}$$

which is interpreted as an equi-weighted sum of the squared input samples.

APPENDIX D. COMPUTATIONAL PROCEDURES

The denominator of output signal-to-noise ratio γ_{IH} in (102) for half-wave rectifiers is

$$\mathrm{Sum}_H = \sum_{k=1}^{\infty} U(k) \sum_{n} \beta(n)\, \rho_0^k(n\Delta) = \sum_{k=1}^{\infty} U(k)\left[1 + 2 \sum_{n=1}^{\infty} \beta(n)\, \rho_0^k(n\Delta)\right] = \qquad \text{(D-1)}$$

$$= 2D(\upsilon) - 1 + 2 \sum_{k=1}^{\infty} U(k)\, S(k)\ , \qquad \text{(D-2)}$$

where we used (141) and defined the inner sum on n in (D-1) as

$$S(k) = \sum_{n=1}^{\infty} \beta(n)\, \rho_0^k(n\Delta) \quad \text{for } k \geq 1\ . \qquad \text{(D-3)}$$

The decay of S(k) with k is fast enough that the infinite sum on k in (D-2) can be terminated and yet realize very accurate results for the quantity Sum_H.

For the S+N versus N input hypotheses of (131) and low input signal-to-noise ratio, the output signal-to-noise ratio (102) becomes approximately

$$\gamma_{IH} \cong \frac{M}{\mathrm{Sum}_H} \frac{\upsilon^2}{4} \left(\frac{S}{N}\right)^2 \quad \text{for } \frac{S}{N} << 1\ . \qquad \text{(D-4)}$$

If this is equated to the standard value in (57) with input signal-to-noise ratio $(S/N)_S$, the amount by which the input signal-to-noise ratio for the half-wave rectifier must be increased is the factor

$$\frac{S/N}{(S/N)_s} = \frac{2}{\upsilon} \left(\frac{TW}{M} \, \mathrm{Sum}_H \right)^{1/2} . \tag{D-5}$$

This quantity is plotted in dB for a variety of values of υ, sampling rates, observation times, and input spectra, as discussed in (59) and (60). The way in which sampling increment Δ is related to the effective duration T of the filter is according to

$$T = M\Delta , \tag{D-6}$$

where M is the effective number of samples of the filter. Thus the ratio of sampling increment to inverse bandwidth is

$$\frac{\Delta}{1/W} = W\Delta = \frac{TW}{M} , \tag{D-7}$$

in terms of the time-bandwidth product TW and number of samples M.

For the full-wave rectifier, the only change is to limit the summation in (D-1) to even k, with the result

$$\mathrm{Sum}_F = \sum_{\substack{k=2 \\ \text{even}}}^{\infty} U(k) \left[1 + 2 \sum_{n=1}^{\infty} \beta(n) \, \rho_0^k(n\Delta) \right] =$$

$$= D(\upsilon) - 1 + 2 \sum_{\substack{k=2 \\ \text{even}}}^{\infty} U(k) \, S(k) , \tag{D-8}$$

where we used (130) and (D-3). The factor corresponding to (D-5) is now

$$\frac{S/N}{(S/N)_s} = \frac{2}{\upsilon} \left(\frac{TW}{M} \, \mathrm{Sum}_F \right)^{1/2} \tag{D-9}$$

for low input signal-to-noise ratio. This quantity has been plotted in dB for various υ, TW, M, and input spectra.

APPENDIX E. EQUIVALENT FREQUENCY DOMAIN REPRESENTATIONS

In this appendix, we derive some useful equivalent representations of the denominator terms in the output signal-to-noise ratios of (91) and (102). We begin by considering a general function $g(\tau)$ with Fourier transform

$$G(f) = \int d\tau \exp(-i2\pi f\tau)\ g(\tau) \ . \tag{E-1}$$

Then the summation of interest is

$$\sum_n \beta(n)\ g(n\Delta) = \frac{1}{b(0)} \sum_n g(n\Delta)\ \Delta \int_{1/\Delta} df\ \left|H(f)\right|^2 \exp(-i2\pi f\Delta n) =$$

$$= \frac{1}{b(0)} \int_{1/\Delta} df\ \left|H(f)\right|^2 \sum_n \exp(-i2\pi f\Delta n)\ g(n\Delta)\ \Delta \ , \tag{E-2}$$

upon use of (68) and (B-6), along with the observation that $b(n)$ in (62) is even in n; the integrals over frequency f are over any interval of length $1/\Delta$. But the summation over n in (E-2) is expressible as

$$\int d\tau\ \exp(-i2\pi f\tau)\ g(\tau) \sum_n \Delta\ \delta(\tau - n\Delta) =$$

$$= G(f) \circledast \sum_n \delta\left(f - \frac{n}{\Delta}\right) = \sum_n G\left(f - \frac{n}{\Delta}\right) \equiv \tilde{G}(f) \ , \tag{E-3}$$

which is the aliased version of $G(f)$ in (E-1). Here we used the fact that the Fourier transform of a product is the convolution of the corresponding Fourier transforms. Employment of (E-3) in (E-2) yields

$$\sum_n \beta(n)\ g(n\Delta) = \frac{1}{b(0)} \int_{1/\Delta} df\ |H(f)|^2\ \tilde{G}(f) \tag{E-4}$$

in terms of the (periodic) power transfer function of the filter H and the aliased spectrum $\tilde{G}$.

Now identify general function g as

$$g(\tau) = \rho^k(\tau)\ , \tag{E-5}$$

in which case

$$G(f) = P^{(k)}(f) = \int d\tau\ \exp(-i2\pi f\tau)\ \rho^k(\tau)\ , \tag{E-6}$$

according to (47). Then (E-4) becomes

$$\sum_n \beta(n)\ \rho^k(n\Delta) = \frac{1}{b(0)} \int_{1/\Delta} df\ |H(f)|^2\ \tilde{P}^{(k)}(f)\ , \tag{E-7}$$

in terms of the aliased spectral versions of $P^{(k)}(f)$.

If the spectral width, 1/T, of $|H(f)|^2$ is narrow relative to the bandwidth W of the spectral functions in (E-7), (see figures 5 and 6), then an approximation to (E-7) is afforded by observing that

$$\sum_n \beta(n)\ \rho^k(n\Delta) = \frac{1}{b(0)} \int_{-.5/\Delta}^{.5/\Delta} df\ |H(f)|^2\ \tilde{P}^{(k)}(f) =$$

$$\cong \frac{1}{b(0)}\ \tilde{P}^{(k)}(0) \int_{-.5/\Delta}^{.5/\Delta} df\ |H(f)|^2 = \frac{1}{\Delta}\ \tilde{P}^{(k)}(0)\ , \tag{E-8}$$

and using (B-4).

According to (E-3) and (E-6), we have, for k = 1,

$$\tilde{p}^{(1)}(f) = \sum_n p^{(1)}\left(f - \frac{n}{\Delta}\right), \tag{E-9}$$

which is the aliased version of the input spectrum to the detection system of interest.

For k = 2, observe first from (E-6) that

$$p^{(2)}(f) = p^{(1)}(f) \circledast p^{(1)}(f) = \int du\; p^{(1)}(u)\; p^{(1)}(f-u)\ . \tag{E-10}$$

Then the aliased version is

$$\tilde{p}^{(2)}(f) = \sum_n p^{(2)}\left(f - \frac{n}{\Delta}\right) = \sum_n \int du\; p^{(1)}(u)\; p^{(1)}\left(f - \frac{n}{\Delta} - u\right) =$$

$$= \int du\; p^{(1)}(u)\; \tilde{p}^{(1)}(f-u) = \int_{1/\Delta} du\; \tilde{p}^{(1)}(u)\; \tilde{p}^{(1)}(f-u)\ , \tag{E-11}$$

by use of (E-9) and the periodicity of $\tilde{p}^{(1)}$. This last relation states that the aliased spectrum $\tilde{p}^{(2)}(f)$ can be found by convolving the aliased input spectrum, $\tilde{p}^{(1)}(f)$, over one period.

In particular, a special case of (E-11) is

$$\tilde{p}^{(2)}(0) = \int_{1/\Delta} du\left[\tilde{p}^{(1)}(u)\right]^2\ , \tag{E-12}$$

using the even character of the input spectrum.

APPENDIX F. VARIOUS INPUT SPECTRA

The input spectra considered in this appendix are characterized by shape f^n for f in the range (f_1,f_2), and are symmetric about the origin f = 0. We still define

$$W = f_2 - f_1 \;, \quad f_c = \frac{f_2 + f_1}{2} \;, \quad Q = \frac{f_c}{W} \;. \tag{F-1}$$

However, the effective bandwidth of the positive frequency components of this spectral shape is

$$W_e = \frac{\left[\int_{f_1}^{f_2} df\ f^n\right]^2}{\int_{f_1}^{f_2} df\ f^{2n}} = \frac{2n + 1}{(n+1)^2} \; \frac{\left(f_2^{n+1} - f_1^{n+1}\right)^2}{f_2^{2n+1} - f_1^{2n+1}} \;, \tag{F-2}$$

and must be accounted for, in the evaluation of the standard output signal-to-noise ratio in (51).

The results for the normalized correlation and the effective bandwidth are listed below for various values of n, where we use the abbreviations

$$\alpha_1 = 2\pi f_1 \tau \,, \quad \alpha_2 = 2\pi f_2 \tau \,. \tag{F-3}$$

n = -2: -6 dB/octave

$$\rho(\tau) = \frac{\alpha_1 \alpha_2}{\alpha_2 - \alpha_1}\left[\mathrm{Si}(\alpha_1) - \mathrm{Si}(\alpha_2) + \frac{\cos(\alpha_1)}{\alpha_1} - \frac{\cos(\alpha_2)}{\alpha_2}\right],$$

$$W_e = W \, \frac{12\,Q^2 - 3}{12\,Q^2 + 1} \,. \tag{F-4}$$

n = -1: -3 dB/octave

$$\rho(\tau) = \frac{\mathrm{Ci}(\alpha_2) - \mathrm{Ci}(\alpha_1)}{\ln(\alpha_2/\alpha_1)} \,,$$

$$W_e = W\left(Q^2 - \frac{1}{4}\right) \ln^2\left(\frac{Q + \frac{1}{2}}{Q - \frac{1}{2}}\right). \tag{F-5}$$

n = 0: 0 dB/octave

$$\rho(\tau) = \frac{\sin(\alpha_2) - \sin(\alpha_1)}{\alpha_2 - \alpha_1} \,,$$

$$W_e = W \,. \tag{F-6}$$

n = 1: +3 dB/octave

$$\rho(\tau) = 2\,\frac{\alpha_2 \sin(\alpha_2) - \alpha_1 \sin(\alpha_1) + \cos(\alpha_2) - \cos(\alpha_1)}{\alpha_2^2 - \alpha_1^2} \,,$$

$$W_e = W \, \frac{12\,Q^2}{12\,Q^2 + 1} \,. \tag{F-7}$$

n = 2: +6 dB/octave

$$\rho(\tau) = 3\left(\alpha_2^3 - \alpha_1^3\right)^{-1} \left[(x^2 - 2)\ \sin(x) + 2\ x\ \cos(x)\right]_{\alpha_1}^{\alpha_2} ,$$

$$W_e = W\ \frac{144\ Q^4 + 24\ Q^2 + 1}{144\ Q^4 + 72\ Q^2 + 1.8} . \tag{F-8}$$

The way in which effective bandwidth W_e enters the standard output signal-to-noise ratio is via (51); namely

$$\gamma_a = \frac{T}{2}\left(\frac{S}{N}\right)_s^2 2W_e , \tag{F-9}$$

since

$$\frac{\left[\int df\ P_0^{(1)}(f)\right]^2}{\int df\ P_0^{(1)^2}(f)} = 2W_e . \tag{F-10}$$

If we equate (F-9) to (158), and solve for the required input signal-to-noise ratio, we obtain

$$\frac{S/N}{(S/N)_s} = \frac{2}{\upsilon}\left(\frac{TW_e}{M}\sum\right)^{1/2} = \frac{2}{\upsilon}\left(\frac{TW}{M}\sum\right)^{1/2}\left(\frac{12\ Q^2 - 3}{12\ Q^2 + 1}\right)^{1/2} , \tag{F-11}$$

where $\sum$ is given by (159); the last equality in (F-11) applies only to the -6 dB/octave spectrum and has utilized (F-4).

APPENDIX G. EVALUATION OF (166) FOR FLAT BANDPASS SPECTRUM

We are interested here in calculating the quantity

$$\tilde{S}(k) = \sum_{n=1}^{\infty} \rho^k(n\Delta) \quad \text{for } k \geq 1 , \tag{G-1}$$

where the relevant normalized correlation is

$$\rho(\tau) = \cos(2\pi f_c \tau)\ \mathrm{sinc}(W\tau) . \tag{G-2}$$

Sampling increment Δ is arbitrary in relation to center frequency f_c and bandwidth W.

Frequency Domain Representation

Since $\rho^k(\tau)$ and $P^{(k)}(f)$ are related by Fourier transform (47),

$$P^{(k)}(f) = \int d\tau \exp(-i2\pi f\tau)\ \rho^k(\tau) , \tag{G-3}$$

their samples are related through Poisson's formula

$$\sum_{n=-\infty}^{\infty} \rho^k(n\Delta) = \frac{1}{\Delta} \sum_{n=-\infty}^{\infty} P^{(k)}\left(\frac{n}{\Delta}\right) ; \tag{G-4}$$

see [5, page 36, (36)], for example. This relation is extremely useful for a bandlimited input spectrum, since its k-fold convolution $P^{(k)}(f)$ will have limited extent in f, leading to <u>finite</u> summations on the right-hand side of (G-4).

A more appropriate version of (G-4) for our use, where $\rho(\tau)$ is real and even, is furnished by the following:

$$\tilde{S}(k) = \sum_{n=1}^{\infty} \rho^k(n\Delta) = \frac{1}{2}\left[\sum_{n=-\infty}^{\infty} \rho^k(n\Delta) - 1\right] =$$

$$= \frac{1}{2\Delta} \sum_{n=-\infty}^{\infty} P^{(k)}\left(\frac{n}{\Delta}\right) - \frac{1}{2} = \frac{1}{\Delta} \sum_{n=1}^{\infty} P^{(k)}\left(\frac{n}{\Delta}\right) + \frac{1}{2\Delta} P^{(k)}(0) - \frac{1}{2} . \quad \text{(G-5)}$$

<u>Evaluation of Auxiliary Functions</u>

Before directly evaluating

$$P^{(k)}(f) = \int d\tau \exp(-i2\pi f\tau) \left[\cos(2\pi f_c\tau) \operatorname{sinc}(W\tau)\right]^k , \quad \text{(G-6)}$$

we first consider the auxiliary functions

$$G_k(u) \equiv \int dx \exp(-i2\pi ux) \operatorname{sinc}^k(x) \quad \text{for } k \geq 1 . \quad \text{(G-7)}$$

It is readily shown that

$$G_1(u) = \operatorname{rect}(u) = \left\{\begin{array}{ll} 1 & \text{for } |u| < 1/2 \\ 1/2 & \text{for } |u| = 1/2 \\ 0 & \text{for } |u| > 1/2 \end{array}\right\} . \quad \text{(G-8)}$$

By repeated convolution, there then follows (see [6, pages 11, 12, 33, 34])

$$G_2(u) = \left\{\begin{array}{ll} 1 - |u| & \text{for } |u| \leq 1 \\ 0 & \text{for } |u| \geq 1 \end{array}\right\} , \quad \text{(G-9)}$$

$$G_3(u) = \left\{\begin{array}{ll} \frac{3}{4} - u^2 & \text{for } |u| \leq \frac{1}{2} \\ \frac{1}{8}(3 - 2|u|)^2 & \text{for } \frac{1}{2} \leq |u| \leq \frac{3}{2} \\ 0 & \text{for } |u| \geq \frac{3}{2} \end{array}\right\} , \quad \text{(G-10)}$$

$$G_4(u) = \begin{Bmatrix} \frac{1}{6}(4 - 6u^2 + 3|u|^3) & \text{for } |u| \le 1 \\ \frac{1}{6}(2 - |u|)^3 & \text{for } 1 \le |u| \le 2 \\ 0 & \text{for } |u| \ge 2 \end{Bmatrix}. \tag{G-11}$$

Generally, $G_k(u) = 0$ for $|u| > k/2$.

<u>Evaluation of $P^{(k)}(f)$</u>

By expanding the k-th power in (G-6) according to

$$\cos^k(y) = \frac{1}{2^k}\left[\exp(iy) + \exp(-iy)\right]^k , \tag{G-12}$$

and using (G-7)-(G-11), there readily follows

$$\frac{1}{\Delta}\, P^{(1)}(f) = \frac{1}{2W\Delta}\, G_1\left(\frac{f \pm f_c}{W}\right) \equiv \frac{1}{2W\Delta}\left[G_1\left(\frac{f - f_c}{W}\right) + G_1\left(\frac{f + f_c}{W}\right)\right], \tag{G-13}$$

$$\frac{1}{\Delta}\, P^{(2)}(f) = \frac{1}{4W\Delta}\left[G_2\left(\frac{f \pm 2f_c}{W}\right) + 2G_2\left(\frac{f}{W}\right)\right], \tag{G-14}$$

$$\frac{1}{\Delta}\, P^{(3)}(f) = \frac{1}{8W\Delta}\left[G_3\left(\frac{f \pm 3f_c}{W}\right) + 3G_3\left(\frac{f \pm f_c}{W}\right)\right], \tag{G-15}$$

$$\frac{1}{\Delta}\, P^{(4)}(f) = \frac{1}{16W\Delta}\left[G_4\left(\frac{f \pm 4f_c}{W}\right) + 4G_4\left(\frac{f \pm 2f_c}{W}\right) + 6G_4\left(\frac{f}{W}\right)\right], \tag{G-16}$$

where the $\pm$ shorthand notation is explained in (G-13).

Equations (G-13)-(G-16) coupled with (G-8)-(G-11) enable us to evaluate the desired quantity in (G-5) for k = 1,2,3,4, in a very efficient manner, since all the sums in (G-5) terminate after a finite number of terms. On the other hand, for $k \ge 5$, we resort to direct numerical evaluation of (G-1) and (G-2), since the summands decay at least as fast as $1/n^5$ and can be terminated with a desired level of error.

Error Analysis

Substitution of (G-2) into (G-1) and use of $\Delta = T/M$ yields

$$\tilde{S}(k) = \sum_{n=1}^{\infty} \left[\cos\left(2\pi Q \frac{TW}{M} n\right) \operatorname{sinc}\left(\frac{TW}{M} n\right)\right]^k . \qquad \text{(G-17)}$$

If this sum is conducted through N terms, the error E is upper bounded according to

$$E \leq \sum_{n=N+1}^{\infty} \frac{1}{(\alpha n)^k} \leq \frac{1}{\alpha^k} \int_N^{\infty} \frac{dx}{x^k} = \frac{1}{\alpha^k (k-1)\, N^{k-1}} , \qquad \text{(G-18)}$$

where $\alpha = \pi TW/M$. Solving for the N required, we obtain

$$N \geq N_k = \frac{1}{\alpha} \exp\left[\frac{-\ln\{(k-1)\, \alpha E\}}{k-1}\right] , \qquad \text{(G-19)}$$

which depends on k, as well as α and specified error E. This limit was used in (G-17) for $k \geq 5$, with E = 1.E-10, to get the results in figures 33 and 34.

APPENDIX H. PROGRAM LISTINGS

In this appendix, we collect all the programs that were used to generate the numerical results and figures in the main body of the report. The auxiliary functions Si(x) and Γ(x) common to these programs are listed in table H-6.

In order to convert table H-1 to the Gaussian spectrum instead of the flat bandpass spectrum, the following changes and additions are required:

```
100     Te=.5*PI*Tw*Tw/(M*M)
111     F=Te*Ns*Ns
112     IF F>100. THEN 210
120     Rho=COS(Tc*Ns)*EXP(-F)        !   GAUSSIAN SPECTRUM
```

In order to convert table H-2 to the Gaussian spectrum, the following changes and additions are required:

```
100     Te=.5*PI*Tw*Tw/(M*M)
111     F=Te*Ns*Ns
112     IF F>100. THEN 200
120     Rho=COS(Tc*Ns)*EXP(-F)        !   GAUSSIAN SPECTRUM
```

In order to convert table H-1 to the RC filter instead of the box car filter, use:

```
101     Te=2./M
110     FOR Ns=1 TO M*15
140     Pk=EXP(-Te*Ns)                !   RC FILTER
```

In order to convert table H-2 to the RC filter, use:

```
101     Te=2./M
110     FOR Ns=1 TO M*15
130     Pk=EXP(-Te*Ns)              ! RC FILTER
```

Table H-5 lists the program used for investigating the long averaging time assumption; however, it is not recommended for use, since the earlier programs are capable of exact evaluation of required signal-to-noise ratios.

The word DOUBLE denotes INTEGER variables in Hewlett-Packard BASIC on the 9000 computer.

Table H-1. Full-Wave Rectifier, Flat Bandpass Spectrum, Box Car Filter

```
10    Tw=50.                          !  TW            FULL-WAVE RECTIFIER
20    Q=5./6.                         !  fc/W >= .5
30    M=1000                          !  M, number of samples
40    K=1000                          !  Number of terms in Sum
50    DOUBLE M,K,Ns,Ks
60    REDIM S(1:K)
70    DIM S(1:1000)
80    MAT S=(0.)
90    Tc=2.*PI*Q*Tw/M
100   Ts=PI*Tw/M
110   FOR Ns=1 TO M-1
120   Rho=COS(Tc*Ns)*SIN(Ts*Ns)/(Ts*Ns)   !  FLAT BANDPASS SPECTRUM
130   Rho2=Rho*Rho
140   Pk=1.-Ns/M                          !  BOX CAR FILTER
150   FOR Ks=2 TO K STEP 2
160   Pk=Pk*Rho2
170   S(Ks)=S(Ks)+Pk
180   IF ABS(Pk)<1.E-12 THEN 200
190   NEXT Ks
200   NEXT Ns
210   PRINT "TW =";Tw;"   Q =";Q;"   M =";M;"   K =";K;"   S(K) =";S(K)
220   INPUT "NU =",V                      !  NU
230   G5=FNGamma(.5*V+.5)
240   U=1.
250   Sum=0.
260   FOR Ks=2 TO K STEP 2
270   T=V+2.-Ks
280   U=U*T*T/(Ks*(Ks-1))
290   Sum=Sum+U*S(Ks)
300   NEXT Ks
310   Dv=SQR(PI)*FNGamma(V+.5)/(G5*G5)
320   Sum=Dv-1.+2.*Sum
330   F=2.*SQR(Tw*Sum/M)/V
340   PRINT V,10.*LGT(F),2.*U*S(K)/Sum
350   GOTO 220
360   END
```

Table H-2. Half-Wave Rectifier, Flat Bandpass Spectrum, Box Car Filter

```
 10     Tw=50.                   !  TW            HALF-WAVE RECTIFIER
 20     Q=5./6.                  !  fc/W >= .5
 30     M=1000                   !  M, number of samples
 40     K=1000                   !  Number of terms in Sum
 50     DOUBLE M,K,Ns,Ks
 60     REDIM S(1:K),U(0:K)
 70     DIM S(1:1000),U(0:1000)
 80     MAT S=(0.)
 90     Tc=2.*PI*Q*Tw/M
100     Ts=PI*Tw/M
110     FOR Ns=1 TO M-1
120     Rho=COS(Tc*Ns)*SIN(Ts*Ns)/(Ts*Ns)  !  FLAT BANDPASS SPECTRUM
130     Pk=1.-Ns/M                         !  BOX CAR FILTER
140     FOR Ks=1 TO K
150     Pk=Pk*Rho
160     S(Ks)=S(Ks)+Pk
170     IF ABS(Pk)<1.E-12 THEN 190
180     NEXT Ks
190     NEXT Ns
200     PRINT "TW =";Tw;"   Q =";Q;"   M =";M;"   K =";K;"  S(K) =";S(K)
210     INPUT "NU =",V                     !  NU
220     G5=FNGamma(.5*V+.5)
230     U(0)=1.
240     U=FNGamma(.5*V+1.)/G5
250     U(1)=2.*U*U
260     Sum=U(1)*S(1)
270     FOR Ks=2 TO K
280     T=V+2.-Ks
290     U(Ks)=U=U(Ks-2)*T*T/(Ks*(Ks-1))
300     Sum=Sum+U*S(Ks)
310     NEXT Ks
320     Dv=SQR(PI)*FNGamma(V+.5)/(G5*G5)
330     Sum=2.*Dv-1.+2.*Sum
340     F=2.*SQR(Tw*Sum/M)/V
350     PRINT V,10.*LGT(F),2.*U*S(K)/Sum
360     GOTO 210
370     END
```

Table H-3. Full-Wave Rectifier, -6 dB/Octave Spectrum, Box Car Filter

```
 10     Tw=50.                        !  TW              FULL-WAVE RECTIFIER
 20     Q=5./6.                       !  fc/W
 30     M=100                         !  M, number of samples
 40     K=1000                        !  Number of terms in Sum
 50     DOUBLE M,K,Ns,Ks
 60     REDIM S(1:K)
 70     DIM S(1:1000)
 80     MAT S=(0.)
 90     C1=2.*PI*Tw*(Q-.5)/M
100     C2=2.*PI*Tw*(Q+.5)/M
110     Sq=12.*Q*Q
120     Sq=SQR((Sq-3.)/(Sq+1.))
130     FOR Ns=1 TO M-1
140     Rho=FNRho(Ns,C1,C2)                        !  -6 dB/OCTAVE SPECTRUM
150     Rho2=Rho*Rho
160     Pk=1.-Ns/M                                 !  BOX CAR FILTER
170     FOR Ks=2 TO K STEP 2
180     Pk=Pk*Rho2
190     S(Ks)=S(Ks)+Pk
200     IF ABS(Pk)<1.E-12 THEN 220
210     NEXT Ks
220     NEXT Ns
230     PRINT "TW =";Tw;"   Q =";Q;"   M =";M;"   K =";K;"  S(K) =";S(K)
240     INPUT "NU =",V                             !  NU
250     G5=FNGamma(.5*V+.5)
260     U=1.
270     Sum=0.
280     FOR Ks=2 TO K STEP 2
290     T=V+2.-Ks
300     U=U*T*T/(Ks*(Ks-1))
310     Sum=Sum+U*S(Ks)
320     NEXT Ks
330     Dv=SQR(PI)*FNGamma(V+.5)/(G5*G5)
340     Sum=Dv-1.+2.*Sum
350     F=2.*SQR(Tw*Sum/M)/V*Sq
360     PRINT V,10.*LGT(F),2.*U*S(K)/Sum
370     GOTO 240
380     END
390     !
400     DEF FNRho(DOUBLE Ns,REAL C1,C2)
410     A1=C1*Ns
420     A2=C2*Ns
430     Rho=FNSi(A1)-FNSi(A2)+COS(A1)/A1-COS(A2)/A2
440     Rho=A1*A2*Rho/(A2-A1)
450     RETURN Rho
460     FNEND
```

Table H-4. Half-Wave Rectifier, -6 dB/Octave Spectrum, Box Car Filter

```
10   Tw=50.                    !  TW              HALF-WAVE RECTIFIER
20   Q=5./6.                   !  fc/W
30   M=100                     !  M, number of samples
40   K=1000                    !  Number of terms in Sum
50   DOUBLE M,K,Ns,Ks
60   REDIM S(1:K),U(0:K)
70   DIM S(1:1000),U(0:1000)
80   MAT S=(0.)
90   C1=2.*PI*Tw*(Q-.5)/M
100  C2=2.*PI*Tw*(Q+.5)/M
110  Sq=12.*Q*Q
120  Sq=SQR((Sq-3.)/(Sq+1.))
130  FOR Ns=1 TO M-1
140  Rho=FNRho(Ns,C1,C2)                    !  -6 dB/OCTAVE SPECTRUM
150  Pk=1.-Ns/M                             !  BOX CAR FILTER
160  FOR Ks=1 TO K
170  Pk=Pk*Rho
180  S(Ks)=S(Ks)+Pk
190  IF ABS(Pk)<1.E-12 THEN 210
200  NEXT Ks
210  NEXT Ns
220  PRINT "TW =";Tw;"   Q =";Q;"   M =";M;"   K =";K;"  S(K) =";S(K)
230  INPUT "NU =",V                         !  NU
240  G5=FNGamma(.5*V+.5)
250  U(0)=1.
260  U=FNGamma(.5*V+1.)/G5
270  U(1)=2.*U*U
280  Sum=U(1)*S(1)
290  FOR Ks=2 TO K
300  T=V+2.-Ks
310  U(Ks)=U=U(Ks-2)*T*T/(Ks*(Ks-1))
320  Sum=Sum+U*S(Ks)
330  NEXT Ks
340  Dv=SQR(PI)*FNGamma(V+.5)/(G5*G5)
350  Sum=2.*Dv-1.+2.*Sum
360  F=2.*SQR(Tw*Sum/M)/V*Sq
370  PRINT V,10.*LGT(F),2.*U*S(K)/Sum
380  GOTO 230
390  END
```

Table H-5. Half-Wave Rectifier, Flat Bandpass Spectrum, Long Averaging Time Assumption

```
 10     Tw=50.                    !  TW                  HALF-WAVE RECTIFIER
 20     Q=.501                    !  fc/W >= .5          LONG AVERAGING TIME
 30     M=1000                    !  M, number of samples      ASSUMPTION
 40     K=1000                    !  Number of terms in Sum
 50     REDIM S(1:K),U(0:K),N(5:K)
 60     DIM S(1:1000),U(0:1000),Rho(1:10000),Rk(1:10000)
 70     DOUBLE N(5:10000),M,K,Ns,Ks,Nmax
 80     Q2=Q+Q
 90     Q3=Q2+Q
100     Q4=Q3+Q
110     S1=FNG1(Q)
120     S2=FNG2(Q2)+FNG2(0.)
130     S3=FNG3(Q3)+3.*FNG3(Q)
140     S4=FNG4(Q4)+4.*FNG4(Q2)+3.*FNG4(0.)
150     Owd=M/Tw
160     Fow=0.
170     Fow=Fow+Owd
180     IF Fow-Q4>=2. THEN 250
190     S1=S1+FNG1(Fow-Q)+FNG1(Fow+Q)
200     S2=S2+FNG2(Fow-Q2)+2.*FNG2(Fow)+FNG2(Fow+Q2)
210     S3=S3+FNG3(Fow-Q3)+3.*FNG3(Fow-Q)+3.*FNG3(Fow+Q)+FNG3(Fow+Q3)
220     S4=S4+FNG4(Fow-Q4)+4.*FNG4(Fow-Q2)+6.*FNG4(Fow)
230     S4=S4+4.*FNG4(Fow+Q2)+FNG4(Fow+Q4)
240     GOTO 170
250     S(1)=.5*Owd*S1-.5
260     S(2)=.25*Owd*S2-.5
270     S(3)=.125*Owd*S3-.5
280     S(4)=.0625*Owd*S4-.5
290     Tc=2.*PI*Q*Tw/M
300     Ts=PI*Tw/M
310     Error=1.E-10
320     C1=1./Ts
330     C2=-LOG(Ts*Error)
340     FOR Ks=5 TO K
350     T=Ks-1
360     N(Ks)=INT(C1*EXP((C2-LOG(T))/T))+1
370     NEXT Ks
380     FOR Ks=K-1 TO 5 STEP -1
390     IF N(Ks)<N(Ks+1) THEN N(Ks)=N(Ks+1)
400     NEXT Ks
410     Nmax=MAX(N(*))
420     REDIM Rho(1:Nmax),Rk(1:Nmax)
430     FOR Ns=1 TO Nmax
440     R=Rho(Ns)=COS(Tc*Ns)*SIN(Ts*Ns)/(Ts*Ns)
450     Rk(Ns)=R*R*R*R
460     NEXT Ns
470     FOR Ks=5 TO K
480     S=0.
490     FOR Ns=1 TO N(Ks)
500     Rk=Rk(Ns)=Rk(Ns)*Rho(Ns)
```

Table H-5 (Cont'd). Half-Wave Rectifier, Flat Bandpass Spectrum, Long Averaging Time Assumption

```
510    S=S+Rk
520    NEXT Ns
530    S(Ks)=S
540    NEXT Ks
550    PRINT "T  =";Tw;"   Q =";Q;"   M =";M;"   K =";K;"  S(K) =";S(K)
560    INPUT "N  =",V                          !  NU
570    G5=FNGam a(.5*V+.5)
580    U(0)=1.
590    U=FNGamm (.5*V+1.)/G5
600    U(1)=2.* *U
610    Sum=U(1  S(1)
620    FOR Ks=. TO K
630    T=V+2.-
640    U(Ks)=U (Ks-2)*T*T/(Ks*(Ks-1))
650    Sum=Sum *S(Ks)
660    NEXT Ks
670    Dv=SQR( )*FNGamma(V+.5)/(G5*G5)
680    Sum=2.* -1.+2.*Sum
690    F=2.*SQ Tw*Sum/M)/V
700    PRINT V 10.*LGT(F),2.*U*S(K)/Sum
710    GOTO 56
720    END
730    !
740    DEF FNC (F)
750    A=ABS(F
760    IF A<.5 THEN RETURN 1.
770    IF A=.5 THEN RETURN .5
780    RETURN  .
790    FNEND
800    !
810    DEF FN .(F)
820    A=ABS(
830    IF A<1  THEN RETURN 1.-A
840    RETURN ).
850    FNEND
860    !
870    DEF FN 3(F)
880    A=ABS(
890    IF A<.  THEN RETURN .75-A*A
900    IF A<1 5 THEN RETURN .125*(3.-A-A)*(3.-A-A)
910    RETURN 0.
920    FNEND
930    !
940    DEF FI 4(F)
950    A=ABS  )
960    A2=A*
970    IF A<   THEN RETURN (4.-6.*A2+3.*A2*A)/6.
980    IF A<   THEN RETURN (2.-A)*(2.-A)*(2.-A)/6.
990    RETUR  0.
1000   FNEND
```

Table H-6. Auxiliary Functions Si(x) and Γ(x)

```
10      DEF FNSi(X)         !  Si(X) via 5.2.8,14,38,39
20      Y=X*X
30      IF Y>1. THEN 70
40      Si=2.83446712018E-5-Y*3.06192435822E-7
50      Si=X*(1.-Y*(.0555555555556-Y*(1.66666666667E-3-Y*Si)))
60      RETURN Si
70      T1=38.102495+Y*(335.677320+Y*(265.187033+Y*(38.027264+Y)))
80      T2=157.105423+Y*(570.236280+Y*(322.624911+Y*(40.021433+Y)))
90      F=T1/(X*T2)
100     T1=21.821899+Y*(352.018498+Y*(302.757865+Y*(42.242855+Y)))
110     T2=449.690326+Y*(1114.978885+Y*(482.485984+Y*(48.196927+Y)))
120     G=T1/(Y*T2)
130     Si=1.57079632679*SGN(X)-F*COS(X)-G*SIN(X)
140     RETURN Si
150     FNEND
```

```
10      DEF FNGamma(X)              !   HART, page 135, #5243
20      DOUBLE N,K
30      N=INT(X)
40      R=X-N
50      IF N>0 OR R>0. THEN 80
60      PRINT "FNGamma(X) IS NOT DEFINED FOR X = ";X
70      STOP
80      IF R>0. THEN 110
90      Gamma2=1.
100     GOTO 180
110     P=439.33044406002567 6+R*(50.108693752970953 0+R*6.7449507245925289 9)
120     P=8762.7102978521489 6+R*(2008.5274013072791 2+R*P)
130     P=42353.689509744089 6+R*(20886.861789269887 4+R*P)
140     Q=499.02852662143904 8-R*(189.49823415702801 6-R*(23.081551524580125-R))
150     Q=9940.3074150827709 0-R*(1528.6072737795220 2+R*Q)
160     Q=42353.689509744090 0+R*(2980.3853309256649 9-R*Q)
170     Gamma2=P/Q                    !  Gamma(2+R) for 0 < R < 1
180     IF N>2 THEN 220
190     IF N<2 THEN 270
200     Gamma=Gamma2
210     RETURN Gamma
220     Gamma=Gamma2
230     FOR K=1 TO N-2
240     Gamma=Gamma*(X-K)
250     NEXT K
260     RETURN Gamma
270     R=1.
280     FOR K=0 TO 1-N
290     R=R*(X+K)
300     NEXT K
310     Gamma=Gamma2/R
320     RETURN Gamma
330     FNEND
```

REFERENCES

1. J. J. Faran and R. Hills, "Correlators for Signal Reception," Technical Memorandum Number 27, ONR-384-903, Acoustics Research Laboratory, Harvard University, Cambridge, MA, 15 September 1952.

2. J. F. Barrett and D. G. Lampard, "An Expansion for Some Second-Order Probability Distributions and its Application to Noise Problems," IRE Transactions on Information Theory, volume IT-1, number 1, pages 10-15, March 1955.

3. Handbook of Mathematical Functions, National Bureau of Standards, Applied Mathematics Series, number 55, U.S. Department of Commerce, U.S. Government Printing Office, Washington, D.C., June 1964.

4. A. H. Nuttall, Signal Processing Studies, NUSC Scientific and Engineering Studies, New London, CT, 1985.

5. P. M. Woodward, Probability and Information Theory, With Applications to Radar, Pergamon Press, N.Y., 1957.

6. A. H. Nuttall, "Spectral Estimation by Means of Overlapped Fast Fourier Transform Processing of Windowed Data," NUSC Technical Report No. 4169, 13 October 1971; also Spectral Estimation, NUSC Scientific and Engineering Studies, New London, CT, 1977.

INIITAL DISTRIBUTION LIST

Addressee	No. of Copies
ASN (RE&S)	1
OUSDR&E (Research and Advanced Technology)	2
DEPUTY USDR&E (Res & Adv Tech)	1
DEPUTY USDR&E (Dir Elect & Phys Sc)	1
ONR, ONR-100, -102, -200, -400, -410, 411 (N. Gerr), -422, -425AC, -430	9
COMSPAWARSYSCOM, SPAWAR 05 (W. R. Hunt)	1
CNO, OP-098, OP-941, OP-951	3
DIA (DT-2C)	10
NRL, Code 5132, (Dr. P. B. Abraham) Code 5370, (W. Gabriel), Code 5135, (N. Yen) (A. A. Gerlach)	4
USRD	1
NORDA	1
USOC, Code 240, Code 241	2
NAVSUBSUPACNLON	1
NAVOCEANO, Code 02	2
NAVELECSYSCOM, ELEX 03, 310	2
NAVSEASYSCOM, SEA-00, -05R, -06F, 63D (D. Early), 63R (E. L. Plummer, CDR E. Graham IV, C. C. Walker), -92R	8
NAVAIRDEVCEN, Warminster	1
NAVAIRDEVCEN, Key West	1
NOSC, Code 8302, Code 6565 (Library), Code 713 (F. Harris)	3
NAVWPNSCEN	1
NCSC, Code 724	1
NAVCIVENGRLAB	1
NAVSWC	1
NAVSURFWPNCEN, Code U31	1
NISC,	1
CNET, Code 017	1
CNTT	1
NAVSUBSCOL	1
NAVTRAEQUIPCENT, Technical Library	1
NAVPGSCOL	2
NAVWARCOL	1
NETC	1
APL/UW, SEATTLE	1
ARL/PENN STATE, STATE COLLEGE	1
CENTER FOR NAVAL ANALYSES (ACQUISITION UNIT)	1
DTIC	2
DARPA, Alan Ellinthorpe	1
NOAA/ERL	1
NATIONAL RESEARCH COUNCIL	1
WOODS HOLE OCEANOGRAPHIC INSTITUTION (Dr. R. C. Spindel)	2
ENGINEERING SOCIETIES LIB, UNITED ENGR CTR	1
NATIONAL INSTITUTE OF HEALTH	1
ARL, UNIV OF TEXAS	1

INIITAL DISTRIBUTION LIST

Addressee	No. of Copies
MARINE PHYSICAL LAB, SCRIPPS	1
UNIVERSITY OF CALIFORNIA, SAN DIEGO	1
NAVSURWEACTR	1
DELSI	1
DIRECTOR SACLANT ASW RES CEN	1
COM SPACE & NAV WAR SYS COM	1
COM NAVAL PERSONNEL R&D CENTER	1
COM NAV SUB COLLEGE	1
B-K DYN INC	1
BBN, Arlington, VA (Dr. H. Cox)	1
BBN, Cambridge, MA (H. Gish)	1
BBN, New London, CT (Dr. P. Cable)	1
EWASCTRI	1
MAR, INC, East Lyme, CT	1
HYDROINC (D. Clark)	1
SUMRESCR (M. Henry)	1
ANALTECHNS, N. Stonington, CT	1
ANALTECHNS, New London, CT	1
EDOCORP (J. Vincenzo)	1
TRA CORP., Austin, TX (Dr. T. Leih, J. Wilkinson)	2
TRA CORP., Groton, CT	1
NETS (R. Medeiros)	1
GESY, D. Bates	1
SONALYSTS, Waterford, CT (J. Morris)	1
ORI CO, INC. (G. Assard)	1
HUGHES AIRCRAFT CO. (S. Autrey)	1
MIT (Prof. A. Baggaroer)	1
RAYTHEON CO. (J. Bartram)	1
Dr. Julius Bendat, 833 Moraga Dr, Los Angeles, CA	1
COOLEY LABORATORY (Prof. T. Birdsall)	1
PROMETHEUS, INC. (Dr. James S. Byrnes)	1
BBN INC., New London, CT (Dr. P. Cable)	1
BBN INC., Arlington VA (Dr. H. Cox)	1
BBN INC., Cambridge, MA (H. Gish)	1
ROYAL MILITARY COLLEGE OF CANADA (Prof. Y. T. Chan)	1
UNIV. OF FLORIDA (D. C. Childers)	1
SANDIA NATIONAL LABORATORY (J. Claasen)	1
COGENT SYSTEMS, INC. (J. P. Costas)	1
IBM CORP. (G. Demuth)	1
UNIV. OF STRATHCLYDE, CLASGOW, SCOTLAND (Prof. T. Durrani)	1
ROCKWELL INTERNATIONAL CORP. (L. T. Einstein and Dr. D. F. Elliott)	2
GENERAL ELECTRIC CO. (Dr. M. Fitelson)	1
HONEYWELL, INC. (D. M. Goodfellow, Dr. Murray Simon, W. Hughey)	3
UNIV. OF TECHNOLOGY, LOUGHBOROUGH, LEICESTERSHIRE, ENGLAND (Prof. J. W. R. Griffiths)	1
HARRIS SCIENTIFIC SERVICES (B. Harris)	1

INITIAL DISTRIBUTION LIST

Addressee	No. of Copies
UNIV OF CALIFORNIA, SAN DIEGO (Prof. C. W. Helstrom)	1
EG&G (Dr. J. Hughen)	1
A&T, INC. (H. Jarvis)	1
BELL COMMUNICATIONS RESEARCH (J. F. Kaiser)	1
UNIV. OF RI (Prof. S. Kay, Prof. L. Scharf, Prof. D. Tufts)	3
MAGNAVOX GOV. & IND. ELEC. CO. (R. Kenefic)	1
DREXEL UNIV. (Prof. Stanislav Kesler)	1
UNIV. OF CT (Prof. C. H. Knapp)	1
APPLIED SEISMIC GROUP (R. Lacoss)	1
ADMIRALITY RESEARCH ESTABLISHMENT, ENGLAND (Dr. L. J. Lloyd)	1
NAVAL SYSTEMS DIV., SIMRAD SUBSEA A/S, NORWAY (E. B. Lunde)	1
DEFENCE RESEARCH ESTAB. ATLANTIC, DARTMOUTH, NOVA SCOTIA CANADA (B. E. Mackey, Library)	1
MARTIN MARIETTA AEROSPACE (S. L. Marple)	1
PSI MARINE SCIENCES (Dr. R. Mellen)	1
Dr. D. Middleton, 127 E. 91st St. NY, NY 10128	1
Dr. P. Mikhalevsky, 803 W. Broad St. Falls Church, VA 22046	1
CANBERRA COLLEGE OF ADV. EDUC., AUSTRALIA 2616 (P. Morgan)	1
NORTHEASTERN UNIV., (Prof. C. L. Nikias)	1
ASTRON RESEARCH & ENGR, (Dr. A. G. Piersol)	1
WESTINGHOUSE ELEC. CORP. (Dr. H. L. Price)	1
M/A-COM GOVT SYSTEMS, (Dr. R. Price)	1
DALHOUSIE UNIV. HALIFAX, NOVA SCOTIA (Dr. B. Ruddick)	1
NATO SACLANT ASW RESEARCH CENTER, LIBRARY, APO NY, NY 09019	1
YALE UNIV. (Prof. M. Schultheiss)	1
NATIONAL RADIO ASTRONOMY OBSERVATORY (F. Schwab)	1
DEFENSE SYSTEMS, INC (Dr. G. S. Sebestyen)	1
NATO SACLANT ASW RESEARCH CENTRE (Dr. E. J. Sullivan)	1
PENN STATE UNIV, APPLIED RESEARCH LAB. (F. W. Symons)	1
NAVAL PG SCHOOL, (Prof. C.W. Therrien)	1
DEFENCE RESEARCH ESTABLISHMENT PACIFIC, VICTORIA, B.C. CANADA VOS 1BO (Dr. D. J. Thomson)	1
Robert J. Urick, 11701 Berwick Rd, Silver Spring, MD 20904	1
RCA CORP (H. Urkowitz)	1
USEA S.P.A. LA SPEZIA, ITALY (H. Van Asselt)	1
NORDA, Code 345 (R. Wagstaff)	1
TEL-AVIV UNIV. ISRAEL (Prof. E. Weinstein)	1
COAST GUARD ACADEMY (Prof. J. J. Wolcin)	1
SPACE PHYSICS LAB, UNIV OF ALBERTA, EDMONTON, CANADA (K. L. Yeung)	1
UNIV. OF IOWA (Prof. D. H. Youn)	1
COLOMBIA RESEARCH CORP. (W. Hahn)	1